

https://dspace.org/

Analysis of the rock mass behaviour as associated with Ventersdorp contact reef stopes, South Africa

Guler, Gokhan

1998
https://hdl.handle.net/10539/28739

Downloaded from a DSpace repository. https://dspace.org/

ANALYSIS OF THE ROCK MASS BEHAVIOUR AS ASSOCIATED WITH VENTERSDORP CONTACT REEF STOPES, SOUTH AFRICA

Gökhan GÜLER

A dissertation submitted to the Faculty of Engineering, University of the Witwatersrand, Johannesburg, in fulfilment of the requirements for the degree of Master of Science in Engineering.

Johannesburg, June 1998.

Declaration

This work is being submitted for the degree of Master of Science in Engineering at the University of the Witwatersrand, Johannesburg.

I declare that this work has not been submitted before for any degree or examination at another university.

Signed this ____ day of _____ 1998.

_____

Gökhan GÜLER

ABSTRACT

In the Far West Rand Goldfields a series of lava flows covers the important, auriferous deposit known as the Ventersdorp Contact Reef (VCR), which separates the lavas from various sedimentary rock types. Until recently, little research had been done aiming at the identification and analysis of rock engineering problems encountered while mining this reef. This is especially surprising when considering that the VCR is one of the major South African gold producers, contributing some 15 % to the overall gold production.

This dissertation consists of three parts: the first concerns the definition and establishment of geotechnical areas in all mines where the VCR is currently being mined. Twelve mines are considered covering a distance exceeding 60 km, and six major geotechnical areas are defined by regions with different combinations of hangingwall lavas and footwall rock types. The second part considers observations and measurements of the rock mass behaviour around geotechnically distinct VCR stopes. This approach is used as it is expected that geotechnical variation influence rock mass behaviour and consequently mining strategy and design of support systems. The last part describes a VCR specific stope support design methodology also considering closure rate variations as a function of face advance rates.

In order to achieve these goals, as a part of the SIMRAC project GAP 102, a series of studies and investigations, involving the division of the orebody into geotechnical areas, underground observations and monitoring, analysis of accident data, laboratory testing, and the assessment of rock mass behaviour, were undertaken. The main results of each of these studies are summarised below:

A) Collation and review of all past rock engineering and geological work undertaken on the VCR by means of a literature survey considering references up to the start of the project, 1993;

- Few documented rock engineering studies were found.
- Several geological studies were of relevance to the project.
- Rock engineering properties of the strata associated with the VCR were not documented.
- Scope existed to use existing geological knowledge as a basis for rock engineering studies.

B) Definition of geotechnical areas;

- As a part of the SIMRAC project GAP 102, a methodology to define primary geotechnical areas on a regional basis has been developed and six primary geotechnical areas based on a combination of three footwall and two hangingwall rock types were delineated.

C) Identification of fracture patterns of different geotechnical areas;

- Distinct fracture attitudes and intensities were associated with different footwall and hangingwall rock type assemblages, including the fracture pattern associated with the soft lava/Jeppestown shale geotechnical domain in which extension fractures in the hangingwall dip towards the back area, a situation almost unique in deep gold mines.

D) Evaluation of the variation in lava type, strength and deformation properties together with friction properties and dilation angles;

- All available rock property data for rock types associated with the VCR were collated and summarised.

- It was shown that large differences exist in the properties of the relevant strata, especially between hard (Alberton Porphyry Formation) and soft (Westonaria Porphyry Formation) lavas.
- No significant difference in rock properties was obtained for compression tests when loading was oriented either normal to stratification or parallel to strike or dip.

E) Assessment of the variability in fracture patterns and stope closure between geotechnical areas;

- A detailed monitoring programme was carried out at two sites in different geotechnical areas to determine differences in rock mass behaviour.
- The measurements and observations made in two different geotechnical areas showed that there are significant differences in: closure rates, 10 mm/day and 5 mm/day; and the amount of the deformation of the strata in the footwall and hangingwall that contributes to the total closure.
- General orientation of the mining induced stress fractures was investigated: in one case dipping between 45° and 55° towards the face in the hangingwall and in the other dipping towards the back area at angles of more than 80°.
- Measurements in the soft lava of the size and nature of falls of ground showed that in the soft lava they extend to heights of more than 1.2 m above the hangingwall and generally comprise relatively small blocks (0.3 m / 0.35 m / 0.4 m), whereas in the hard lava the equivalent figure for falls of ground is 1.8 m and they are made up of relatively few but large blocks (1.0 m / 1.1 m / 0.4 m).
- This finding on block size is of major significance to support design, particularly with respect to spacing of support units, the need for area coverage and the dimensions of load spreaders.

- It was shown that the amount of closure measured at a point in a stope is a function of the rate of face advance. Where the rate of face advance is high the closure rate, expressed in mm/day, is higher than if the face were advanced at a lower rate. However, if the rate is expressed in mm/m face advance, which is of significance to support design, the rates are substantially different. The results of this finding have been used to develop a modification to the Support Design Analysis (SDA) presented in the SIMRAC project GAP 032.

F) Numerical analyses to quantitatively understand rock mass behaviour:

- MINSIM-D modelling was used to compare actual closures recorded with the expected convergences. The results show that more inelastic behaviour is taking place in geotechnical areas with soft lava overlying Jeppestown shale than in areas with hard lava overlying quartzite-conglomerate.
- A mechanism that may account for the observed differences in mining induced stress fracturing, associated with different geotechnical conditions at Deelkraal, and East Driefontein Gold Mines, is illustrated. This is based on the hypothesis that the difference in modulus between hangingwall and footwall formations influences the position, relative to the stope horizon, at which the dip of fractures changes from towards the face to away from the face. However, in the FLAC numerical models exaggerated moduli values had to be used to achieve this effect.

G) Analysis of data from fatal accident inquiries (using the developed database):

- A database incorporating information gathered from the Department of Minerals and Energy (DME) on fatal accident inquiries from 1990 onwards

was used to calculate the cumulative percentages of rockfall thicknesses in VCR stopes. The height of 95 % of all fallouts is 1.2 m and 1.8 m for soft and hard lava hangingwalls, respectively.

- The equivalent figures for rockburst ejection thicknesses for soft and hard lava are 2.1 m and 1.8 m respectively. These figures were used to calculate overall support design criteria for soft and hard lava hangingwalls. These are
  - Soft lava: 33.0 kN/m^2.
  - Hard lava: 49.5 kN/m^2.
- The energy absorption criterion for dynamic loading at 3 m/s and to arrest the closure within 0.2 m for
  - Soft lava: 37.3 kJ/m^2.
  - Hard lava: 32.0 kJ/m^2.

  However, mines should calculate their own criteria based on local circumstances and should include an appropriate factor of safety.

H) Identification of a suitable approach to support design in VCR stopes.

Detailed monitoring and analysis of closure measurements carried out in this project have allowed the development of a modification to the support design methodology presented in the SIMRAC project GAP 032. This expresses the closure rate as a function of face advance rate. This methodology is thus available to rock engineers involved in support design on mines.

ACKNOWLEDGEMENTS

I would like to gratefully acknowledge that the work reported in this dissertation results from funding provided by SIMRAC (Safety in Mines Research Advisory Committee), project GAP102, (Improved support design by an increased understanding of the rock mass behaviour around the Ventersdorp Contact Reef, Rock Engineering Programme, CSIR: Division of Mining Technology). The constructive criticism and support of the SIMRAC Group Rock Mechanic Engineers is appreciated, and their permission to publish this work is gratefully acknowledged. This study would not have been possible without the support and co-operation of the management and staff of the East Driefontein, Deelkraal and Western Areas Gold Mines.

I am grateful to Mr WA Naismith, my supervisor, for giving me the opportunity to work on this project and for his patient guidance. I am also grateful for technical support and encouragement by Mr JK Schweitzer.

The project team of the GAP 102 project, especially, Mr MKC Roberts, Mr AJ Jager, Dr RA Eve, Mr GB Quaye and Mr J Glisson, are acknowledged for their contributions. Special thanks go to Dr RG Gürtunca for his continuous support.

In addition, grateful acknowledgements are given to Mrs C Langbridge for support in editing and Miss JB Collins for detailed drafting of the figures.

Contents **Page**

Declaration.. .. .. .

Chapter 3.....17

3 Geotechnical areas.. 17

3.1 Establishment of geotechnical areas.. 17

3.2 Geological discontinuities.. 21

Summary.. .. .. .22

Chapter 4.....24

4 Rock property tests.. .. .. .24

4.1 Rock property results for strata associated with the Ventersdorp Contact Reef.. 24

4.2 Uniaxial compressive strengths as deduced from point-load tests.. .. .. .32

Chapter 5.....36

5 Analysis of the rock mass behaviour as associated with Ventersdorp Contact Reef stopes.. 36

5.1 Ventersdorp Contact Reef study sites .. .. .36

5.1.1 East Driefontein Gold Mine.. 38

5.1.1.1 Mining induced stress fracture mapping.. .. .. .38

5.1.1.2 Closure-ride stations.. 44

5.1.1.3 Anomalous closure associated with seismicity.. 51

5.1.1.4 Extensometer stations.. .. .. .56

5.1.2 Deelkraal Gold Mine.. 60

5.1.2.1 Mining induced stress fracture mapping.. .. .. .60

5.1.2.2 Closure-ride stations.. 65

5.1.2.3 Extensometer stations.. .. .. .72

5.1.2.4 Analysis of falls of ground sizes.. 78

Chapter 6.....81

6 Numerical modelling.. .. .. .

8.2 Recommendations.. 142

References.. .. .. .144

Appendix A

Mining induced stress fracturing : East Driefontein Gold Mine.. 150

Appendix B

Mining induced stress fracturing : Deelkraal Gold Mine.. 155

List of Figures **Page**

Figure 1.1 Location of defunct (indicated by a star) and active VCR mines.. 2

Figure 2.1 Stratigraphic column of the Witwatersrand and the lower Ventersdorp Supergroups and the stratigraphic position of the VCR. (modified after SACS, 1980).. 8

Figure 2.2 VCR channels distribution in the southwestern portion of Vaal Reefs Gold Mine (after Chapman et al., 1986).. 9

Figure 3.1 Hangingwall plan of the VCR mines under consideration (West Rand and Carletonville Goldfields). Grey colour delineates area of "false" hard lava thickness due to erosion by Black Reef (Schweitzer, pers. comm.,1993).. .. ..

Figures 4.2 a and b Average UCS values for the hard and soft lavas and the various footwall rock types.. 29

Figures 4.3 a and b Average Young's Modulus values for the hard and soft lavas and the various footwall rock types.. .. .. .30

Figures 4.4 a and b Average Poisson's ratio values for the hard and soft lavas and the various footwall rock types.. 31

Figures 4.5 a to c Uniaxial compressive strength results of point-load tests of cores containing soft lava from Western Areas Gold Mine.. .34

Figures 4.5 a to c Continued.. .. .. .34

Figures 4.5 a to c Continued.. .. .. .35

Figure 5.1 Location of underground monitoring sites.. 37

Figure 5.2 VCR footwall plan of East Driefontein Gold Mine (Schweitzer, pers. comm.,1993).. 39

Figure 5.3 VCR hangingwall plan of East Driefontein Gold Mine (Schweitzer, pers. comm.,1993).. 40

Figure 5.4 Geotechnical area plan of East Driefontein Gold Mine (Schweitzer, pers. comm.,1993).. 41

Figure 5.5 Locality of underground monitoring site (32 Level 37 Line) at East Driefontein Gold Mine (Schweitzer, pers. comm.,1993).. 42

Figure 5.6 Attitude of mining induced stress fracturing at East Driefontein Gold Mine. The point of inflection is interpreted as to occur in the hangingwall of the excavation.. 43

Figure 5.7 The general panel layout, face position and location of each station at the monitoring site on 32 Level, 37 Line, No 4 Shaft, East Driefontein Gold Mine.. 45

Figures 5.8 a to d Closure rates at the permanent station (a), at the temporary stations at the bottom (b), middle (c) and top (d) of the face in West 4 panel, 32 Level, 37 Line, No 4 Shaft, East Driefontein Gold Mine.. .. .. .48

Figures 5.9 a to d Closure rates at the permanent station (a), at the temporary stations at the bottom (b), middle (c) and top (d) of the face in West 5 panel, 32 Level, 37 Line, No 4 Shaft, East Driefontein Gold Mine.. .. .. .49

Figures 5.10 a to d Closure rates at the permanent station (a), at the temporary stations at the bottom (b), middle (c) and top (d) of the face in West 6 panel, 32 Level, 37 Line, No 4 Shaft, East Driefontein Gold Mine.. .. .. .50

Figure 5.11. Panel layout and the positions of falls of ground (dotted area) in W4 panel, 32 Level, 37 Line, Eastdriefontein Gold Mine.. 51

Figures 5.12 a and b Extensometer results from the first borehole in the hangingwall (a) and the footwall (b) along West 5 gully, 32 Level, 37 Line, No 4 Shaft, East Driefontein Gold Mine.. 57

Figures 5.13 a and b Extensometer results from the second borehole in the hangingwall (a) and footwall (b) along West 5 gully, 32 Level, 37 Line, No 4 Shaft, East Driefontein Gold Mine.. 58

Figures 5.14 a and b Extensometer results from the borehole in the hangingwall (a) and in the footwall (b) along West 6 gully, 32 Level 37 Line, No 4 Shaft, East Driefontein Gold Mine.. 59

Figure 5.15 VCR footwall subcrop plan, Deelkraal Gold Mine (Schweitzer, pers. comm.,1993).. 61

Figure 5.16 VCR hangingwall plan of Deelkraal Gold Mine. Grey colour delineates area of "false" hard lava thickness due to erosion by Black Reef (Schweitzer, pers. comm.,1993).. 62

Figure 5.17 Geotechnical plan of Deelkraal Gold Mine (Schweitzer, pers. comm.,1993).. 63

Figure 5.18 Locality of underground monitoring site (Schweitzer, pers. comm.,1993) 64

Figure 5.19 Attitude of mining induced stress fracturing at Deelkraal Gold Mine. The point of inflection occurs in the footwall of the excavation.. 65

Figure 5.20 The general panel layout, face position, and location of each station at the monitoring site on 27 Level, 15 Line, Deelkraal Gold Mine.. 66

Figures 5.21 a to d Closure rates at the permanent station (a), and the temporary stations at the top (b), middle (c) and bottom (d) of the face in East 1 panel, 27 Level, 15 Line, Deelkraal Gold Mine.. 67

Figures 5.22 a to d Closure rates at the permanent station (a), and the temporary stations at the top (b), middle (c) and bottom (d) of the face in East 5 panel, 27 Level, 15 Line, Deelkraal Gold Mine... 68

Figures 5.23 a to d Closure rates at the permanent station (a), and the temporary stations at the top (b), middle (c) and bottom (d) of the face in East 4 panel, 27 Level, 15 Line, Deelkraal Gold Mine.. 69

Figures 5.24 a to d Closure rates at the permanent station (a), and the temporary stations at the top (b), middle (c) and bottom (d) of the face in East 3 panel, 27 Level, 15 Line, Deelkraal Gold Mine.. 70

Figures 5.25 a to c Closure rates at the permanent station (a), and the temporary stations at the top (b), and middle (c) of the face in East 1 panel, 27 Level, 15 Line, Deelkraal Gold Mine.. 71

Figure 5.26 Location of boreholes (shown as blue circles) and seismic events (shown as red crosses) on 27 Level, 15 Line, Deelkraal Gold.. 73

Figures 5.27 a and b Extensometer results from the borehole in the hangingwall (a) and footwall (b), East 1 gully, 27 Level, 15 Line, Deelkraal Gold Mine.. 74

Figures 5.28 a and b Extensometer results from the borehole in the hangingwall (a) and footwall (b), East 4 gully, 27 Level, 15 Line, Deelkraal Gold Mine.. 75

Figures 5.29 a and b Extensometer results from the borehole in the hangingwall (a) and footwall (b), East 3 panel, 27 Level, 15 Line, Deelkraal Gold Mine.. 76

Figures 5.30 a and b Position of fractures and borehole extensometers installed in the boreholes drilled in the hangingwall (a) and footwall (b) and in East 3 panel, 27 Level 15 Line, Deelkraal Gold Mine. Circled numbers refer to the number of fractures that were observed.. 77

Figure 5.31 Panel layout and the positions of falls of ground (grey area) in E3 panel, 27 Level, 15 Line, Deelkraal Gold Mine.. 78

Figure 5.32 Observed thicknesses of falls of ground in E3 panel, 27 Level, 15 Line, Deelkraal Gold Mine. *The thick red line delineates the average of all the* lines measured in this panel.. 80

Figure 6.1 Digitised plan showing the extent of mining on the VCR from August 1993 to April 1994, East Driefontein Gold Mine. The six coarse windows (C1-C6) are also shown.. 83

Figure 6.2 Fine window identifying mining steps at the monitoring site from August 1993 to April 1994, 32 Level, 37 Line, East Driefontein Gold Mine.. .. 83

Figures 6.3 a and b Comparison of MINSIM-D runs for different Young's Moduli, with actual underground measurements considering closure versus distance to face (a) and closure versus number of days (b).. 85

Figure 6.4 Digitised plan showing the extent of VCR mining from August 1993 to May 1994, 15 Line, Deelkraal Gold Mine. The positions of the coarse windows are also indicated.. 87

Figure 6.5 Fine window showing mining steps on the monitoring site from August 1993 to May 1994, 27 Level, 15 Line, Deelkraal Gold.. 87

Figures 6.6 a ω d Comparison of MINSIM-D runs for different Young's Moduli with actual measurements taken from underground, in the graphs of closure versus distance to face (a) and closure versus number of days (b).. 88

Figure 6.7 The basic model including position of grids, interfaces and boundary conditions.. 91

Figures 6.8 a and b Modelling results considering maximum principal stress around the stopes at East Driefontein (Fig. 6.8 a) and Deelkraal Gold Mines (Fig. 6.8 b).. 96

Figures 6.9 a and b Modelled maximum principal stress, the directions and angles of the calculated fracture around the model stope, East Driefontein Gold Mine, using the Mohr-Coulomb model.. 97

Figures 6.10 a and b Modelled maximum principal stress, and the directions and angles of the fracture around the model stope, East Driefontein Gold Mine, using the Mohr-Coulomb model. The hangingwall, footwall, and reef strengths were assumed to be 75 % softer than those measured in the laboratory.. .. .. .98

Figures 6.11 a and b Modelled maximum principal stress, the directions and angles of the calculated fracture around the model stope, Deelkraal Gold Mine, using the Mohr-Coulomb model.. 99

Figures 6.12 a and b Idealised stress-strain characteristics of soft lava hangingwall to use in strain-softening test for East Driefontein site.. .. .. .100

Figures 6.13 a and b Idealised stress-strain characteristics of Jeppestown shale footwall to use in strain-softening tests for East Driefontein site.. .. .. 1..

Figures 6.14 a and b Idealised stress-strain characteristics or hard lava hangingwall to use in strain-softening test for Deelkraal site.. 102

Figures 6.15 a and b Idealised stress-strain characteristics of quartzite-conglomerate footwall to use in strain-softening tests for Deelkraal site.. 103

Figures 7.1 a and b Typical support resistance deformation curves (Anon, 1988).. .. .. .108

Figure 7.2 Comparison of different support systems (Roberts, pers. comm., 1995).. .. .. .109

Figure 7.3 Different support systems with expected closure rate lines (Roberts, pers. comm., 1995).. 110

Figures 7.4 a and b Selection and design of stope support systems (Anon, 1988).. .. .. .111

Figures 7.5 a to c The force-deformation (a), support resistance-deformation (b) and energy absorption-deformation behaviour of profile props (Roberts, 1996).. 114

Figure 7.6 Energy-deformation curve showing the decrease in energy absorption ability with increasing deformation (Roberts, 1996).. 116

Figure 7.7 The support resistance-deformation curve, as a function of stope closure and distance behind the stope face props (Roberts, 1996).. 117

Figure 7.8 The support resistance-deformation curves of various support systems, as a function of stope closure and distance behind the stope face, for the face and permanent support areas (Roberts, 1996).. 117

Figure 7.9 Energy absorption-deformation curve as a function of stope closure and distance behind the stope face props (Roberts, 1996).. 118

Figure 7.10 Determination of critical velocity (V_c) using an energy-deformation curve as a function of stope closure and distance behind the stope face (Roberts, 1996).. 119

Figure 7.11 Critical velocity variation for a constant energy absorption capability (Roberts, 1996).. 120

Figure 7.12 Comparison of critical velocities (V_c) for various support systems with different energy absorption ability as a function of stope closure and distance behind the stope face (Roberts, 1996).. .. .. .121

Figure 7.13 Analysis of fallout thicknesses in VCR stopes with soft lava hangingwall from 1990 to 1995 (Source: RSA, DME, 1996).. 123

Figure 7.14 Analysis of fallout thicknesses in VCR stopes with hard lava hangingwall from 1990 to 1995 (Source: RSA, DME, 1996).. .. .. .124

Figure 7.15 Analysis of rockburst ejection thicknesses in VCR stopes with soft lava hangingwall using data from 1990 to 1995 (Source: RSA, DME, 1996).. .. ..

Figure 7.16 Analysis of rockburst ejection thicknesses in VCR stopes with hard lava hangingwall using data from 1990 to 1995 (Source: RSA, DME, 1996).. 126

Figure 7.17 The equation for the linear line in the graph of deformation versus distance behind the stope face (the fourth quadrant) in the defined SDA.. 129

Figure 7.18 Closure measured in the closure-ride station installed in the face area at the middle of the West 5 panel, East Driefontein Gold Mine, 32 Level, 37 Line. R^2=0.985.. 131

Figure 7.19 Graph showing the relationship between average face advance per month versus the value of "slope" for five closure-ride stations analysed with the best fit line having a correlation factor of 0.86.. 132

Figure 7.20 The calculated relationship between closure and average face advance in a stope with soft lava hangingwall in East Driefontein Gold Mine, 32 Level 37 Line.. 133

Figure 7.21 The graph showing the relationship between average face advance per month and the value of "slope", the best fit line has a correlation factor of 0.82.. 135

Figure 7.22 Calculated relationship between closure and average face advance in a stope with hard lava hangingwall in Deelkraal Gold Mine, 27 Level 15 Line.. 135

Figure 7.23 A summary of energy absorption criterions for soft lava and hard lava hangingwalls for different face advance rates.. 136

Figure 7.24 The effect of different face advance rates on the amount of closure experienced at a particular distance behind the face and hence amount of available energy to be absorbed by the support system.. .. .. .137

List of Tables **Page**

Table 1.1 VCR production during 1992 (Annual Reports).. 3

Table 2.1 Number of tests obtained from CSIR Mining Technology test laboratory considering the mines of the Gold Fields Group.. .. .15

Table 2.2 Average uniaxial compressive strength (MPa) analyses considering samples with known position and geological information (Group A) from Kloof Gold Mine.. .. .. .15

Table 2.3 Average rock property analyses considering samples where geological information is available (Group B).. .. .. .16

Table 3.1 Approximate percentages of geotechnical areas as per individual VCR mine.. 21

Table 4.1 Average uniaxial compressive strength values. The numbers in brackets indicate the number of analyses.. 26

Table 4.2 Average Poisson's ratios. The numbers in brackets indicate the number of analyses.. 27

Table 4.3 Average Young's Modulus values. The numbers in brackets indicate the number of analyses.. .. .. .28

Table 6.1 Summary of input values as utilised during MINSIM-D modelling for the East Driefontein Gold Mine site.. 84

Table 6.2 Summary of input values considering during the MINSIM-D modelling for the Deelkraal Gold Mine.. .. .. .86

Table 6.3 Material properties used during the numerical modelling. 93

Table 7.1. Summary of rock related (rockburst and rockfall) fatalities on South African tabular gold mines that occurred during last six years from 1990 to 1995 (Source: RSA, DME, 1996). 123

Table 7.2 The fallout thickness for the 95 % frequency level and the associated support resistance criteria for VCR soft and lavas.. 124

Table 7.3 The minimum energy absorption requirements per m^2 of soft lava hangingwall.. 127

Table 7.4 Minimum energy absorption requirements per m^2 of hard lava hangingwall.. 127

Table 7.5 The fallout thickness for the 95 % frequency level and the associated energy absorption criterion for VCR soft and lavas.. .. ..

List of Photographs **Page**

Photograph 5.1 Damage observed on packs installed along the gully of West 4 panel, 32 Level, 37 Line, East Driefontein Gold Mine (number 1 indicates the direction of this picture in Fig. 5.11).. .. .. .53

Photograph 5.2 Observed local fall of ground in West 4 panel due to a seismic event occurred. The hangingwall blocks were small and very fragmented (number 2 indicates the direction of this picture in Fig. 5.11).. .. .. .53

Photograph 5.3 Damage observed on the gully packs due to a seismic event occurred in West 4 panel, 32 Level, 32 Line, East Driefontein Gold Mine (number 3 indicates the direction of this picture in Fig. 5.11).. .. .. .54

Photograph 5.4 A downdip view of damage observed on the gully packs due to a seismic event occurred in West 4 panel, 32 Level, 32 Line, East Driefontein Gold Mine (number 4 indicates the direction of this picture in Fig. 5.11).. 54

Photograph 5.5 Damage of seismic event on another pack installed next to gully of West 4 panel, 32 Level, 37 Line, East Driefontein Gold Mine (number 5 indicates the direction of this picture in Fig. 5.11).. .. .. .55

Photograph 5.6 *Observed damage due to a seismic event on another pack installed next to gully of West 4 panel, 32 Level, 37 Line, East Driefontein Gold Mine (number 6 indicates the direction of this picture in Fig. 5.11).. .. .. .55*

Photographs A1 and A2 Fractures observed in hangingwall along West 6 Gully in 32 Level 37 Line at # 4 shaft, East Driefontein Gold Mine. The arrow shows the direction of mining operations.. 151

Photographs A3 and A4 Fractures observed in footwall along West 6 Gully in 32 Level 37 Line at # 4 shaft, East Driefontein Gold Mine. The arrow shows the direction of mining operations.. 152

Photographs A5 and A6 Fractures observed in hangingwall in West 5 Stope in 32 Level 37 Line at # 4 shaft, East Driefontein Gold Mine. The arrow shows the direction of mining operations.. 153

Photographs A7 and A8. Fractures observed in hangingwall in West 7 Stope (above) and in West 6 Stope (below) 32 Level 37 Line at # 4 shaft, East Driefontein Gold Mine. The arrow shows the direction of mining operations.. 154

Photographs B1 and B2 Fractures observed in hangingwall in East 1 panel on 27 Level 15 Line Deelkraal Gold Mine. The arrow shows the direction of mining operations.. 156

Photographs B3 and B4 Fractures observed in hangingwall in East 5 panel on 27 Level 15 Line Deelkraal Gold Mine. The arrow shows the direction of mining operations.. 157

Photographs B5 and B6. :Fractures observed in hangingwall and footwall along East 4 panel and fractures in hangingwall in East 4 panel on 27 Level 15 Line Deelkraal Gold Mine. The arrow shows the direction of mining operations.. 158

Photographs B7 and B8. :Fractures observed in hangingwall in East 3 panel and East 2 panels on 27 Level 15 Line Deelkraal Gold Mine. The arrow shows the direction of mining operations.. .. .. .159

CHAPTER 1

1 INTRODUCTION

In 1993, Gold Fields of South Africa contracted the CSIR: Mining Technology, through the Chamber of Mines of South Africa, to investigate the rock mass behaviour associated with the Ventersdorp Contact Reef (VCR). In 1994 the remaining five mining houses joined the VCR Project through SIMRAC, which led to the consideration of 12 mines mining the VCR.

1.1 PROBLEM DEFINITION

In the West Rand and Carletonville goldfields, the VCR is the main gold producing orebody, contributing about 15 % to the total annual gold production of South Africa. The VCR is mined at 12 major gold mines situated in the Klerksdorp, Carletonville and West Rand mining districts (Fig. 1.1). Seven mines under Gold Fields of South Africa Limited management, GFSA, (situated within the West Rand and Carletonville areas), three mines of Anglo American Corporation of South Africa Limited, AAC, (situated within the Carletonville and the Klerksdorp areas), two mines of General Mining, Metals and Minerals Limited, GENMIN, (situated within the Klerksdorp area, closed recently), three mines of Johannesburg Consolidated Investment Limited, JCI, (situated within the West Rand) and one mine under management of First Wesgold Mining, FWM, (situated within the West Rand area) are considered. Currently, GFSA and AAC derive a tonnage of approximately 73 % and 23 % (Annual Reports of related mines), respectively, of their total tonnage from the VCR (Table 1.1). This is likely to increase in the future, predominantly sourced from greater depths.

Previously, rock engineering research with respect to gold mine stoping has been primarily directed towards understanding the behaviour of stratified quartzite rocks surrounding reefs such as the Carbon Leader and the Vaal Reef. Little attention was given to the stratigraphy associated with VCR stopes, which have an unbedded, jointed lava hangingwall.

The potential geotechnical differences between the VCR and the older Witwatersrand orebodies, e.g. closure rates, contribution of hangingwall and footwall to the total closure, sizes of falls of ground and responses to seismicity, can, to a large extent, be attributed to the geological setting. Shales, quartzites or conglomerates comprises the footwall of the VCR. The hangingwall consists of several types of lavas. The various rock types encountered within the footwall and hangingwall exhibit different rock strengths and natural fracture patterns, which control the behaviour of the hangingwall. It is therefore important that the rock mass behaviour of VCR stopes is well understood to facilitate rock mechanics and support system design.

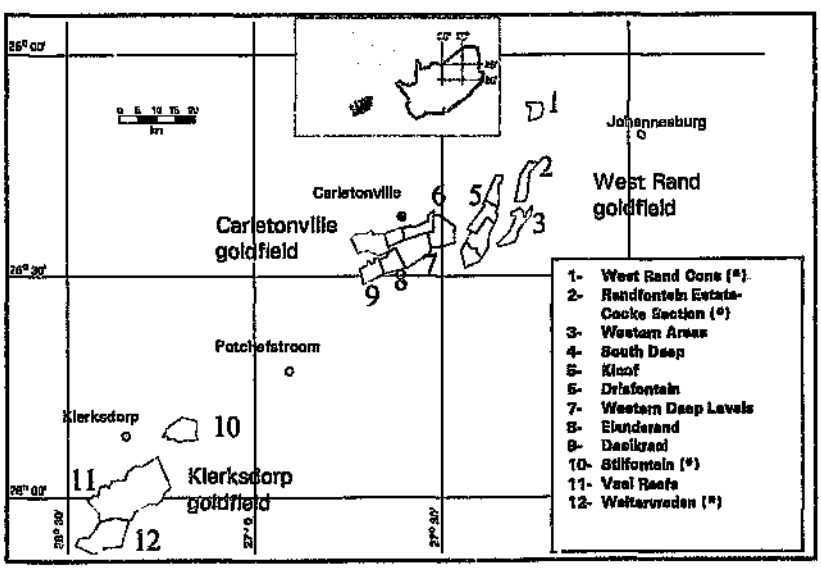

Figure 1.1. Location of defunct (indicated by a star) and active VCR mines.

Table 1.1. VCR production during 1992 (Annual Reports).

MINE HOUSE		TOTAL VCR (t)	TOTAL PRODUCTION (t)	% VCR OF TOTAL (%)
GFSA	DEELKRAAL G.M.	1 149 588	1 183 636	97
	EAST DRIEFONTEIN G.M.	2 515 000	3 485 000	72
	WEST DRIEFONTEIN G.M.	3 267 000	5 447 000	60
	LEEUDOORN G.M.	802 000	802 000	100
	KLOOF G.M.	3 259 000	3 436 000	95
	VENTERSPOST G.M.	249 000	1 115 000	22
	Sub Total	**11 231 588**	**15 468 636**	**73**
AAC	VAAL REEFS G.M.	202 000	24 312 000	0.8
	WESTERN DEEP LEVELS G.M.	2 926 000	5 790 000	51
	ELANDSRAND G.M.	4 836 000	4 836 000	100
	Sub Total	**7 963 000**	**34 938 000**	**23**

1.2 AIMS AND OBJECTIVES

The main expectation in the definition of geotechnical areas by combination of different hangingwall and footwall of the reef may potentially result in various rock mass behaviour around the VCR stopes, therefore influencing support strategies.

This study had two main objectives: firstly, to improve the understanding of the controls that rock strength and natural fracture patterns have on hangingwall failure modes in order to provide the basis for the development of a conceptual model for rock mass behaviour around VCR stopes. Secondly, this study aimed to improve safety and to reduce production losses due to rockfalls and rockbursts through application of the knowledge gained on VCR stopes to the design of efficient support systems for static and dynamic conditions.

Understanding of the rock mass behaviour around the VCR excavations is a prerequisite to make support recommendations. In order to achieve these goals, the following analyses and studies were undertaken:

1- collation and review of all past rock engineering work undertaken on the VCR by means of a literature survey,

2- definition of geotechnical areas,

3- evaluation of the variation in lava type, strength and deformation properties together with friction properties and dilation angles,

4- identification and documentation of fracture patterns as present in different geotechnical areas in VCR stopes,

5- determination of the variability in stope closure by means of closure stations and extensometers,

6- numerical analysis to quantitatively understand rock mass behaviour.

7- application of findings to VCR support design methodology.

CHAPTER 2

2 LITERATURE REVIEW

2.1 ORIGIN OF THE NAME: VENTERSDORP CONTACT REEF

In 1937, the first reference to the "Ventersdorp Contact Reef (VCR)" was published by Pelletier (1937) who stated that "We have given the name of Ventersdorp Contact Reef to a reef which occurs at the base of the Ventersdorp lava".

De Kock (1940) indicated that the name VCR is applied to a conglomerate layer, which occurs at the base of the Ventersdorp System. It owes its preservation to the outpouring of the lavas and can be regarded as a basal conglomerate of the Ventersdorp System. He also emphasised that the term "Contact Reef" has no significance in the sense of pyrometasomic or pyrometamorphic deposits. Its coupling with "Ventersdorp" is not intended to convey genetic affinity with the Ventersdorp magmatic event, which has definitely not contributed any gold and is responsible only for small additions of volcanic ash to the matrix of the reef. The name in summary was originally chosen to indicate the stratigraphic position of the reef at the contact between the Ventersdorp and Witwatersrand Systems and also to distinguish it from a true Witwatersrand Banket (De Kock, 1940).

2.2 THE VENTERSDORP CONTACT REEF: HISTORY OF MINING

Mining of the VCR has contributed significantly to the Klerksdorp Goldfield production. Although most mining was from the south-western part of the present Vaal Reefs Mine, i.e. Vaal Reefs West, other promising values were exposed (Chunnett, 1994).

De Kock (1940) indicated that the VCR was worked as far back as 1889, on the property of the New Steyn Estate Gold Mines Limited, Klerksdorp area. There, it was known as the Steyn Estate or Contact Reef, while the VCR was assumed to be the equivalent of the Randfontein Leader or South Reef at Western Rand Estates Limited. Chapman et al., (1986) reported that the Orkney mine in the Klerksdorp area first started in 1888 and closed due to collapse of the local stock market. In 1891 the Orkney mine was restarted on reefs which were later identified as Elsburg and VCR and Klerksdorp Gold Estates mine was opened. The Nooitgedacht had increased its battery to sixty stamps in 1890 and in 1891 started acquiring other small mines such as the Klerksdorp, the Argosy, the Foxdale, and the New Nooitgedacht. The VCR was also worked by the Luipaards Vlei Estate and Gold Mine Corporation Limited, where it was known as the Montana Reef, and by the Lincoln Gold Mines on a few claims formerly held by a Mr. Le Roux on the eastern boundary of the Randfontein Mine (De Kock, 1940).

Chunnett (1994) reported that the discovery of the VCR was intimately linked to the events that followed George Harrison's discovery of the Main Reef on Langlaagte early in 1886. History shows that, by the end of 1886, the Central, East and West Rand, and Klerksdorp areas were all a hive of activity. He also indicated that, although the prime target was the exceptionally rich Main Reef, other reefs including the VCR were found, explored and, in some cases, mined. The VCR was not regarded as the primary economic reef in the first mines to be opened along the West Wits Line, with the Middelvlei and Carbon Leader Reefs east and west of the Bank Fault, respectively, being the prime targets. However, the VCR certainly played an important part in establishing the Venterspost, Libanon, West Driefontein, Western Areas and particularly Western Deep Levels Gold Mines. Drilling and development provided information which led to the elucidation of the pre-Ventersdorp Contact Reef geomorphological characteristics across several areas, and this resulted in the opening of Kloof (in 1968) and East Driefontein Gold Mining Companies, while the Deelkraal

and Elandsrand mines, which derive the vast majority of their income from the VCR, started some 10 years later. The incorporation of the North Driefontein lease area into Driefontein Consolidated and the establishment of the Leeudoorn Gold Mine is the latest evidence of the foresight of the pioneers who had confidence in the economic potential of this reef horizon.

2.3 GEOLOGICAL STUDIES

De Kock (1940) proposed that the VCR represents the erosional product of the immediately underlying Witwatersrand formation during the period which intervened between the deposition of the Witwatersrand System and the outpouring of the Ventersdorp lavas. The bulk of its constituent materials, such as the pebbles, the larger quartz particles of the matrix and the gold, was undoubtedly derived from the Witwatersrand beds and collected on the old land surface in the form of a thin layer of eluvial scree which accumulated in thicker alluvial sheets in depressions, valleys and stream beds. In the more deeply scooped out portions of the land surface there is evidence of successive layers of conglomerate being washed in, frequently separated by layers of sand, sandy tuff or tuff. De Kock (1940) emphasised that, during the initial diastrophic phase or phases of the eruptions which culminated in the extrusion of the Ventersdorp lavas, a certain amount of tuffaceous material was deposited over the existing land surface to become intermingled with the relatively coarse surface debris on which it fell.

Nicolaysen et al., (1963) have reported that the sediments of the Witwatersrand Basin were formed between 2895 and 2700 Ma, a time frame given by Barton et al., (1986) and Armstrong et al., (1986). The stratigraphic position of the VCR is shown in the South African Handbook of Stratigraphy, (1980), (Fig. 2.1).

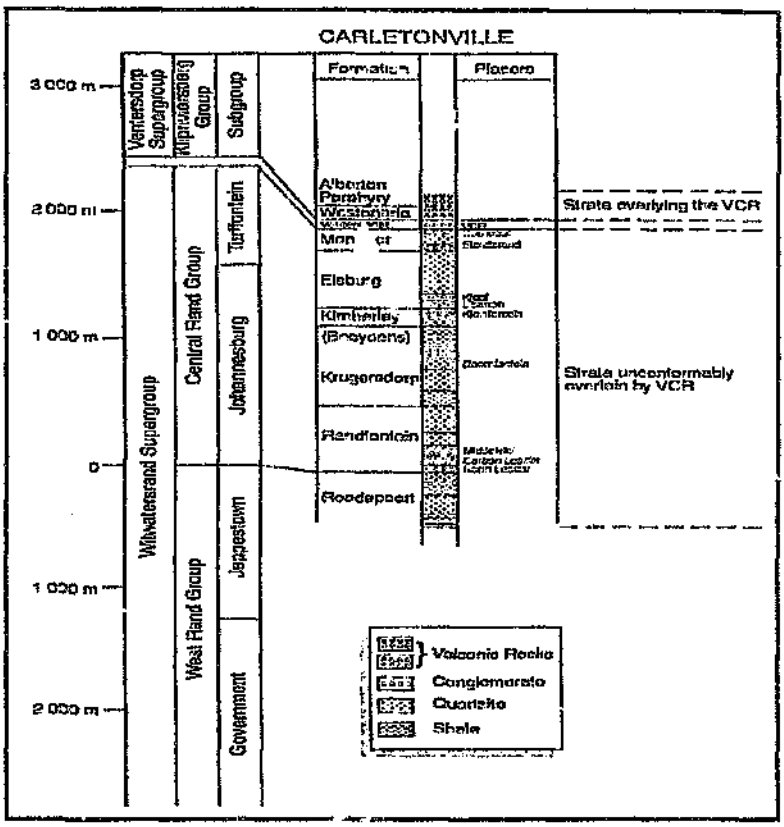

Figure 2.1. Stratigraphic column of the Witwatersrand and the lower Ventersdorp Supergroups and the stratigraphic position of the VCR. (modified after SACS, 1980).

Along the north-western margin of the Witwatersrand Basin, from Krugersdorp to Klerksdorp, an angular unconformity with up to 5 degrees discordance has been recognised together with block faulting that produced grabens and half grabens (Tankard et al., 1982). Unconformities that strike obliquely to those in the Central Rand Group were initiated during late Witwatersrand times.

The VCR rests with an angular unconformity on the Witwatersrand deposits and is conformably overlain by volcanic flows of the Ventersdorp Supergroup

(Turner, 1979). As a result of this unconformable relationship between the VCR and its underlying beds, the VCR truncates up to 3000 m of upper and lower Witwatersrand stratigraphy, which could correspond to a paleoslope distance of 27 km (Schweitzer et al., 1994). Like the Central Rand Group reefs, the VCR is an auriferous, uraniferous, pyritic, oligomictic conglomerate (Chapman et al., 1986). Similarities to the West Rand Group reefs with respect to its deposition, in that there is a marked channel development, resulting in a Channel Facies and a Terrace Facies, do exist. The Terrace Facies generally represents a thin band (maximum 80 cm) with generally poor gold values, with the Channel Facies reaching channel widths of up to 7 m in thickness (Fig. 2.2, Chapman et al., 1986).

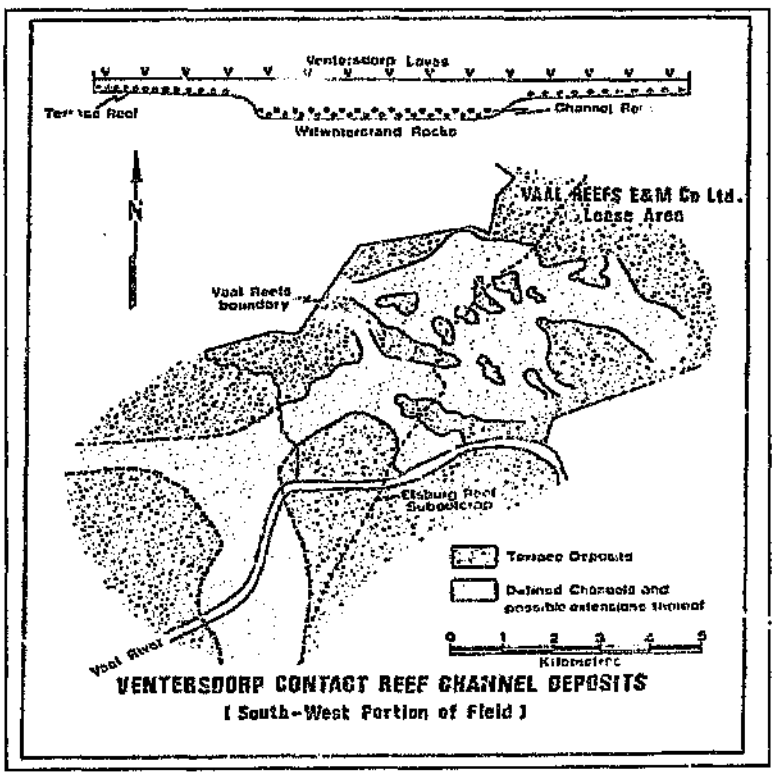

Figure 2.2. VCR channels distribution in the southwestern portion of Vaal Reefs Gold Mine (after Chapman et al., 1986).

The contact between the VCR and the Ventersdorp lava at Western Deep Levels Gold Mine is irregular (Knowles, 1966). For example, pillow structures developed in the basal lavas deformed the underlying reef. The presence of pillow lavas indicates that certain areas of the VCR were under water when the first lava flowed over the landsurface. The weight of the initial lava forced the top portion of the unconsolidated VCR into the voids between the pillows, giving rise to this irregular contact between the VCR and the Ventersdorp lava (load casting). Pillows may be up to 1 m in size. Adjacent pillows are separated from one another by loose, unconsolidated brecciated material, which has, at a later stage, been infilled by vein quartz. Adjacent pillows are, therefore, separated by reef pinnacles. Pillows only become detached under certain conditions and good cohesion occurs between the chilled skins of adjacent pillow structures. Hangingwall instability occurs when reef pinnacles and large amounts of inter-pillow breccia are present.

Metamorphism played an important role in the history of the reefs within the Witwatersrand Supergroup resulting in considerable changes in composition, grain shape and size.

2.4 ROCK ENGINEERING STUDIES

Rock engineering research with respect to gold mine stoping has been, prior to this study, primarily directed towards understanding the behaviour of stratified quartzite rocks surrounding reefs (e.g. Carbon Leader and Vaal Reef). Little attention was given to the rocks associated with VCR stopes, which have an unbedded, jointed lava hangingwall.

The frequency and magnitude of rockbursts are a function of, mainly, the nature and geological discontinuities, the associated footwall and hangingwall rock types, and the type of stope layout. Roberts and Jager

(1991) analysed all rock related accidents on South African gold mines during 1990 and reported that, in three major gold mining regions, namely the Far West Rand, the Orange Free State and the Klerksdorp regions, a total of 226 fatalities related to rockbursts (52 %) and rockfalls (48 %) occurred. Of fatalities recorded in the Far West Rand, where predominantly VCR is mined and both scattered longwall and longwall mining are practised, 91 resulted from rockbursts (87 %) and rockfalls (13 %). Roberts and Jager (op. cit.) also emphasised that in the Far West Rand the face support systems in use were inadequate to prevent rockburst damage.

There have been only a few rock engineering studies on the VCR, and most studies viewed the rock engineering aspects associated with the mining of Witwatersrand orebodies regionally. Gürtunca and Adams (1991), for example, argued that the rock mass, for modelling purposes, may generally be assumed to be a homogeneous isotropic elastic body, with the influence of joints, geological discontinuities, and different strata to be considered. They, furthermore, propose that three major factors affect the overall response of the rock mass to mining, also causing the documented differences between profiles of measured and modelled closure. These factors are: joints in the rock mass; strata having different mechanical properties and inelastic behaviour such as fracture, dilation; and bed separation. Gürtunca and Adams (1991) also reported that differences in geological stratigraphy in the Central Rand, West Rand, and the Orange Free State goldfields influence rock mass behaviour. The rock mass response varied due to different orientations and spacing of joints as well as values of Young's Modulus for the strata. These values were derived by comparing the actual underground measurements with the results obtained from MINSIM-D elastic modelling and are: Carletonville, 52 GPa; Klerksdorp, 35 to 40 GPa; and the Orange Free State, 30 to 35 GPa.

A study at a depth of 2150 m, considering the VCR at Western Deep Levels (WDL), revealed that cemented backfill can be used for local and regional

support in areas of high (4 m) stoping width (York and Squelch, 1992, Gürtunca et al., 1993). Cemented backfill provided an almost immediate resistance to closure, was considered to be stiff, and showed little or no shrinkage. Clamping of the hangingwall occurred at vertical stresses of less than 2 MPa, which is less than the stresses measured in quartzite hangingwalls. This was assumed to be due to limited inelastic closure in the VCR hangingwall as a result of smaller dip spans and lack of bedding planes (York and Squelch, 1992; Gürtunca et al., 1993). MINSIM-D elastic modelling showed that degradation of the laboratory modulus, to values in the range of 45-50 GPa, was necessary to reproduce observed closures. This suggests that a significant component of inelastic closure is present, a feature similar to reefs with stratified quartzite rocks, in both the hangingwall and footwall.

The VCR at Western Deep Levels South Mine (WDL-S) is underlain by quartzites which are generally well bedded with intact-rock uniaxial compressive strengths of between 200 to 250 MPa (Gürtunca et al., 1993). At the same time Ventersdorp lavas comprise the hangingwall. These are exceptionally strong and stiff, having a compressive strength in excess of 300 MPa, and a modulus of approximately 110 GPa. The lavas often contain discontinuities at 0,5 to 1 m intervals, which are intersected by several sets of weakly cohesive, steeply inclined quartz-filled joints. The combination of these leads to blocky and joint-bounded rockfalls in the stopes. In the same study, it was also reported that the values of in situ modulus compared well with the values quoted by Gürtunca and Adams (1991), and McKinnon (1989). These estimated 52 GPa for the in situ rock mass modulus from measurements in the Carbon Leader Reef at Western Deep Levels, and the Main Reef at East Rand Proprietary Mine (ERPM). The same in situ rock mass modulus was therefore used for the VCR and Carbon Leader Reef, despite the greater material stiffness of most of the VCR lava hangingwall. Nevertheless, Gürtunca et al., (1993) argued that closure

associated with the VCR hangingwall was significant (not merely elastic), confirming the findings of York and Squelch (1992).

In situ stress measurements on the VCR at Kloof Gold Mine using the "doorstopper" technique were taken at a depth of 2957 m below surface, in the vicinity of a strike stabilising pillar (Smith and Vlietstra, 1992). There the VCR is under-and overlain by quartzite and porphyritic lavas, respectively. Nine laboratory tests, three uniaxial and six triaxial at confining stresses of 10 MPa, 20 MPa and 40 MPa, were completed for the footwall quartzites. Average values of the quartzite strength properties, i.e. uniaxial compressive strength (185 MPa), Poisson's ratio (0.21±0.009) and Young's Modulus (70±14.4 GPa), were obtained. Petroscoping of holes drilled in sidewalls indicated the following fracture frequency:

10 fractures / m at 0.0 to 1.0 m.
5 fractures / m at 1.0 to 2.0 m.
3-4 fractures / m at 2.0 to 5.0 m.

Subsequently, Vlietstra (1995) carried out in situ stress measurements using the same technique at two further sites at Kloof Gold Mine, in gritty footwall quartzite, 17 m beneath the VCR stope. On the basis of uniaxial tests, an average secant Young's Modulus of 81.6 GPa and 70.2 GPa, and average Poisson's ratios of 0.19 and 0.16 were used for data reduction at two sites. The maximum stress measured was 36 MPa which is equivalent to a depth of 1300 m, indicating that it was likely that complete closure had taken place in the stope, allowing transmission of stress through the stope. Such closure would give some relief to stabilising pillars that are functioning as regional support.

2.4.1 Previous rock property analyses

The establis ment of the rock engineering properties of the VCR and associated stratigraphy is required to determine conceptual models of rock

mass behaviour. A considerable number of rock engineering tests on rock material associated with the VCR has been undertaken in the past. However, most records are incomplete as detailed locations and other information pertaining to the samples are not available. Using the information provided by the mines and data from the CSIR: Mining Technology test laboratory, three categories are defined :

Group A: Geological information and locality are known,
Group B: Geological information is available but locality is unknown,
Group C: Both geological information and locality are unknown.

The information for Groups A and B (Table 2.1) is summarised in Tables 2.2 and 2.3. It is noted that major differences in the rock properties exist between the hard (e.g. UCS exceeding 300 MPa) and soft lava (e.g. UCS less than 150 MPa) (Table 2.3). It is in addition concluded that little rock engineering information concerning the VCR is available. The rock mass behaviour around VCR excavations is consequently not well defined and understood. It is important to establish in detail all different rock strength parameters (e.g. UCS, Poisson's ratio and Young's Modulus) controlling the mode of failure of the hangingwall and footwall. These failure criteria are the major parameters in support design.

In summary: the literature review reveals that, prior to 1992, several geological and few rock engineering studies had been performed. Most of the rock engineering studies were directed towards the understanding of reefs with stratified quartzitic surroundings. The rock mass behaviour associated with the VCR is ill understood due to limited rock engineering work. The rock mass behaviour and associated rock engineering properties of the stratigraphy associated with the VCR are undocumented, despite their importance for support design.

Table 2.1. Number of tests obtained from CSIR: Mining Technology test laboratory considering the mines of the Gold Fields group.

		Uniaxial Compressive Strength Test	Triaxial Compressive Strength Test	Brazilian Test	Indentation Test
DEELKRAAL	A	-	-	-	-
	B	15	22	-	1
	C	-	-	-	-
WEST DRIEFONTEIN	A	-	-	-	-
	B	4	4	3	-
	C	5	2	1	-
EAST DRIEFONTEIN	A	-	-	-	-
	B	3	4	-	-
	C	5	6	-	3
KLOOF	A	22	-	-	-
	B	5	7	3	5
	C	14	4	2	2
LIBANON	A	-	-	-	-
	B	-	-	-	7
	C	-	-	-	-
DOORNFONTEIN	A	-	-	-	-
	B	12	-	-	-
	C	-	-	-	-

Table 2.2. Average uniaxial compressive strength (MPa) analyses considering samples with known position and geological information (Group A) from Kloof Gold Mine.

UNIAXIAL COMPRESSIVE STRENGTH TESTS (MPa)	KLOOF GOLD MINE							
	A	A	A	A	A	A	A	A
	Booysens shale	Elsburg quartzite	Jeanette Formation	Edenville Formation	Alberton Formation	Westonaria Formation	Orkney Formation	Loraine Formation
Maximum Stress (MPa)	156	181	604	208	341	151	598	404
Number of Analysis	3	4	1	6	4	4	6	1

Table 2.3. Average rock property analyses considering samples where geological information is available (Group B).

UNIAXIAL COMPRESSIVE STRENGTH TESTS	DEELKRAAL		WEST DRIEFONTEIN		EAST DRIEFONTEIN			DOORNFONTEIN	WESTERN DEEP LEVELS		KLOOF
	B		B		B			B	B		B
	Hard Lava	Mondeor quartzite	Middle square pebble quartzite	Square pebble quartzite	Upper Jeppestown shale	Square pebble quartzite	Jeppestown shale	Jeppestown shale	Booysens shale	Hard Lava	Rietgat Formation
Max. Stress (MPa)	341	191	183	187	184	159	180	186	166	316	210
Yield Point (MPa)	-	172	-	-	-	-	-	-	84	250	-
Young's Modulus (GPa)	81	66	69	58	48	43	67	55	92	117	71
Inferred shear strength (MPa)	48	41	41	39	43	17	25	-	34	-	42
Calculated UCS from regression analysis (MPa)	330	193	185	192	185	148	182	-	140	-	208
Number of analysis	6	28	6	5	1	1	1	17	7	15	11

BRAZILIAN TESTS											
Max. Stress (Tensile) (MPa)	-	-	-	18.62	-	-	-	-	-	-	18.62
Number of analysis	-	-	-	8	-	-	-	-	-	-	8

ORIENTATION TESTS											
Load @ 1st break (kN)	48.2	-	-	-	-	-	-	-	-	-	28.52
Penetration @major break (mm)	0.79	-	-	-	-	-	-	-	-	-	0.74
Number of analysis	2	-	-	-	-	-	-	-	-	-	10

CHAPTER 3

3 GEOTECHNICAL AREAS

Geotechnical areas are areas which are expected to have different rock mass behaviour. The main motivation behind defining "geotechnical areas" is the expectation that different combinations of rock types in the hangingwall and footwall of the reef may potentially result in different rock mass behaviour around the tabular excavation. If proven this will influence support and mining strategies.

3.1 ESTABLISHMENT OF GEOTECHNICAL AREAS

The various geotechnical areas were identified by using information which was provided by the Geology Departments of mines. These geotechnical areas are defined by superimposing the various groups of footwall and hangingwall rock type assemblages with similar mechanical properties.

The hangingwall lavas are of two types, the "hard" (Alberton Porphyry Formation) and "soft" (Westonaria Formation). In view of the large differences in mechanical properties (Tables 2.2 and 2.3), these are referred to as the "hard" and "soft" lavas (Fig. 3.1).

The major footwall lithologies underlying the VCR are Booysens and Jeppestown shales, quartzite and conglomerate. Quartzite and conglomerate are treated as "one" rock type for the delineation of geotechnical areas, because they are proposed to have the same rock engineering properties (Fig. 3.2). Overall, six geotechnical areas are defined for the mines in the West Rand and Carletonville areas (Fig. 3.3).

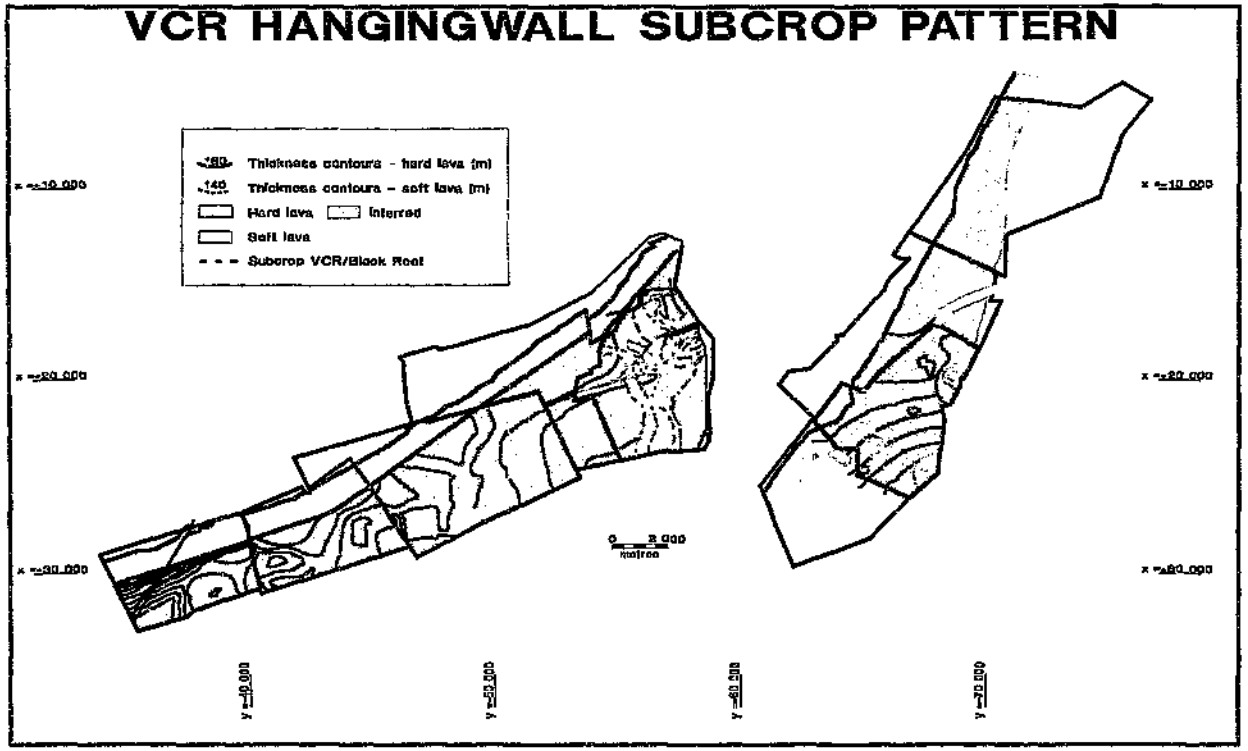

Figure 3.1. Hangingwall plan of the VCR mines under consideration (West Rand and Carletonville goldfields). Grey colour delineates area of "false" hard lava thickness due to erosion by Black Reef (Schweitzer, pers. comm.,1993).

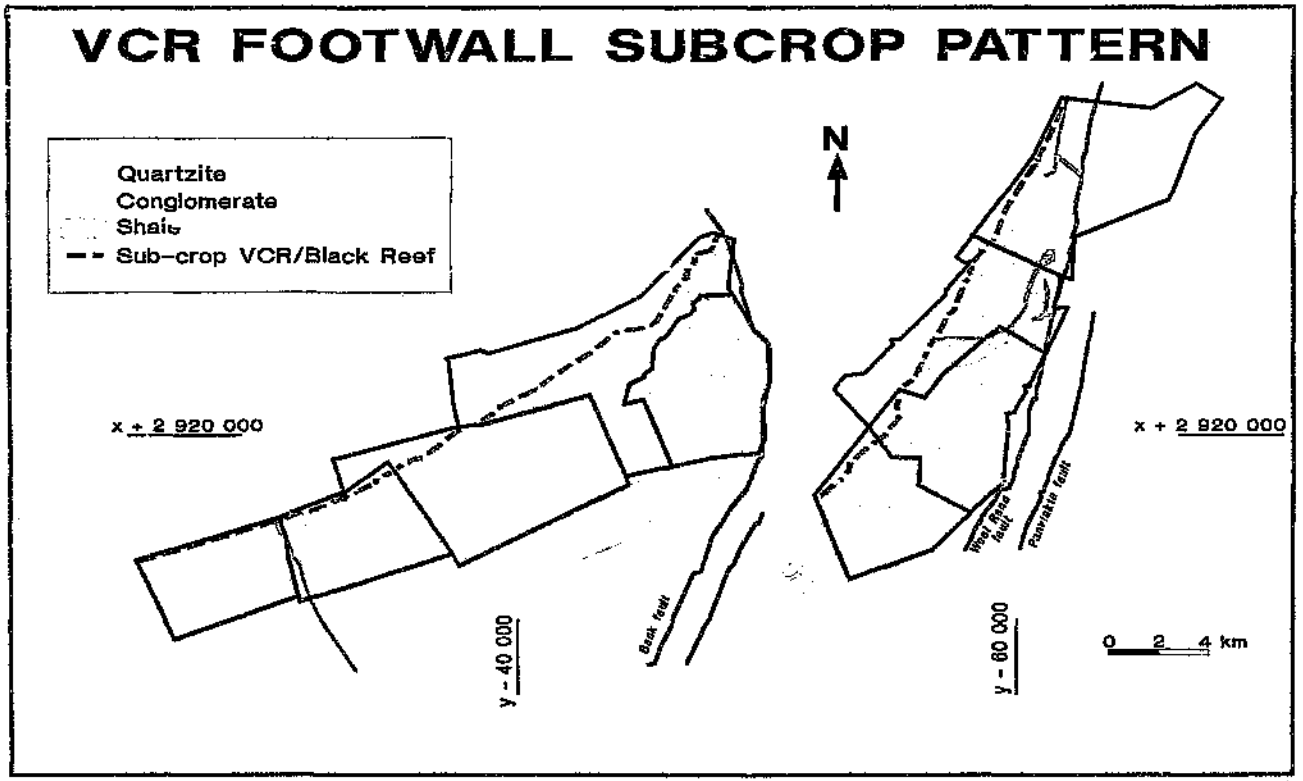

Figure 3.2. Footwall plan of the VCR mines under consideration (West Rand and Carletonville goldfields) (Schweitzer, pers. comm.,1993).

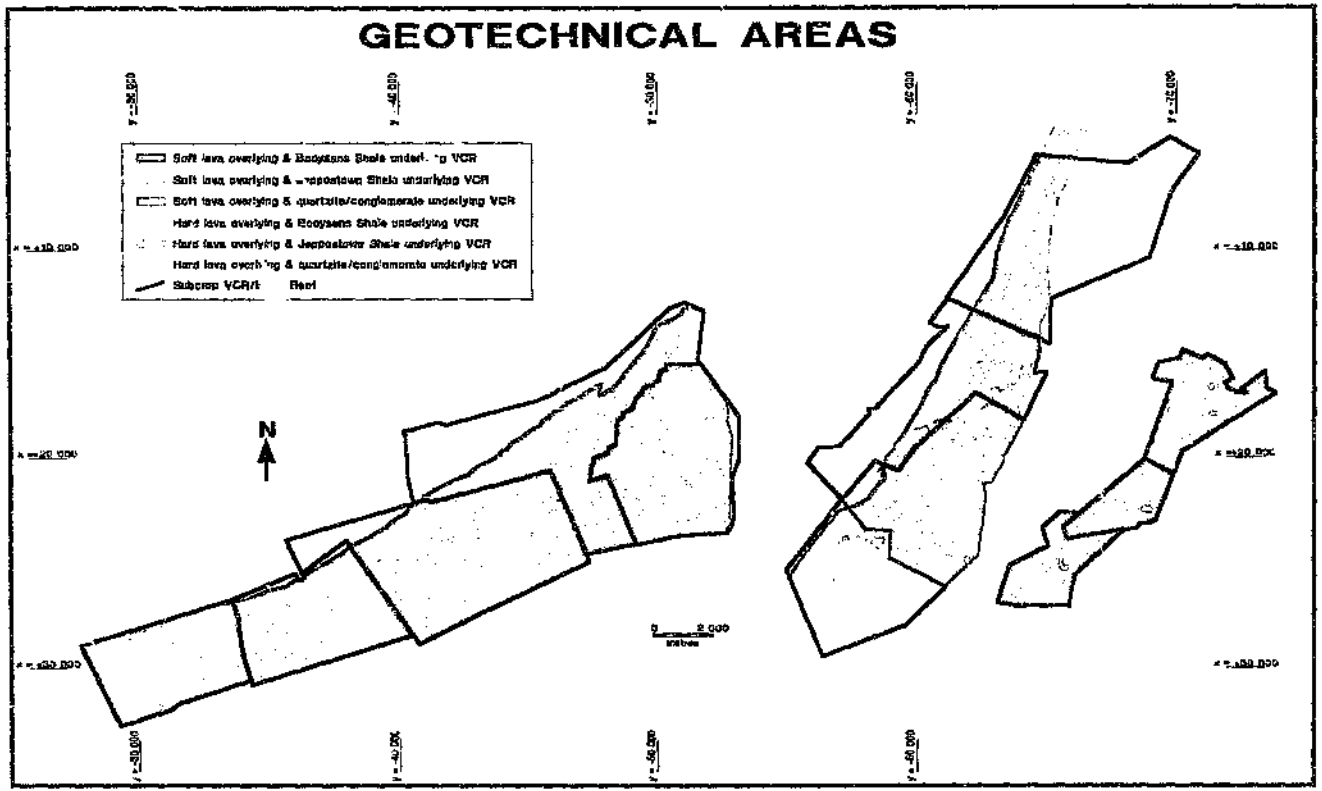

Figure 3.3. Geotechnical plan of the VCR mines under consideration (West Rand and Carletonville goldfields) (Schweitzer, pers. comm.,1993).

The approximate percentage of occurrence of individual geotechnical areas for each mine is summarised in Table 3 1.

Table 3.1. Approximate percentages of geotechnical areas as per individual VCR mine.

MINE	Hangingwall	Hard lava	Hard lava	Hard lava	Soft lava	Soft lava	Soft lava
	Footwall	Qtz/cong.	Boo[illegible]n's	Jeppestown shale	Qtz/cong.	Booysen's shale	Jeppestown shale
Doelkraal GM		100 %		-	-	-	-
West Driefontein GM		84 %	7 %	7 %	2 %	-	-
East Driefontein GM		42 %	-	22 %	6 %	-	30 %
Leeudoorn, Kloof and Venterdsdrop GM		30 %	8 %	-	58 %	4 %	-
Libanon GM		34 %	18 %	-	45 %	3 %	
Western Deep Levels Gold Mines		90 %	10 %	-			-
Elandsrand GM		100 %	-	-	-	-	-
Vaal Reefs GM		100 %	-	-	-	-	-
First Wesgold GM		-	-	-	100 %	-	-
Western Areas and South Deep GM		10 %	-	-	90 %	-	-
Cooke Section 2		-	-	-	100 %	-	-

3.2 GEOLOGICAL DISCONTINUITIES

Sub-areas exist within individual geotechnical areas. These may consider thicknesses and contact relationships of various lithologies, major partings and their characteristics (e.g. spacing, mineral composition) and their distances to footwall/reef and reef/lava contacts. Major partings, for example, could be seismically active. Some of the above information is utilised to compile maps considering the distance from the VCR to the footwall and hangingwall features (Fig. 3.4). Features are the intensely bedded Booysen's shale with its overlying Libanon Reef, commonly sheared at the bottom contact (especially at Libanon, Kloof, Leeudoorn and

Driefontein Gold Mines), the sheared, shaly Green Bar horizon, the Master Bedding Plane Fault (at Driefontein Gold Mine), and a shear zone associated with the Deelkraal Reef Zone (Deelkraal Gold Mine).

The most prominent parting in the hangingwall of the VCR is developed along the contact of the soft and hard lavas. The distance of this parting to the VCR has been delineated where possible, and varies from a few centimetres to 10 m.

The VCR was deposited on an unconformity characterised by pronounced topographic variations, expressed as "rolling". Topographic variations are observed, although to varying degrees, at all of the mines under consideration. "Pilloidal" structures are occasionally associated with these slopes, especially at Elandsrand, Deelkraal and Western Deep Levels Gold Mines. They have also been observed at Vaal Reefs Gold Mine. These have previously been identified as to be responsible for hazardous hangingwall conditions (J.P.E Hamman, pers. comm., 1993).

SUMMARY

The definition of geotechnical areas, with the expectation that different combinations of rock types in the hangingwall and footwall of the reef may potentially result in different rock mass behaviour around tabular excavations, was completed. In total, six geotechnical areas considering three footwall and two hangingwall rock types are defined.

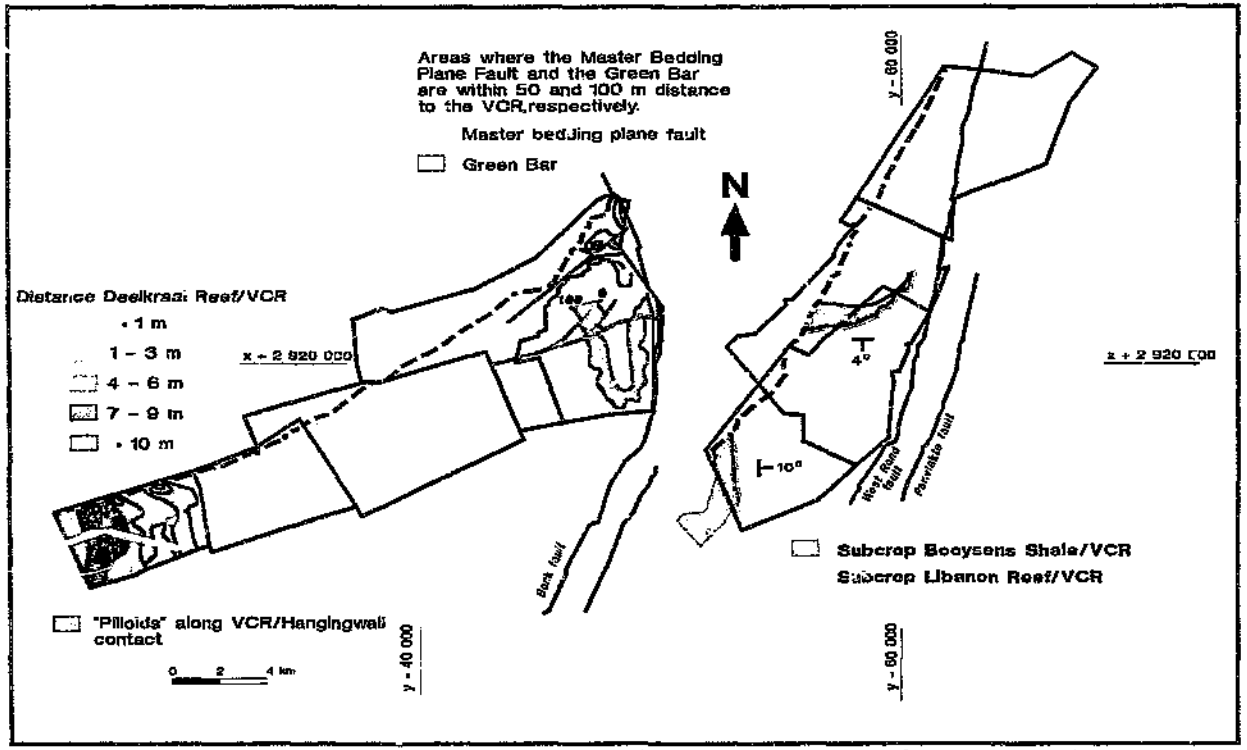

Figure 3.4. Location and distances of partings to the VCR as encountered in the footwall. The areas where Booysens shale and Libanon Reef subcrop against the VCR exhibit pronounced shearing and are also shown. (West Rand and Carletonville goldfields) (Schweitzer, pers. comm.,1994).

CHAPTER 4

4 ROCK PROPERTY TESTS

The literature survey, also considering rock engineering properties, revealed that there is little information on the rock strength parameters of the hangingwall and footwall formations around VCR stopes. The first step towards creating a better understanding of the rock mass behaviour associated with the VCR was, therefore, the establishment of a database considering the properties of the relevant rock types.

4.1 ROCK PROPERTY RESULTS FOR STRATIGRAPHY ASSOCIATED WITH THE VCR

A considerable number of samples of the different rock types were collected (Fig 4.1) and tested (Tables 4.1 to 4.3). Over 30 hangingwall and footwall rock samples were collected from the various geotechnical areas. Core samples measuring 76.2 mm in length and 25.2 mm in diameter were also prepared from 25 samples.

Uniaxial tests were performed by gradually loading the sample along its longest axis until it failed. The triaxial tests were carried out at 10 MPa, 20 MPa, and 40 MPa confinements. Each of these four test conditions was applied to specimens prepared from the samples in three orientations, i.e. dip, strike and 90° relative to the reef plane, so as to ascertain whether the rocks exhibit any anisotropy. The dip and strike of the lava samples were obtained by extrapolation of those of the VCR. However, no consistent or significant differences between the different directions are noted (Tables 4.1 to 4.3).

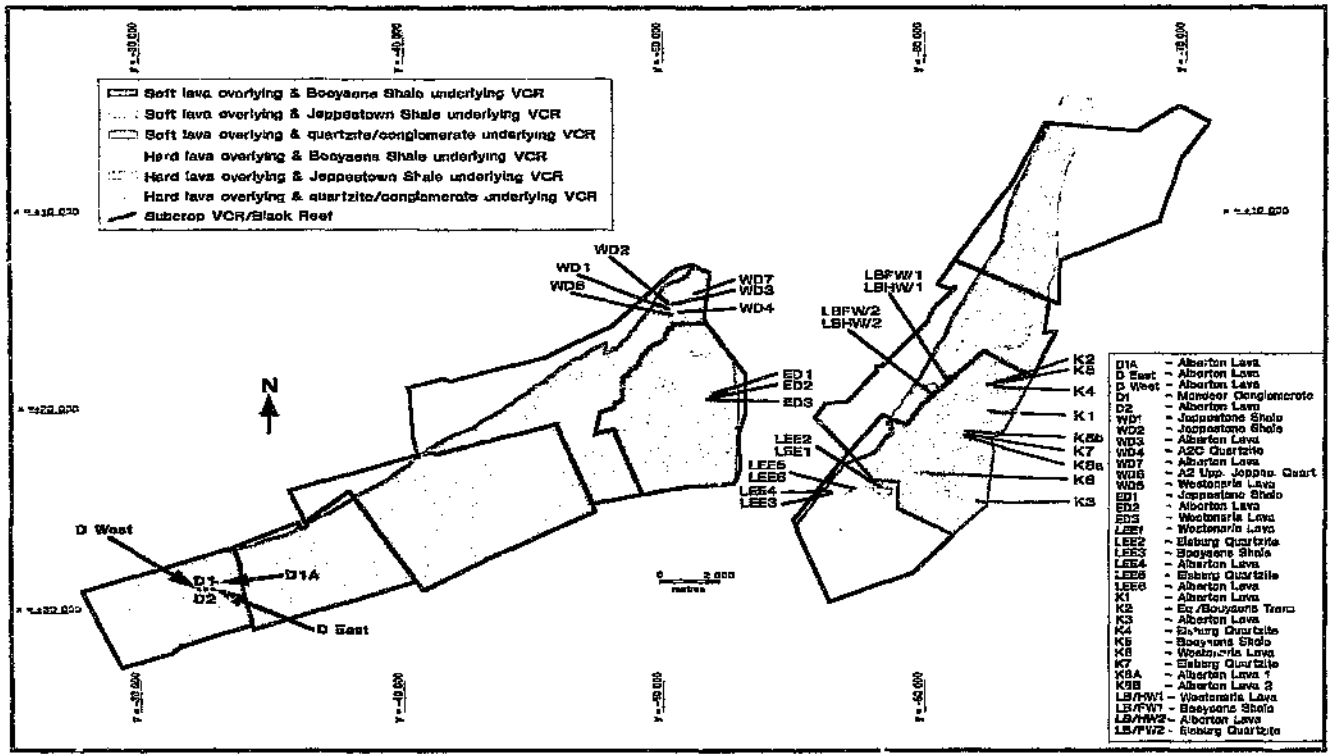

Figure 4.1. Location of samples collected for rock engineering property analyses during the course of this study (Schweitzer, pers. comm.,1993)..

The results obtained from the laboratory tests show that the uniaxial compressive strength (UCS) of hard lava averages around 269 MPa, with a median value close to 226 MPa. The soft lava was weaker with an average UCS of about 157 MPa and a median value of 165 MPa. The Young's Modulus values recorded for the hard lava vary between 66 - 80 GPa with a median value close to 75.1 GPa, whereas the soft lava has values lying between 60 - 71 GPa and a median value of 63.8 GPa. The results of the Poisson's ratio for the two rock types show no significant differences. Average values of the hard lava lie between 0.19 - 0.24 with the soft lava having values between 0.19 - 0.27.

Table 4.1. Average uniaxial compressive strength values. The numbers in brackets indicate the number of analyses.

MINE	ROCK TYPE	STRIKE DIRECTION	DIP DIRECTION	PERPENDICULAR DIRECTION
DEELKRAAL G.M.	HARD LAVA	241 ± 32 (3)	NO TEST	NO TEST
	HARD LAVA	252 ± 19 (3)	NO TEST	NO TEST
	HARD LAVA	217 ± 40 (3)	237 ± 22 (4)	191 ± 75 (3)
FAST DRIEFONTEIN G.M.	HARD LAVA	296 ± 51 (3)	171 ± 62 (3)	216 ± 52 (3)
KLOOF G.M.	HARD LAVA	450 ± 234 (3)	577 ± 66 (3)	454 ± 243 (3)
	HARD LAVA	206 (1)	N/A	212 ± 30 (2)
	HARD LAVA	98 (1)	186 (1)	167 (1)
WEST DRIEFONTEIN G.M.	HARD LAVA	222 (1)	192 ± 10 (3)	214 (1)
WEST. DEEP LEVELS G.M.	HARD LAVA	233 ± 35 (3)		
KLOOF G.M.	SOFT LAVA	174 ± 18 (3)	161 ± 20 (3)	177 ± 11 (3)
EAST DRIEFONTEIN G.M.	SOFT LAVA	150 ± 13 (3)	82 ± 23 (3)	114 ± 27 (3)
LIBANON G.M.	SOFT LAVA	175 ± 56 (3)	176 ± 24 (3)	204 ± 29 (3)
EAST DRIEFONTEIN G.M.	JEPPESTOWN SHALE	119 ± 28 (3)	96 ± 34 (3)	160 ± 23 (3)
WEST DRIEFONTEIN G.M.	JEPPESTOWN SHALE	N/A	153 ± 52 (2)	262 ± 2 (2)
KLOOF G.M	TRANSITION SHALE	196 ± 86 (2)	217 ± 50 (3)	203 ± 69 (3)
KLOOF G.M.	BOOYSEN'S SHALE	128 ± 20 (3)	155 ± 24 (3)	150 ± 45 (3)
LEEUDOORN G.M.	BOOYSEN'S SHALE	119 ± 8 (3)	102 ± 7 (3)	101 ± 24 (3)
LIBANON G.M	BOOYSEN'S SHALE	216 ± 5 (2)	145 (1)	125 (1)
KLOOF G.M.	ELSBURG QUARTZITE	296 ± 8 (3)	260 ± 22 (3)	255 ± 23 (3)
KLOOF G.M.	ELSBURG QUARTZITE	286 (1)	333 (1)	221 (1)
LEEUDOORN G.M.	ELSBURG QUARTZITE	N/A	N/A	225 ± 25 (2)
LEEUDOORN G.M.	ELSBURG QUARTZITE	N/A	221 ± 46 (3)	N/A
WEST. DEEP LEVELS G.M.	ELSBURG QUARTZITE	173 ± 11 (3)		
DEELKRAAL G.M.	MONDEOR CONG.	274 (1)	181 (1)	261 ± 6 (2)
DEELKRAAL G.M.	MONDEOR CONG.	171 ± 26 (2)	151 ± 52 (2)	114 ± 43 (2)

The Transition shale appears to be the hardest when compared to Jeppestown shale and Booysen's shale. It has an average UCS value of about 205 MPa and Poisson's ratio of about 0.15. The Booysen's shale has an average UCS value of 135 MPa with a median value of about 126 MPa, and Poisson's ratio values varying between 0.18 - 0.25. The Jeppestown shale, which has properties lying between these two extremes, has an average UCS value of about 149 MPa, with a median value of 142 MPa, and a Poisson's ratio varying between 0.21 - 0.26.

Table 4.2. Average Poisson's ratios. The numbers in brackets indicate the number of analyses.

MINE	ROCK TYPE	STRIKE DIRECTION	DIP DIRECTION	PERPENDICULAR DIRECTION
DEELKRAAL G.M.	HARD LAVA	0.21 ± 0.018 (9)	NO TEST	NO TEST
	HARD LAVA	0.23 ± 0.015 (9)	NO TEST	NO TEST
	HARD LAVA	0.21 ± 0.011 (7)	0.21 ± 0.009 (6)	0.22± 0.010 (6)
EAST DRIEFONTEIN G.M.	HARD LAVA	0.23 ± 0.020 (5)	0.24 ± 0.011 (6)	0.22± 0.009 (6)
KLOOF G.M.	HARD LAVA	0.19 ± 0.010 (4)	0.19 ± 0.010 (6)	0.19± 0.010 (6)
	HARD LAVA	0.21 ± 0.020 (4)	N/A	0.16± 0.040 (4)
	HARD LAVA	0.20 (3)	0.19 (4)	0.22± 0.009 (3)
WEST DRIEFONTEIN G.M.	HARD LAVA	0.24 ± 0.016 (5)	0.21 ± 0.027 (6)	0.22± 0.012 (3)
WEST. DEEP LEVELS G.M.	HARD LAVA	0.20 ± 0.018 (9)		
KLOOF G.M.	SOFT LAVA	0.26 ± 0.012 (6)	0.27 ± 0.022 (6)	0.24± 0.011 (5)
EAST DRIEFONTEIN G.M.	SOFT LAVA	0.22 ± 0.014 (6)	0.22 ± 0.028 (6)	0.22± 0.013 (6)
LIBANON G.M.	SOFT LAVA	0.19 ± 0.011 (6)	0.18 ± 0.018 (4)	0.19± 0.022 (6)
EAST DRIEFONTEIN G.M.	JEPPESTOWN SHALE	0.26 ± 0.019 (5)	0.25 ± 0.040 (5)	0.23± 0.001 (6)
WEST DRIEFONTEIN G.M.	JEPPESTOWN SHALE	N/A	0.21 ± 0.004 (3)	0.21± 0.009 (3)
KLOOF G.M	TRANSITION SHALE	0.14 ± 0.007 (4)	0.15 ± 0.010 (6)	0.16± 0.010 (6)
KLOOF G.M.	BOOYSEN'S SHALE	0.24 ± 0.027 (6)	0.21 ± 0.028 (6)	0.25± 0.013 (6)
LEEUDOORN G.M.	BOOYSEN'S SHALE	0.25 ± 0.019 (6)	0.25 ± 0.017 (6)	0.25± 0.011 (6)
LIBANON G.M	BOOYSEN'S SHALE	0.18 ± 0.012 (3)	0.18 (3)	0.19± 0.011 (4)
KLOOF G.M.	ELSBURG QUARTZITE	0.11 ± 0.010 (6)	0.11 ± 0.001 (5)	0.11± 0.010 (6)
KLOOF G.M.	ELSBURG QUARTZITE	0.10 ± 0.015 (4)	0.11 ± 0.007 (4)	0.12± 0.009 (4)
LEEUDOORN G.M.	ELSBURG QUARTZITE	0.12 ± 0.015 (6)	N/A	0.13± 0.020 (6)
LEEUDOORN G.M.	ELSBURG QUARTZITE	N/A	0.10 ± 0.001 (6)	N/A
WEST. DEEP LEVELS G.M.	ELSBURG QUARTZITE	0.17 ± 0.016 (9)		
DEELKRAAL G.M.	MONDEOR CONG.	0.11 ± 0.005 (3)	0.11 ± 0.008 (4)	0.11± 0.004 (3)
DEELKRAAL G.M.	MONDEOR CONG.	0.10 ± 0.005 (3)	0.13 ± 0.017 (3)	0.14± 0.031 (3)

In terms of the values of Young's Modulus, the Transition shale has an average value of about 71.6 GPa, followed by Jeppestown shale with an average value of around 65.8 GPa and a median value of 63.8 GPa, and the Booysen's shale at about 64.7 GPa and a median value of 66.4 GPa. The other two rock types, namely Elsburg quartzite and Mondeor conglomerate have average UCS values of 244 MPa and 185 MPa, respectively. They have median values around 239 MPa and 171 MPa respectively. The Poisson's ratio values of the Elsburg quartzite varies between 0.09 - 0.17, whereas that of the Mondeor conglomerate is about 0.11. Young's Modulus values for Elsburg quartzite varies between 63.5 - 84.2 GPa with a median value of about 74.8 GPa, whereas the Mondeor conglomerate has an average value of 70.9 GPa with a median value of 69.5 GPa.

Table 4.3. Average Young's Modulus values. The numbers in brackets indicate the number of analyses.

MINE	ROCK TYPE	STRIKE DIRECTION	DIP DIRECTION	PERPENDICULAR DIRECTION
DEELKRAAL G.M.	HARD LAVA	70.7 ± 2.9 (12)	NO TEST	NO TEST
	HARD LAVA	70.1 ± 3.4 (12)	NO TEST	NO TEST
	HARD LAVA	79.0 ± 2.6 (10)	76.6 ± 2.5 (10)	76.0 ± 2.2 (9)
EAST DRIEFONTEIN G.M.	HARD LAVA	76.0 ± 1.8 (9)	71.7 ± 2.6 (9)	71.2 ± 3.0 (9)
KLOOF G.M.	HARD LAVA	93.7 ± 3.2 (9)	94.8 ± 1.6 (9)	93.2 ± 4.0 (9)
	HARD LAVA	74.7 ± 2.5 (5)		73.0 ± 1.3 (6)
	HARD LAVA	78.2 ± 2.7 (4)	80.4 ± 1.8 (5)	76.6 ± 0.9 (4)
WEST DRIEFONTEIN G.M.	HARD LAVA	77.9 ± 5.2 (6)	66.4 ± 2.2 (9)	67.4 ± 2.2 (4)
WEST. DEEP LEVELS G.M.	HARD LAVA	69.6 ± 2.1 (12)		
KLOOF G.M.	SOFT LAVA	70.4 ± 4.6 (9)	65.9 ± 4.9 (9)	66.9 ± 4.3 (6)
EAST DRIEFONTEIN G.M.	SOFT LAVA	69.4 ± 5.1 (9)	65.5 ± 3.4 (9)	60.7 ± 5.2 (6)
LIBANON G.M.	SOFT LAVA	70.0 ± 1.9 (9)	68.2 ± 2.6 (8)	71.4 ± 1.2 (9)
EAST DRIEFONTEIN G.M.	JEPPEST.WN SHALE	56.2 ± 3.2 (8)	56.2 ± 8.9 (8)	65.9 ± 1.6 (9)
WEST DRIEFONTEIN G.M.	JEPPESTOWN SHALE	N/A	76.7 ± 4.4 (5)	66.4 ± 2.2 (5)
KLOOF G.M	TRANSITION SHALE	70.8 ± 4.4 (8)	72.7 ± 1.8 (9)	71.4 ± 4.5 (9)
KLOOF G.M.	BOOYSEN'S SHALE	66.6 ± 4.6 (9)	59.6 ± 5.4 (9)	69.6 ± 4.2 (9)
LEEUDOORN G.M.	BOOYSEN'S SHALE	63.1 ± 2.3 (9)	56.7 ± 3.3 (9)	64.4 ± 2.6 (9)
LIBANON G.M	BOOYSEN'S SHALE	71.0 ± 0.9 (5)	72.4 ± 1.0 (4)	68.7 ± 2.9 (5)
KLOOF G.M.	ELSBURG QUARTZITE	77.2 ± 1.7 (9)	72.0 ± 1.1 (8)	74.8 ± 2.0 (9)
KLOOF G.M.	ELSBURG QUARTZITE	81.4 ± 2.0 (5)	80.1 ± 6.1 (5)	80.0 ± 2.0 (5)
LEEUDOORN G.M.	ELSBURG QUARTZITE	77.0 ± 1.4 (6)	N/A	73.2 ± 1.7 (8)
LEEUDOORN G.M.	ELSBURG QUARTZITE	N/A	84.2 ± 2.4 (9)	N/A
WEST. DEEP LEVELS G.M.	ELSBURG QUARTZITE	65.1 ± 2.0 (12)		
DEELKRAAL G.M.	MONDEOR CONG.	81.2 ± 1.0 (4)	78.0 ± 1.9 (5)	82.8 ± 0.9 (5)
DEELKRAAL G.M.	MONDEOR CONG.	65.7 ± 1.0 (5)	61.5 ± 4.2 (5)	58.6 ± 5.0 (5)

A graphical representation of the UCS, Young's Modulus and the Poisson's ratio values for the various hangingwall and footwall rock types, arranged in a sequential manner from west to east along the 'West Wits Line', is shown in the following Figures 4.2 a and b to 4.4 a and b.

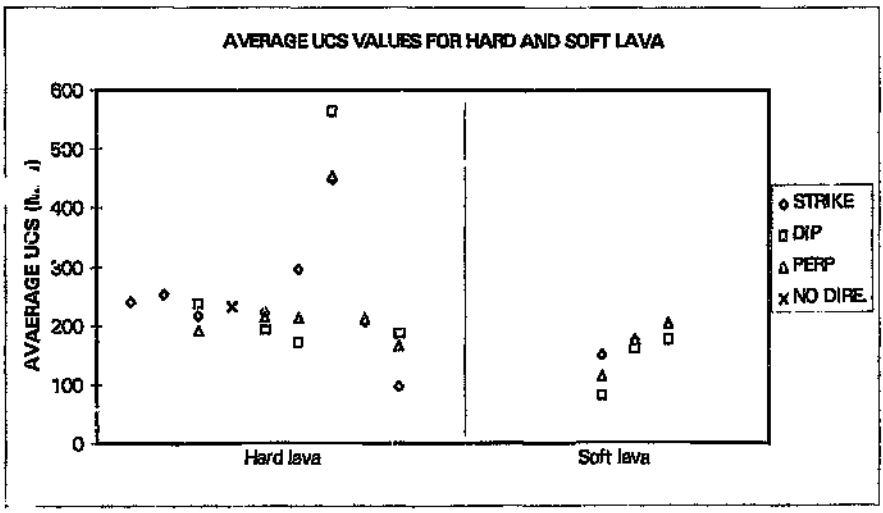

a

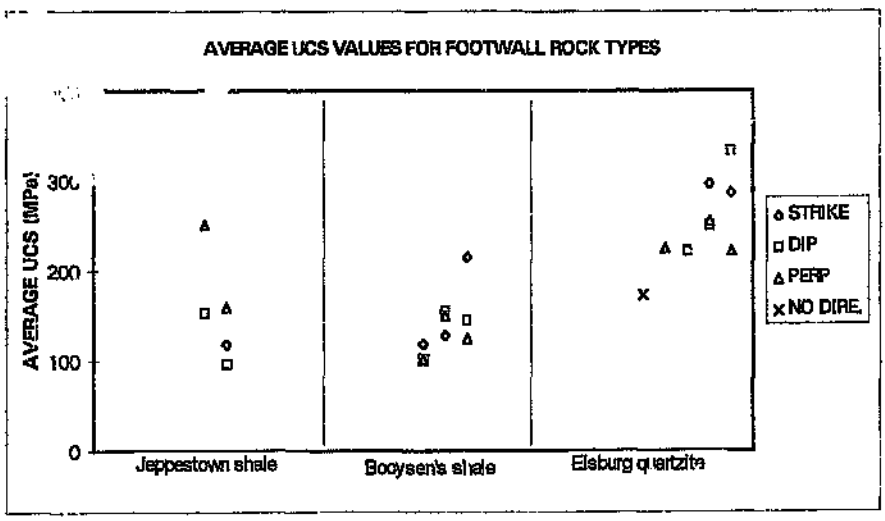

b

Figures 4.2 a and b. Average UCS values for the hard and soft lavas and the various footwall rock types.

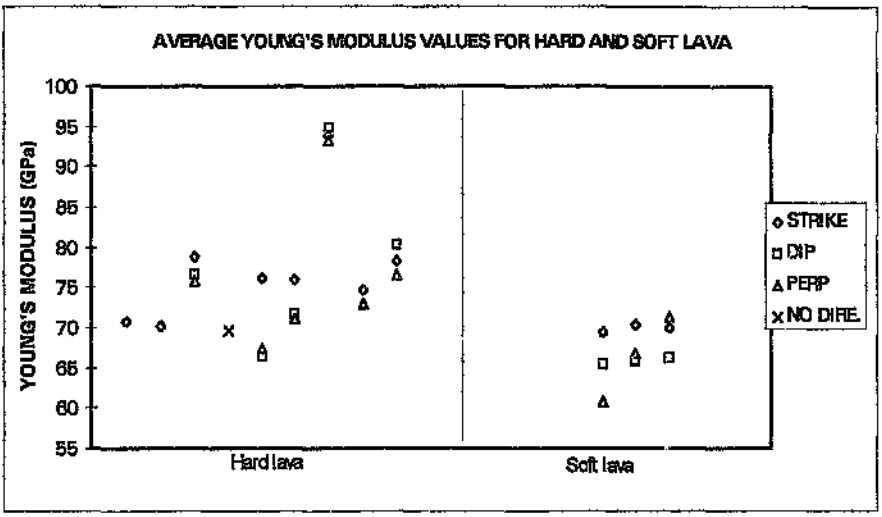

a

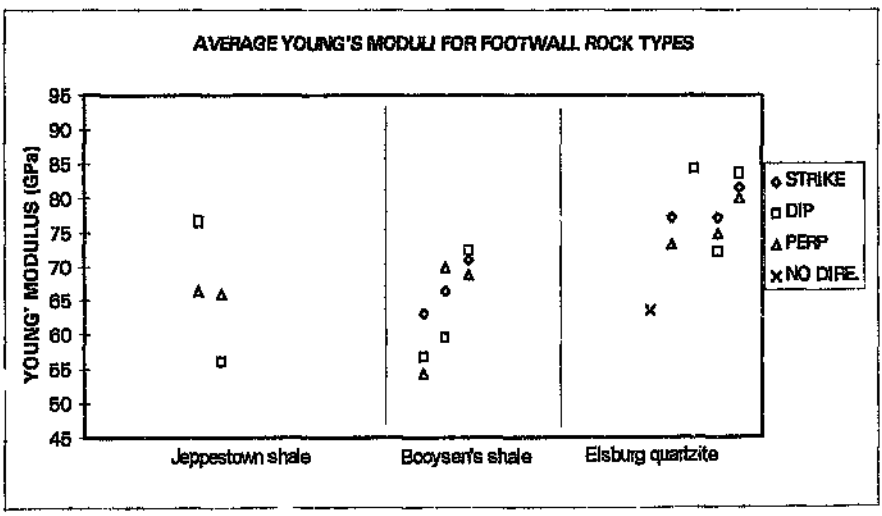

b

Figures 4.3 a and b. Average Young's Modulus values for the hard and soft lavas and the various footwall rock types.

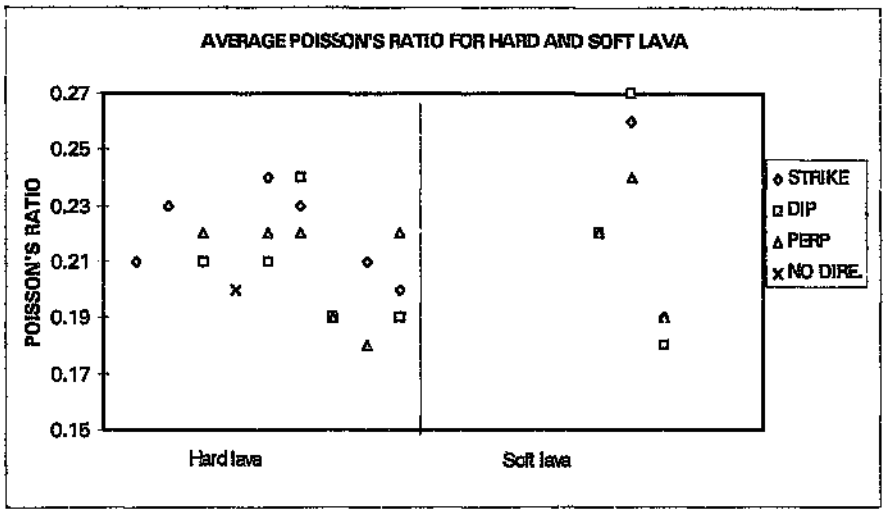

a

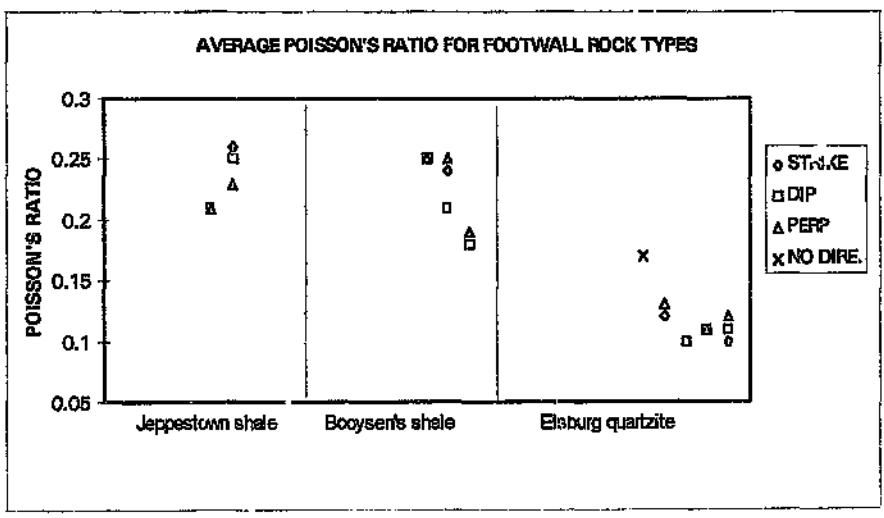

b

Figures 4.4 a and b. Average Poisson's ratio values for the hard and soft lavas and the various footwall rock types.

4.2 UNIAXIAL COMPRESSIVE STRENGTHS AS DEDUCED FROM POINT LOAD TESTS

More than 1000 point load tests were performed on nine underground borehole cores drilled at Western Areas Gold Mine. The depth of drilling figures were converted into actual stratigraphic heights to facilitate comparison of the uniaxial compressive strength values as obtained from the different cores.

A correlation of the results with the lithological/geochemical variations in the soft lavas performed by JK Schweitzer, reveals the existence of three distinct soft lava types as shown in Figures 4.5a to c: Talcose High-Mg Basalt, Mottled High-Mg Basalt and Olivine Cumulate. The values of uniaxial compressive strength for Talcose High-Mg Basalt are generally less than 150 MPa (Figs. 4.5a to c) while Olivine Cumulate and Mottled High-Mg Basalt have uniaxial compressive strengths generally exceeding 150 MPa (Figs. 4.5b and c). The soft lava may therefore be subdivided, from a rock engineering point of view, into two broad categories. It is noteworthy that the fault rock (pseudotachylite) possesses uniaxial compressive strengths of just less than 150 MPa (Fig. 4.5c).

The results indicate th ' marked differences exist in the properties of the different hangingwall and footwall rock types. The two types of lava, namely hard and soft, which constitute the VCR hangingwall rock types, have significantly different rock properties. As the name implies, the soft lava is the weaker of the two. Lithological/geochemical variations and the resulting differences in rock properties of the soft lava suggest that a subdivision defining "strong" and "weak" soft lava is possible. Based on the chemical composition, three soft lava types were identified (Coetzer and Lambert, 1993). The JCI Group defined these distinct soft lava types as: Talcose High-Mg Basalt, Mottled High-Mg Basalt, and Olivine Cumulate (H. Swart, pers. comm., 1995). Detailed investigations have not been carried

out on the hard lava but the large variations in the test results suggest that similar classes could exist. The hard lava type, for example, referred to as "K3" at Kloof Gold Mine (Table 4.1), is far stronger than what has been identified at other mines. Similar differences in rock properties have been noted between the footwall formations underlying the VCR stopes. The Transition shale at Kloof Gold Mine is stronger than the Booysen's and Jeppestown shales in all the three directions tested. Apart from the relatively weak Elsburg quartzite at Western Deep Levels Gold Mine, there are no appreciable differences in strength of this rock type when compared to other areas.

In summary: as a result of testing the stratigraphy associated with the VCR, a database has been compiled. This data base includes 13 hangingwall and 12 footwall samples and corresponding uniaxial compressive strength (UCS), Poisson's ratio, and Young's Modulus values. The results show that there is a significant difference in the properties of the relevant rock type, especially for soft and hard lava, and no remarkable differences with direction of testing. The analyses of lithological/geochemical variations in the soft lavas and point load tests reveal the existence of three distinct soft lava types.

A considerable amount of information on the strength properties of the various rock types surrounding the VCR stopes has been gathered. The foundations for a data base have been laid.

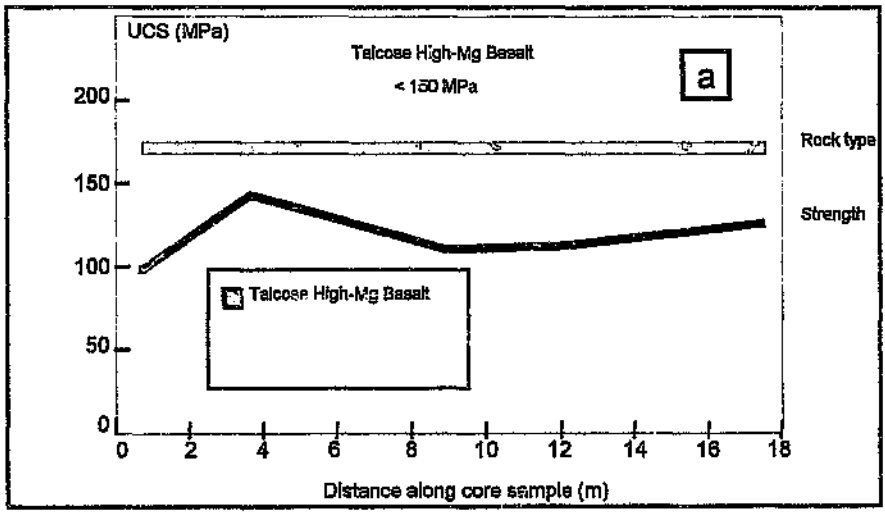

Figures 4.5 a to c: Uniaxial compressive strength results of point-load tests of cores containing soft lava from Western Areas Gold Mine.

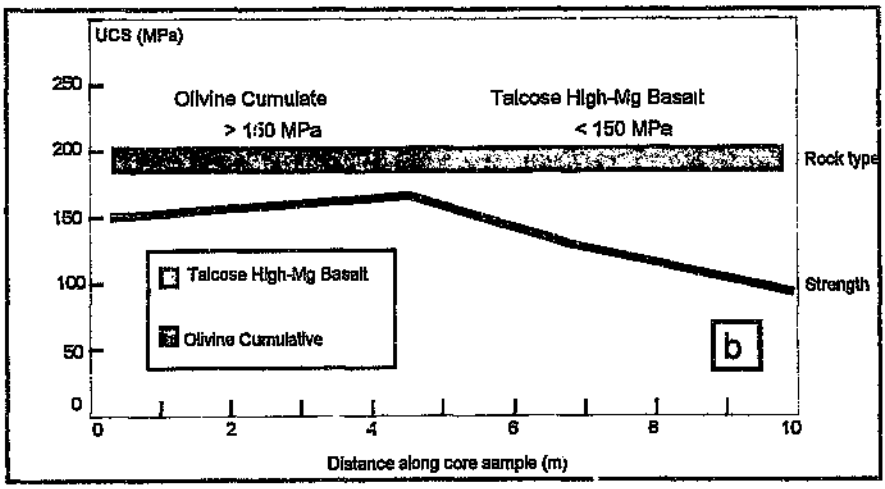

Figures 4.5 a to c: Continued.

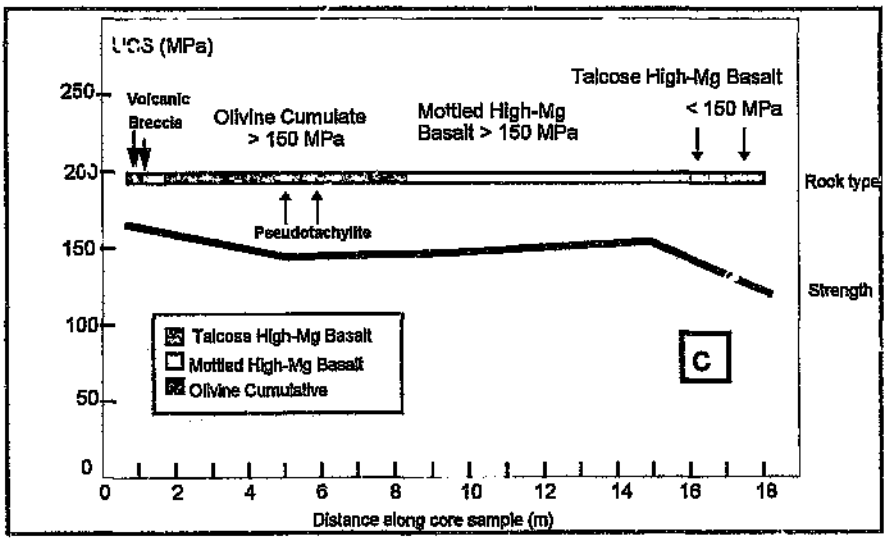

Figures 4.5a to c: Continued.

CHAPTER 5

5 ANALYSIS OF ROCK MASS BEHAVIOUR ASSOCIATED WITH VCR STOPES

In the mines under the management of GFSA and AAC, the major type of geotechnical area defined is hard lava overlying the VCR and quartzite-conglomerate underlying the VCR (Table 3.1). The second most important area is defined as a combination of soft lava hangingwall and quartzite-conglomerate footwall, especially prominent at the JCI mines at First Wesgold. The third one is defined as soft lava overlying the VCR and Jeppestown shale underlying the VCR, of specific importance to East Driefontein Gold Mine.

Two different geotechnical areas were selected for monitoring, which especially includes closure-ride and extensometer measurement (Fig. 5.1):

- the first area is a combination of hard lava hangingwall and quartzite or conglomerate footwall and it is the major geotechnical area,

- the second area is defined as soft lava hangingwall with Jeppestown shale footwall.

5.1 VCR STUDY SITES

The first geotechnical area is defined as soft lava overlying and Jeppestown shale underlying the VCR at a depth of 2600 m below datum at East Driefontein Gold Mine. The site is located on 32 Level 37 Longwall at 4 Shaft. The second site is situated at Deelkraal Gold Mine. This site is located on 27 Level 15 Longwall. There, hard lava overlies and quartzite-conglomerate underlies the

VCR with the depth varying between 2690 and 2730 m below datum. All digitised detailed plans showing the general face positions at these two sites are shown in Figures 6.1 to 6.5 (Chapter 6).

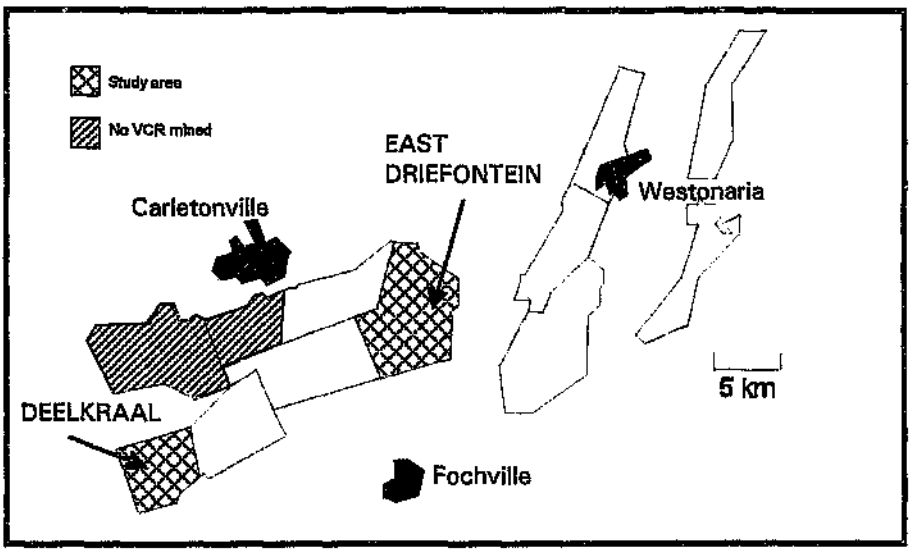

Figure 5.1. Location of underground monitoring sites.

The rock mass behaviour at both East Driefontein and Deelkraal Gold Mines was monitored over a period of two years. Measurements were taken using two methods:

- Extensometer measurements (a method to observe "internal", inelastic rock mass deformation),
- Closure-ride deformation measurements (a method to observe the total "external", inelastic rock mass deformation).

Analysis of the mining induced stress fracturing and fall of ground characteristics was also carried out at each of the sites. Underground investigations also aimed at the identification of potential differences in mining induced stress and shear fracturing in different geotechnical areas.

5.1.1 East Driefontein Gold Mine

At East Driefontein Gold Mine, Jeppestown shale and quartzite/conglomerate comprise the footwall (Fig. 5.2). The soft lava is the hangingwall lithology over major portions of the lease area (Fig. 5.3), resulting in the definition of two geotechnical areas. Two additional geotechnical areas are defined by hard lava hangingwall and quartzite-conglomerate or Jeppestown shale footwall (Fig. 5.4).

The site is located on 32 Level 37 Line, at 4# Shaft (Fig. 5.5, Fig. 6.1 and Fig. 6.2). There, soft lava overlies and Jeppestown shale underlies the VCR at a depth of 2450 m below surface. The VCR dips at 10° towards the southeast. Underground monitoring and observations were carried out in three panels, West 4, 5 and 6.

5.1.1.1 Mining induced stress fracture mapping

A number of underground visits were made to underground monitoring sites to identify mining induced stress fracturing, the orientation, and other characteristics of joints, faults, and dykes within the footwall and hangingwall of the VCR.

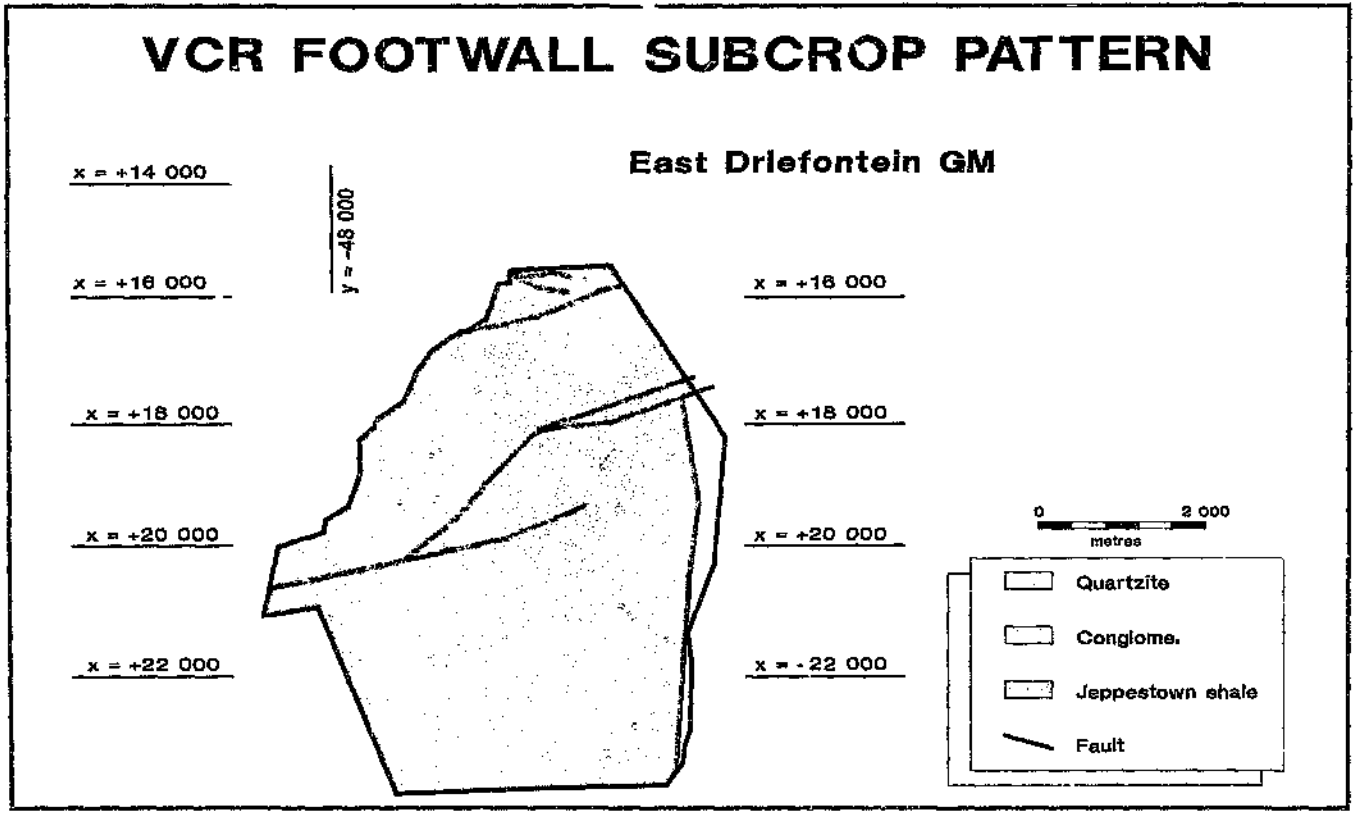

Figure 5.2. VCR footwall plan of East Driefontein Gold Mine (Schweitzer, pers. comm.,1993).

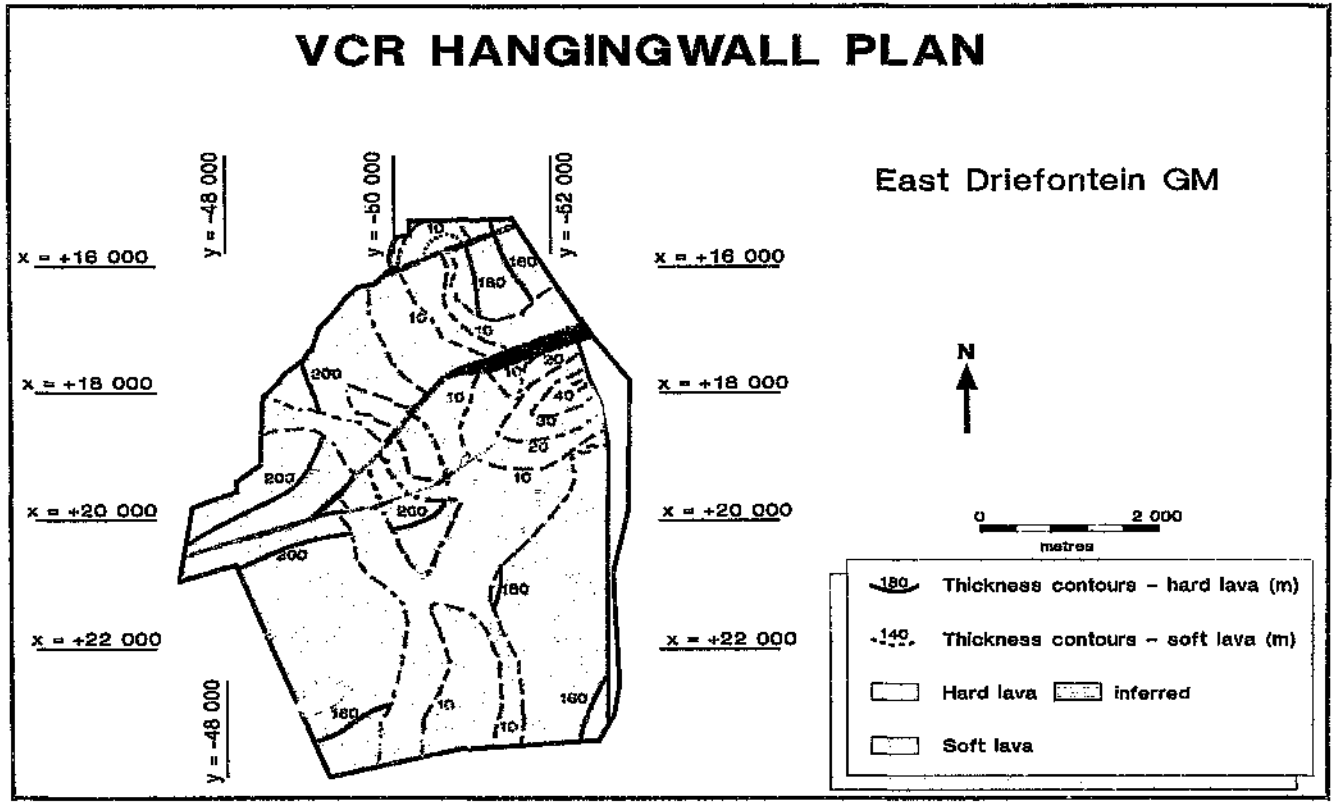

Figure 5.3. VCR hangingwall plan of East Driefontein Gold Mine (Schweitzer, pers. comm.,1993).

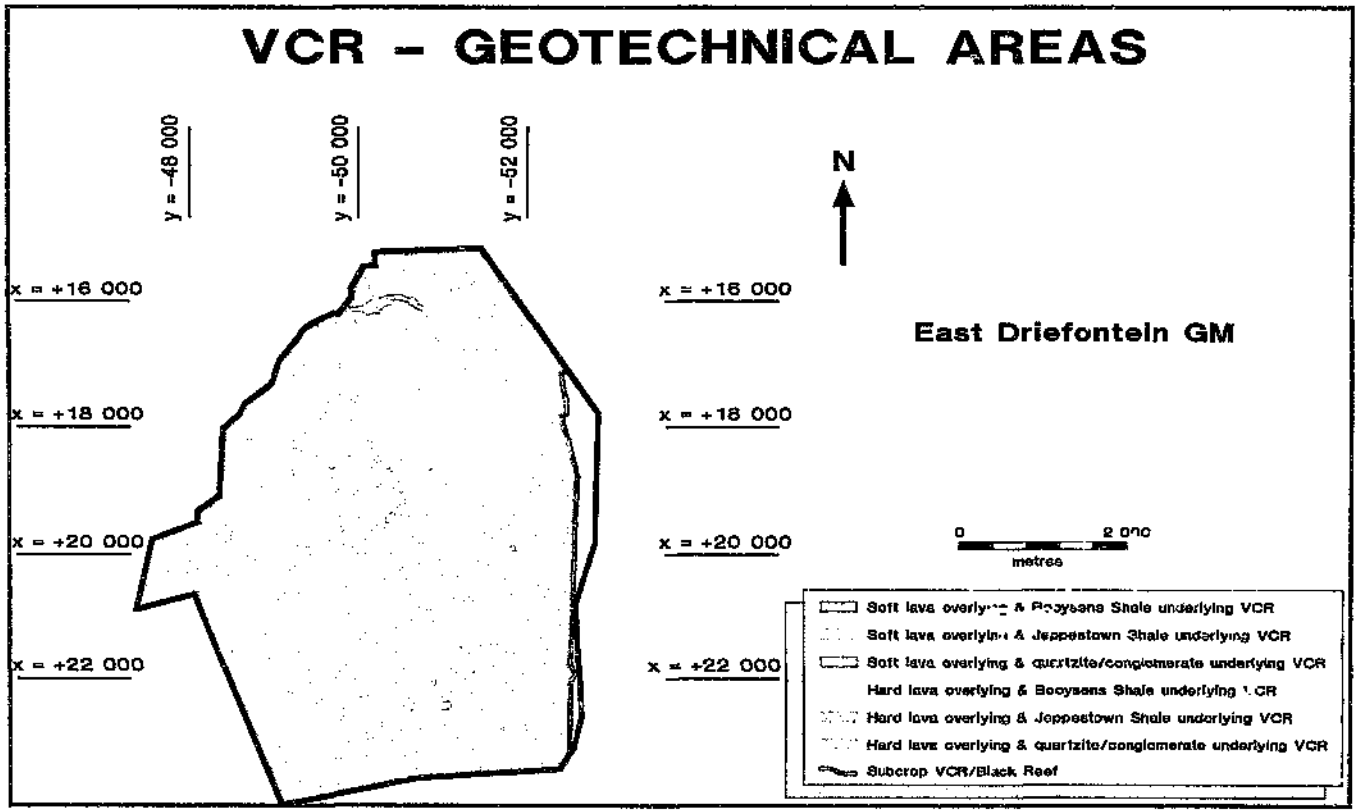

Figure 5.4. Geotechnical area plan of East Driefontein Gold Mine (Schweitzer, pers. comm.,1993).

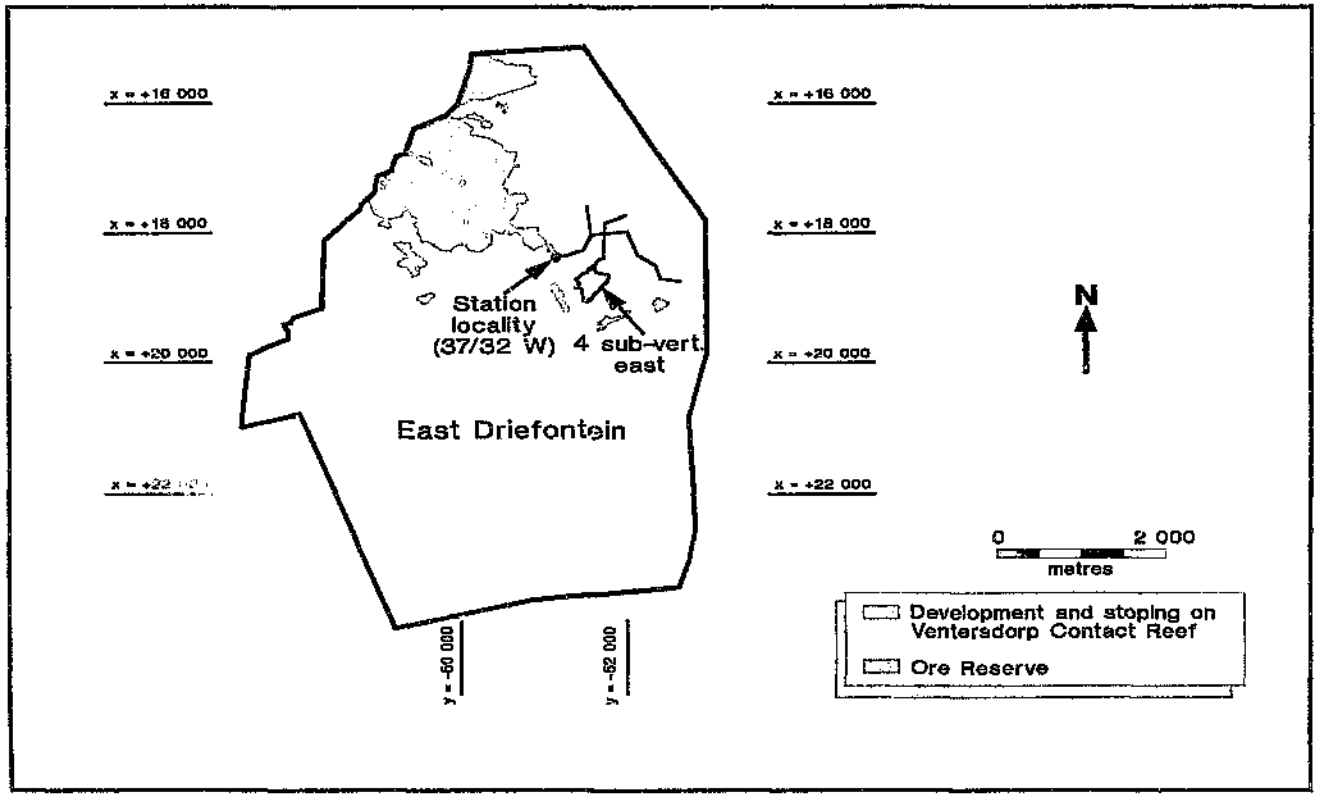

Figure 5.5. Locality of underground monitoring site (32 Level 37 Line) at East Driefontein Gold Mine (Schweitzer, pers. comm.,1993).

In general, mining induced stress fractures at the underground monitoring site at East Driefontein Gold Mine are very steep (about 70° to 80°) and dip away from the face in the Jeppestown shale footwall. The orientation of fractures observed in soft lava hangingwall was anomalous, dipping in the "wrong" direction (Fig. 5.5) when compared to reefs that have sedimentary footwall and hangingwall rocks or to areas where the VCR is overlain by hard lava. The other visits to the east side of the longwall showed the same configuration of mining induced stress fracturing.

Stresses around the face of the stope are influenced by the variation in stiffness and extent of damage between footwall and hangingwall. Fractures forming in a direction associated with the direction of maximum compressive principal stress may have been generated with the point of inflection that is in hangingwall (Fig. 5.6). A photographic record of the mining induced stress fracturing as observed at the site is shown in Appendix A.

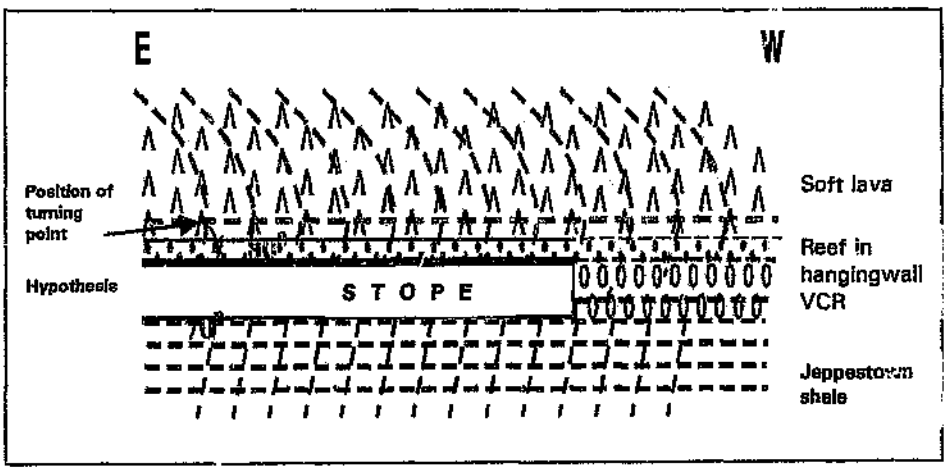

Figure 5.6. Attitude of mining induced stress fracturing at East Driefontein Gold Mine. The point of inflection is interpreted as to occur in the hangingwall of the excavation.

The hangingwall is strongly fragmented in appearance, associated with small-sized (characteristically 30 cm / 25 cm / 30 cm) falls of ground. The sizes of the falls of ground are controlled by the joint frequency and attitude and the mining induced extension fractures.

5.1.1.2 *Closure-ride stations*

The closure-ride movements were continuously monitored. All stations were classified as either temporary or permanent stations. Three temporary stations were installed at the top, middle and bottom of the panel and one permanent station was established along each advanced strike gully (Fig. 5.7). The temporary stations were installed as close as possible to the face (usually within 4-5 m). When the distance exceeded 12 m, a new line of closure ride stations was installed. The general panel layout, face position and the locations of each station at this site during monitoring are shown in Figure 5.7.

The theory of station installation and calculation of the closure was explained by Piper and Gürtunca (1987) as follows:

a) Three holes are drilled in the hangingwall to form the corners of an approximate right triangle, preferably with one side along dip and one side along strike. Convergence pegs are installed and the distances between them are measured.
b) A hole is drilled in the footwall vertically below the apex of the hangingwall triangle (if covered with broken rock, the "lost" peg can be found later by dropping a stone from the apex).
c) The spring loaded vernier is now used to measure the initial distance between each of the hangingwall pegs and the footwall peg. Extension pieces of known length usually need to be attached to the vernier to measure the distance between the footwall and hangingwall.

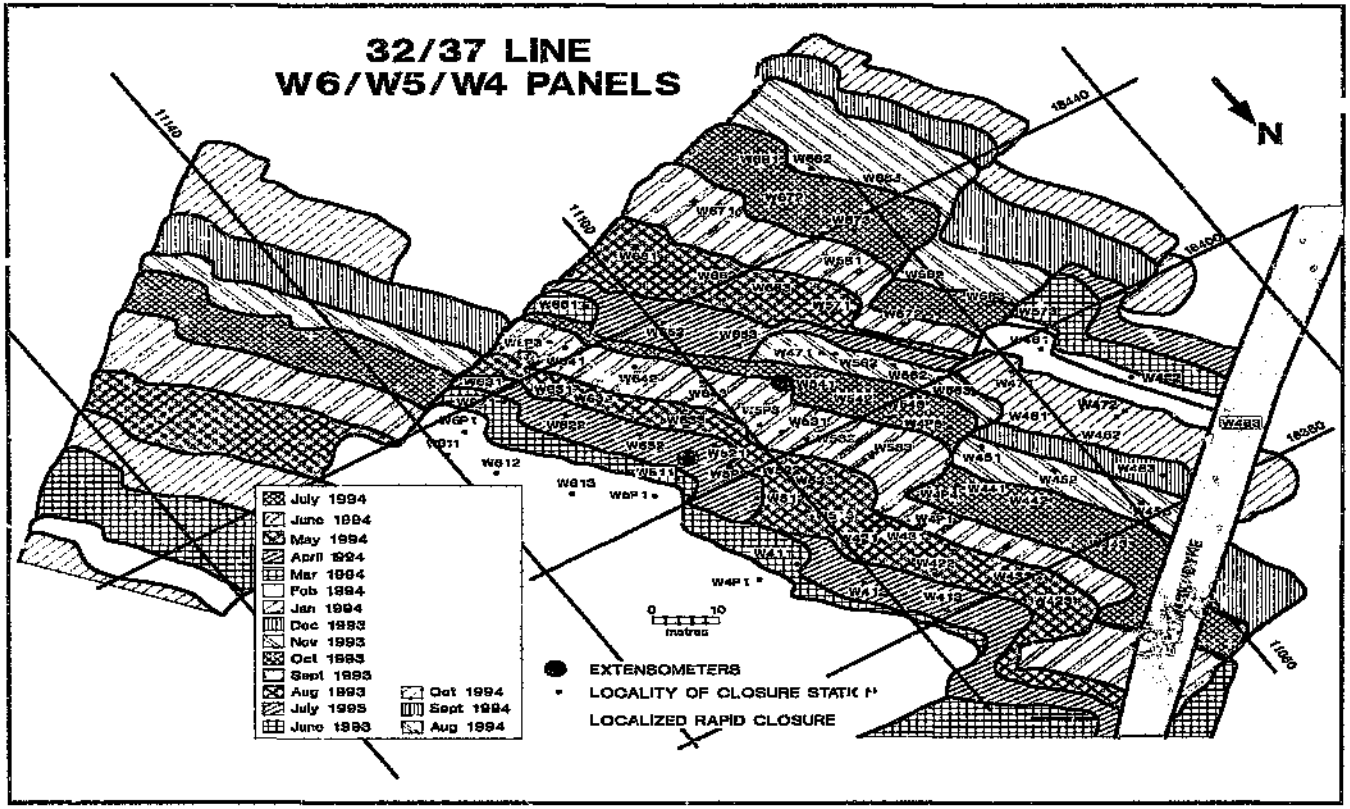

Figure 5.7. The general panel layout, face position and location of each station at the monitoring site on 32 Level, 37 Line, No 4 Shaft, East Driefontein Gold Mine.

When the three distances between the hangingwall and footwall pegs are subsequently measured, the new position of the footwall peg can be found from the following equations:

b_1, b_2, b_3 = Lengths of base triangle,

l_1, l_2, l_3 = Measured lengths between footwall and hangingwall pegs,

f_1, f_2, f_3 = Co-ordinates of the footwall peg with respect to the hangingwall triangle

First calculate the temporary variables x_3 and y_3;

$$x_3 = (b_1^2 + b_2^2 - b_3^2) / (2 b_1^2) \qquad y_3 = (b_2^2 - x_3^2)^{0.5}$$

Now calculate the new co-ordinates of the footwall peg ;

$$f_1 = (b_1^2 + l_1^2 - l_2^2) / (2b_1) \qquad \text{(Strike ride)}$$

$$f_2 = (l_2^2 - l_3^2 - b_1^2 + x_3^2 + y_3^2 + 2 f_1 (b_1 - x_3)) / (2y_3) \qquad \text{(Dip ride)}$$

$$f_3 = (l_1^2 - f_1^2 - f_2^2)^{0.5} \qquad \text{(Closure)}$$

The initial mining at the site on 32 Level 37 Line took place in West 6 panel, in June 1993. This was followed by West 5 and West 4 panels over the next few weeks. Mining continued uninterrupted in all three panels for the next four months but at different rates. The average face advance rates for this period were 7.5 m per month, 7.5 m per month and 5.0 m per month, in panels West 4, 5 and 6, respectively.

Mining was stopped on West 4 panel in April 1994 to allow the 25 m lag to panel 5 to be reduced. Thus only panels 5 and 6 and the more distant panel 7 were advanced from this date until the end of the monitoring period. In West 4 panel, the initial closure rates were as high as 10 to 14 mm per day. These rates were reduced to 3 mm per day when the mining in this panel discontinued. It was not possible to observe ongoing closure rates in this particular panel because no further face advance was made before this site was closed (Fig. 5.8).

At the early stage of monitoring of the closure ride stations in West 5 panel, the rate of closure was about 8 mm per day. Production was stopped for about six months from October 1993 to April 1994, in West 5 and 6 panels, because of a pronounced roll, which was almost along strike direction and about 4 m in height. During this period mining took place only in West 4 and 7. As could be expected, a significant decrease in the closure rates at all stations in West 5 and 6 panels was noticed. However, a closure rate of about 3 mm per day was maintained during this period indicating the influence of mining adjacent panels on the closure and possibly also time effects. As soon as production recommenced in those panels, a significant increase in closure rate was observed with rates of 10 mm and 8 mm per day (Figs. 5.9 and 5.10).

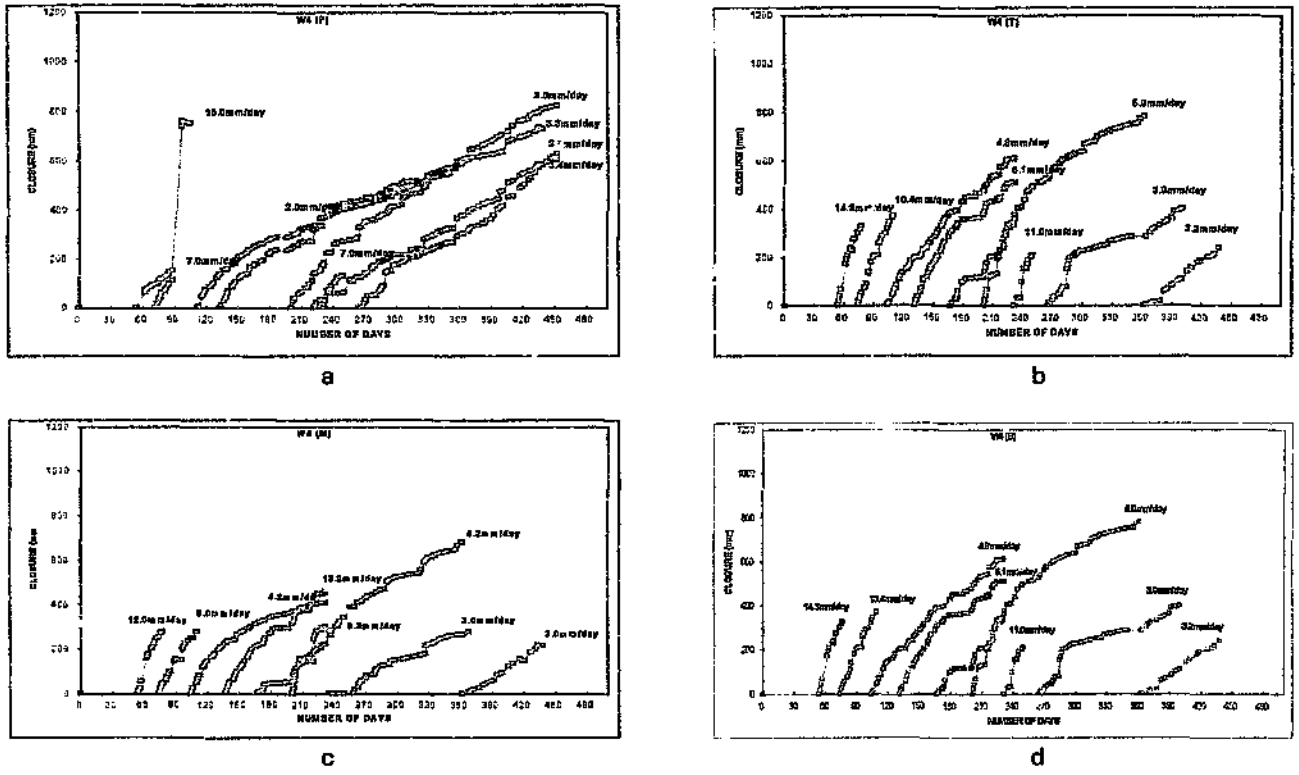

Figures 5.8 a to d. Closure rates at the permanent station (a), at the temporary stations at the bottom (b), middle (c) and top (d) of the face in West 4 panel, 32 Level, 37 Line, No 4 Shaft, East Driefontein Gold Mine.

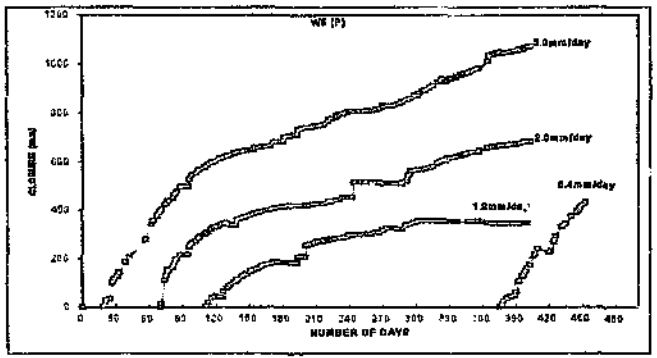

a

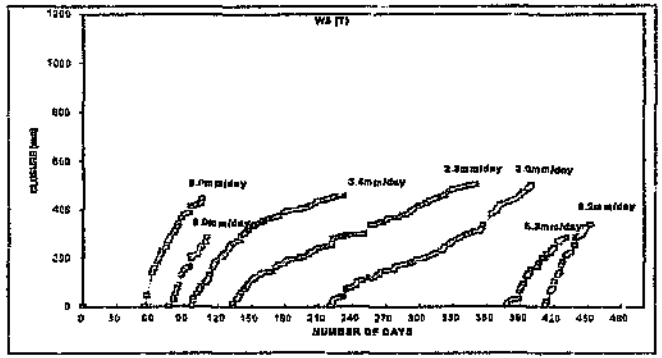

b

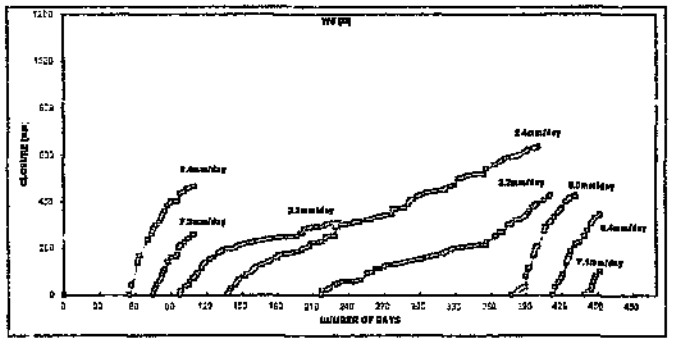

c

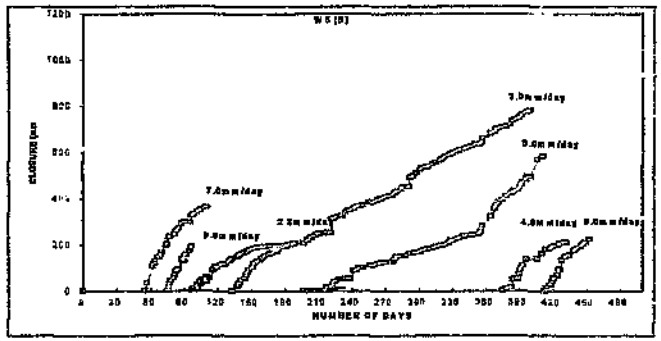

d

Figures 5.9 a to d. Closure rates at the permanent station (a), at the temporary stations at the bottom (b), middle (c) and top (d) of the face in West 5 panel, 32 Level, 37 Line, No 4 Shaft, East Driefontein Gold Mine.

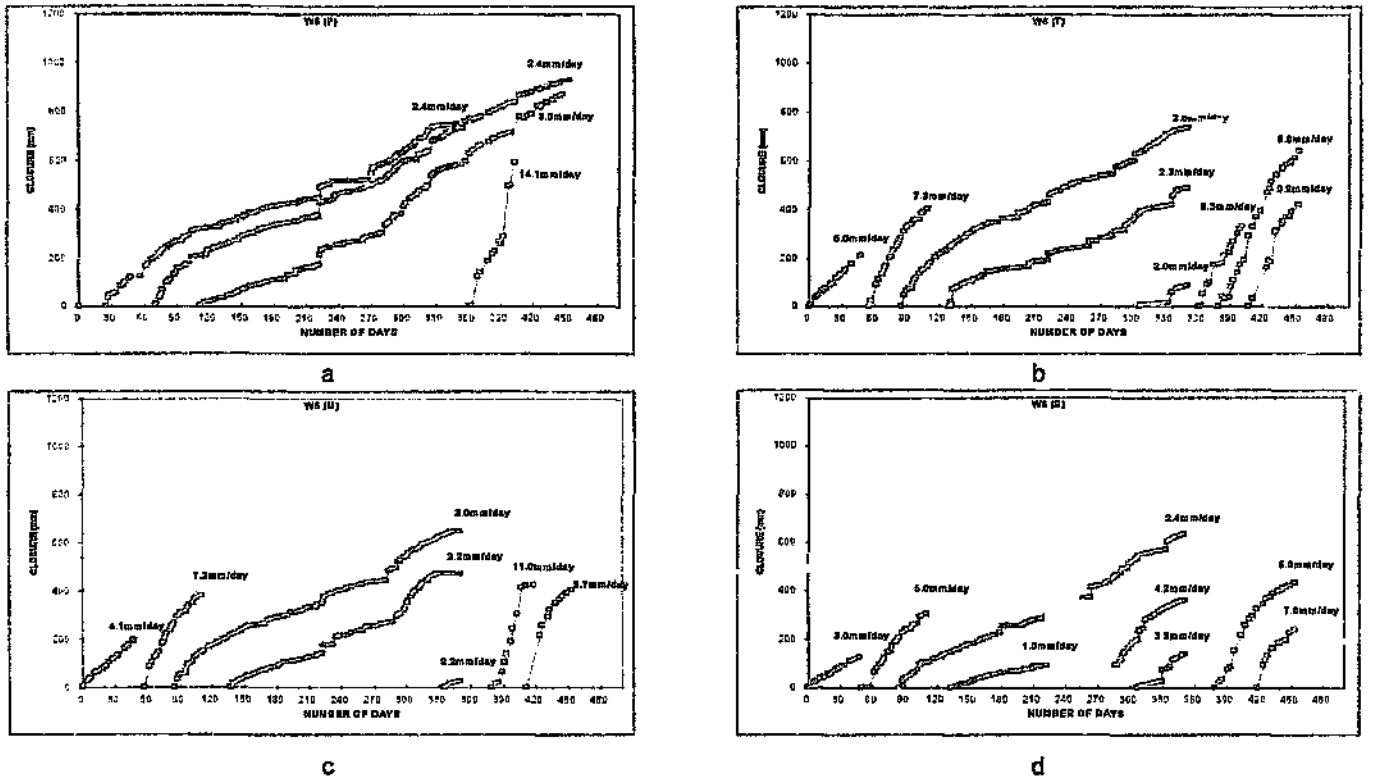

Figures 5.10 a to d. Closure rates at the permanent station (a), at the temporary stations at the bottom (b), middle (c) and top (d) of the face in West 6 panel, 32 Level, 37 Line, No 4 Shaft, East Driefontein Gold Mine.

5.1.1.3 Anomalous closure associated with seismicity

High closure occurred at the first permanent station, namely W4P1 (Fig. 5.7) along the advanced strike gully in West 4 panel. The location of this station is about 6 m back from the face position at this time. Figure 5.11 shows the panel layout, position of packs installed, fall of ground, and direction of pictures taken to indicate damage on the packs as well as the size of fall of ground.

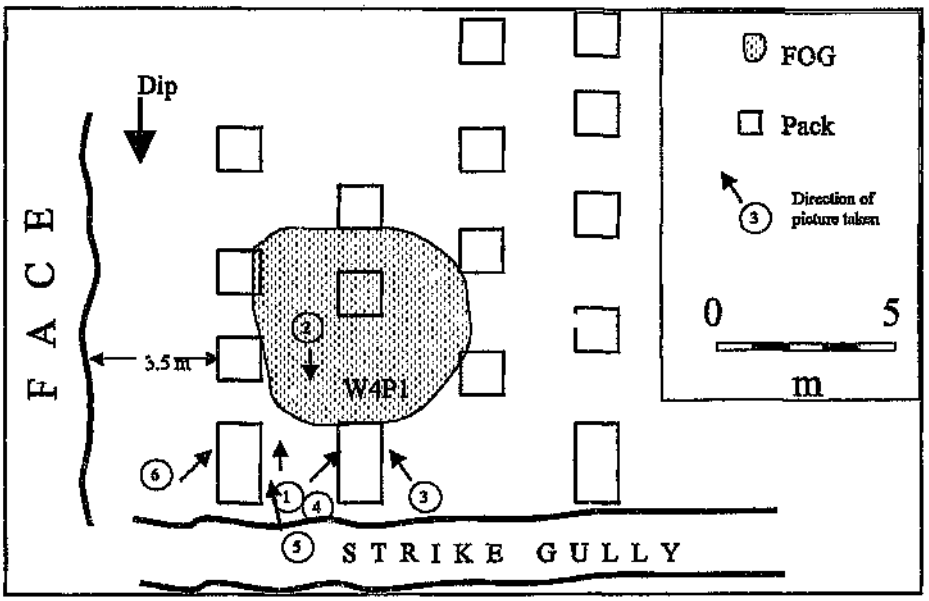

Figure 5.11. Panel layout and the positions of falls of ground (dotted area) in W4 panel, 32 Level, 37 Line, East Driefontein Gold Mine.

Up to 27/09/93, the average value of the measured closure rate was 5 mm per day at this particular station. On 06/10/93, a closure measurement of 587 mm was recorded. Eight days later, the hangingwall in the vicinity of this station collapsed following which the measured closure rate was reduced to about

2 mm per day. Seven seismic events with magnitudes ranging between -0.64 and 1.64 occurred between 27/09/93 and 06/10/93. On 14/10/93, on which a fall of ground was documented, five seismic events with magnitudes of between -0.39 and 2.7 occurred.

Approximately 25 m² of the hangingwall between the packs along the strike gully collapsed. The hangingwall blocks were small (0.3 m / 0.35 m / 0.4 m) and very fragmented defined by new fractures. The upper portion of each pack was found to have ridden away from the face, and in an updip direction. The initial height of the first pack was 2030 mm (the width of each timber slab was originally 145 mm and the packsetter was originally 150 mm), but, after the fall of ground, the average height of the pack was measured as 1210 mm. The total difference in height is 800 mm, due to sudden closure.

Analyses of the other closure ride stations in West 4 panel, such as W423, W422 and W421, for the same time period reveals that, although some increases in closure rates were measured, these increases were insignificant when compared to that recorded at station W4P1. It is therefore deduced that considerable closure due to seismicity affected only a small (25 m^2) area of the stope.

Photographs 5.1 to 5.6 show all damages due to seismic event, in the hangingwall, and on the packs installed in this panel.



Photograph 5.1. Damage observed on packs installed along the gully of West 4 panel, 32 Level, 37 Line, East Driefontein Gold Mine (number 1 indicates the direction of this picture in Fig. 5.11).



Photograph 5.2. Observed local fall of ground in West 4 panel due to a seismic event occurred. Note that the hangingwall blocks were small and very fragmented (number 2 indicates the direction of this picture in Fig. 5.11).



Photograph 5.3. Damage observed on the gully packs due to a seismic event occurred in West 4 panel, 32 Level, 32 Line, East Driefontein Gold Mine (number 3 indicates the direction of this picture in Fig. 5.11).

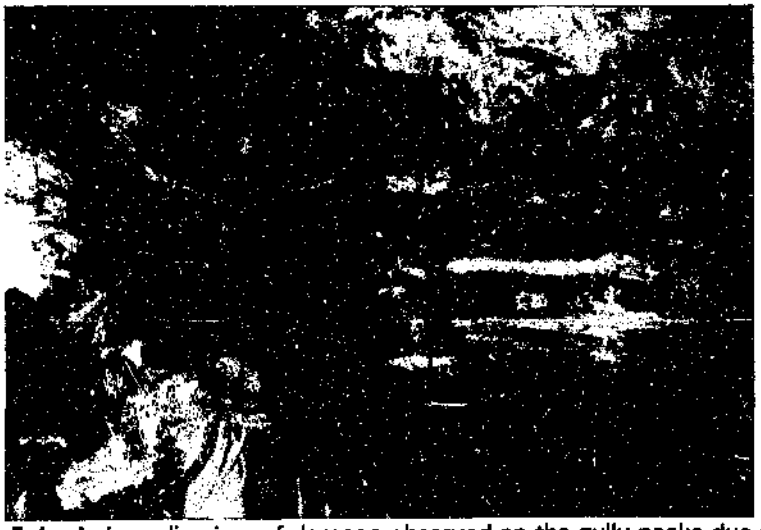

Photograph 5.4. A downdip view of damage observed on the gully packs due to a seismic event occurred in West 4 panel, 32 Level, 32 Line, East Driefontein Gold Mine (number 4 indicates the direction of this picture in Fig. 5.11).

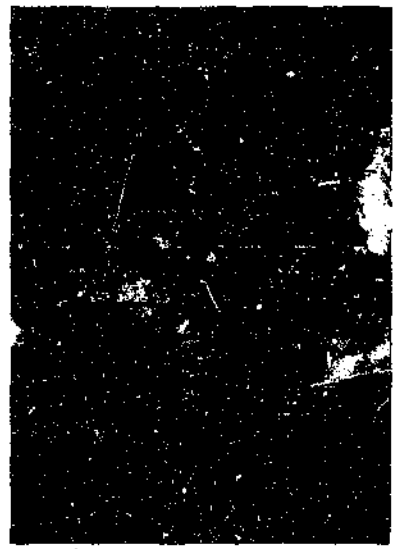

Photograph 5.5. Damage of seismic event on another pack installed next to gully of West 4 panel, 32 Level, 37 Line, East Driefontein Gold Mine (number 5 indicates the direction of this picture in Fig. 5.11).



Photograph 5.6. Observed damage due to a seismic event on another pack installed next to gully of West 4 panel, 32 Level, 37 Line, East Driefontein Gold Mine (number 6 indicates the direction of this picture in Fig. 5.11).

5.1.1.4 Extensometer stations

In order to identify the relative hangingwall and footwall contributions to the total closure, six boreholes (three hangingwall, three footwall) of 10 m depth were drilled in pairs in three different areas along the strike gullies (Fig. 5.7). These boreholes were equipped with extensometer anchors at 2 m intervals.

Extensometer readings indicate localised hangingwall separation (Figs. 5.12 to 5.14) with most of the separation being initiated by seismic events. A significant contribution from the footwall Jeppestown shale is not observed.

On 08/02/1994 a seismic event with a magnitude of 2.08 was recorded. The epicentre of this seismic event was 65 m away from the position of the extensometer along West 6 gully. The extensometer measurements (Figs. 5.14 a and) show that this event resulted in localised separation, confined to the hangingwall along the West 6 gully. The measurements in the footwall borehole and the second set of the hangingwall and the footwall boreholes along West 5 panel did not show any significant movement.

Three more seismic events were recorded on 25/05/1994, 06/06/1994, and 16/06/1994 confirming that seismically induced hangingwall separation is confined to the hangingwall (Fig 5.14 a).

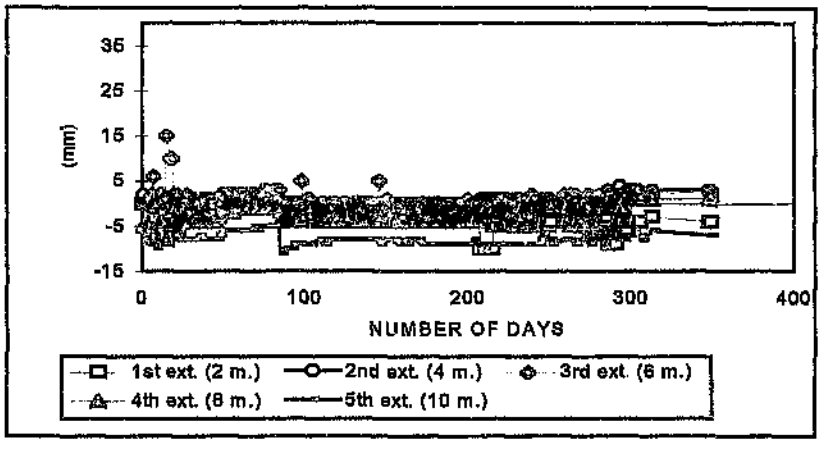

a

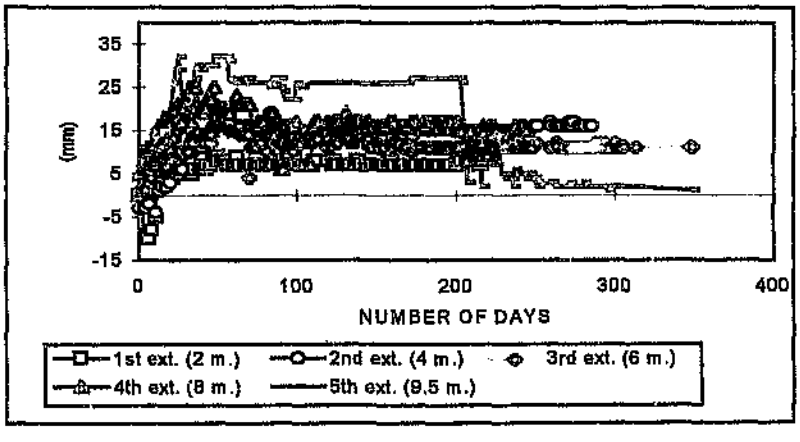

b

Figures 5.12 a and b. *Extensometer results from the first borehole in the hangingwall (a) and the footwall (b) along West 5 gully, 32 Level, 37 Line, No 4 Shaft, East Driefontein Gold Mine.*

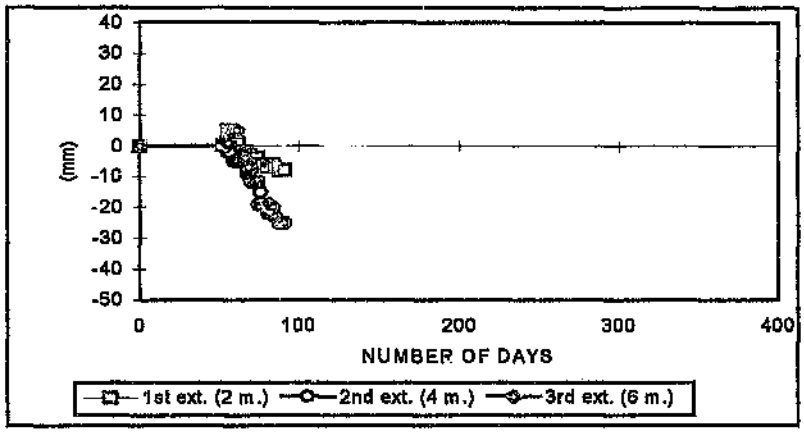

a

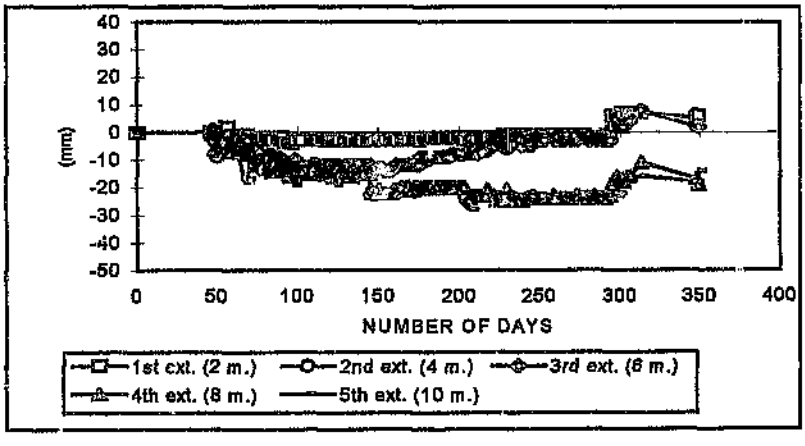

b

Figures 5.13 a and b. Extensometer results from the second borehole in the hangingwall (a) and footwall (b) along West 5 gully, 32 Level, 37 Line, No 4 Shaft, East Driefontein Gold Mine.

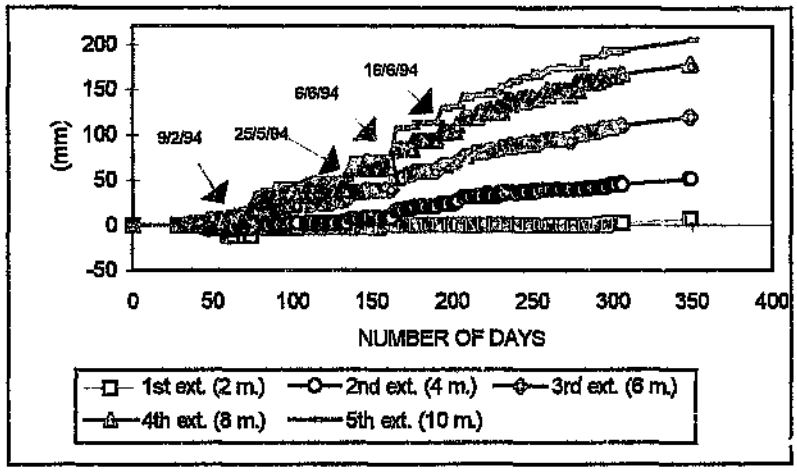

a

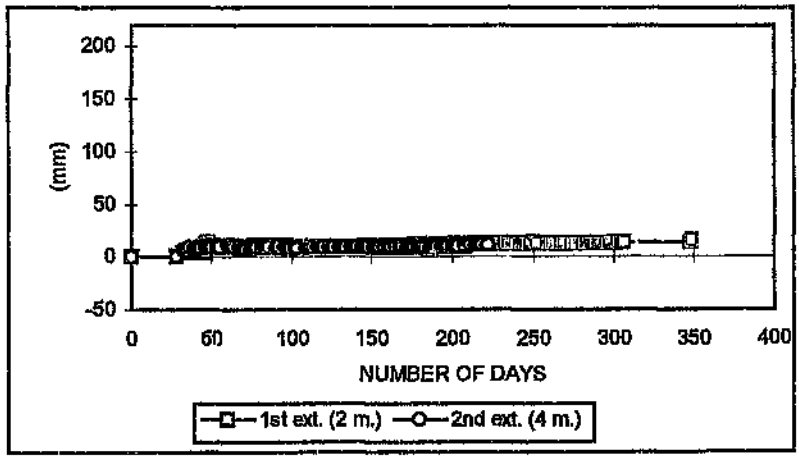

b

Figures 5.14 a and b. Extensometer results from the borehole in the hangingwall (a) and in the footwall (b) along West 6 gully, 32 Level 37 Line, No 4 Shaft, East Driefontein Gold Mine.

5.1.2 Deelkraal Gold Mine

At Deelkraal Gold Mine, quartzite/conglomerate comprises the footwall (Fig. 5.15). The hard lava is the hangingwall lithology over the total lease area (Fig. 5.16). One type of geotechnical area is defined by hard lava hangingwall and quartzite/conglomerate footwall (Fig. 5.17). The site is located on 27 Level 15 Line (Fig. 5.18). The VCR dips at 27 degrees and the depth varies between 2690 m and 2730 m. below datum. Underground monitoring and observations were carried out in five panels.

5.1.2.1 Mining induced stress fracture mapping

At the Deelkraal Gold Mine site, the general direction of mining induced stress fracturing in quartzite/conglomerate footwall was observed to be steeply dipping away from the face. The fractures in hard lava hangingwall are flat (about 45° to 55°). The point of inflection observed at the underground monitoring site at Deelkraal Gold Mine is in the footwall, (Fig. 5.19). Photographs of the mining induced stress fractures in the footwall and hangingwall are shown in Appendix B.

The hangingwall is massive in appearance, associated with large-sized falls of ground. The size of the falls of ground is controlled by the joint frequency and attitude, and the mining induced extension fracturing. The blocks of rock which can fall out are as large as 1.0 m / 1.1 m / 0.4 m in this geotechnical area.

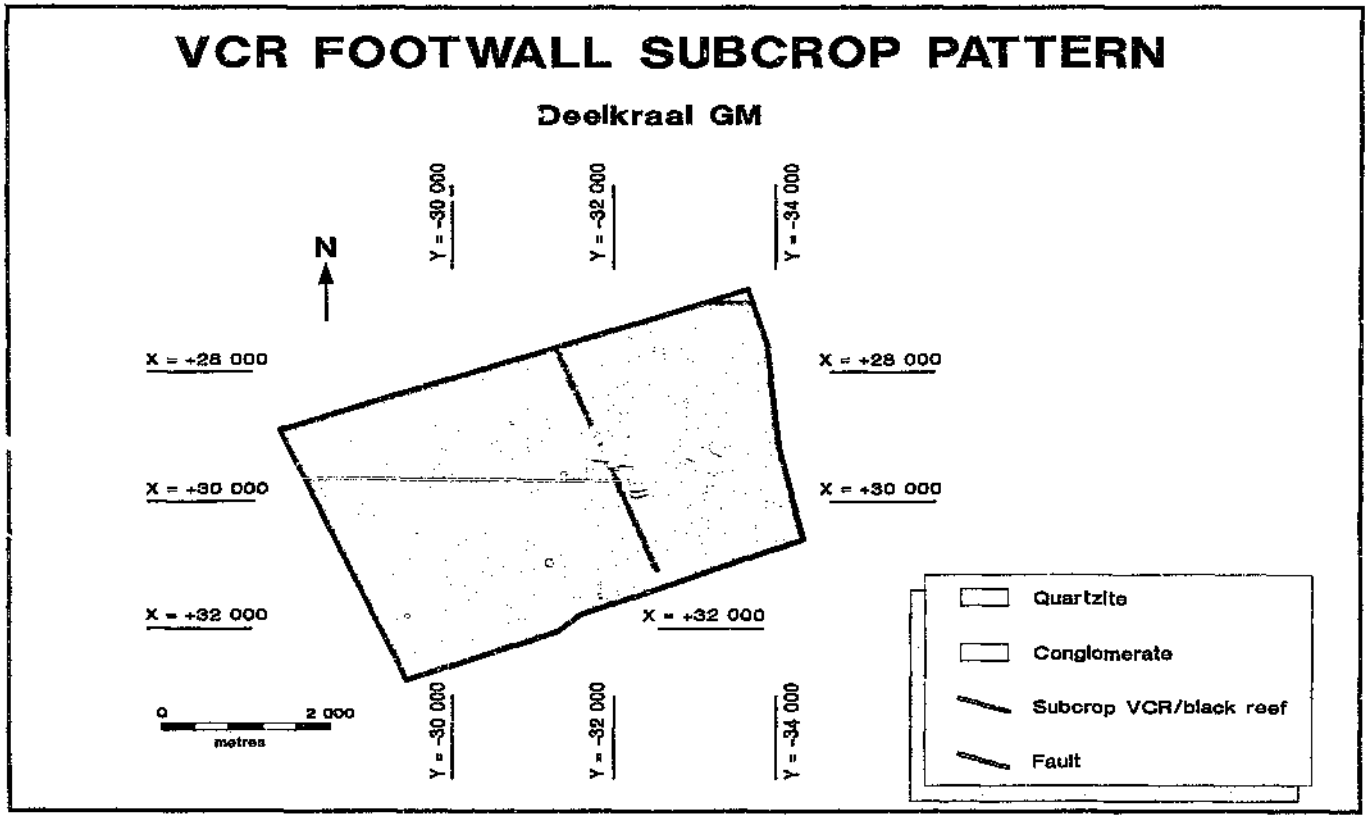

Figure 5.15. VCR footwall subcrop plan, Deelkraal Gold Mine (Schweitzer, pers. comm.,1993).

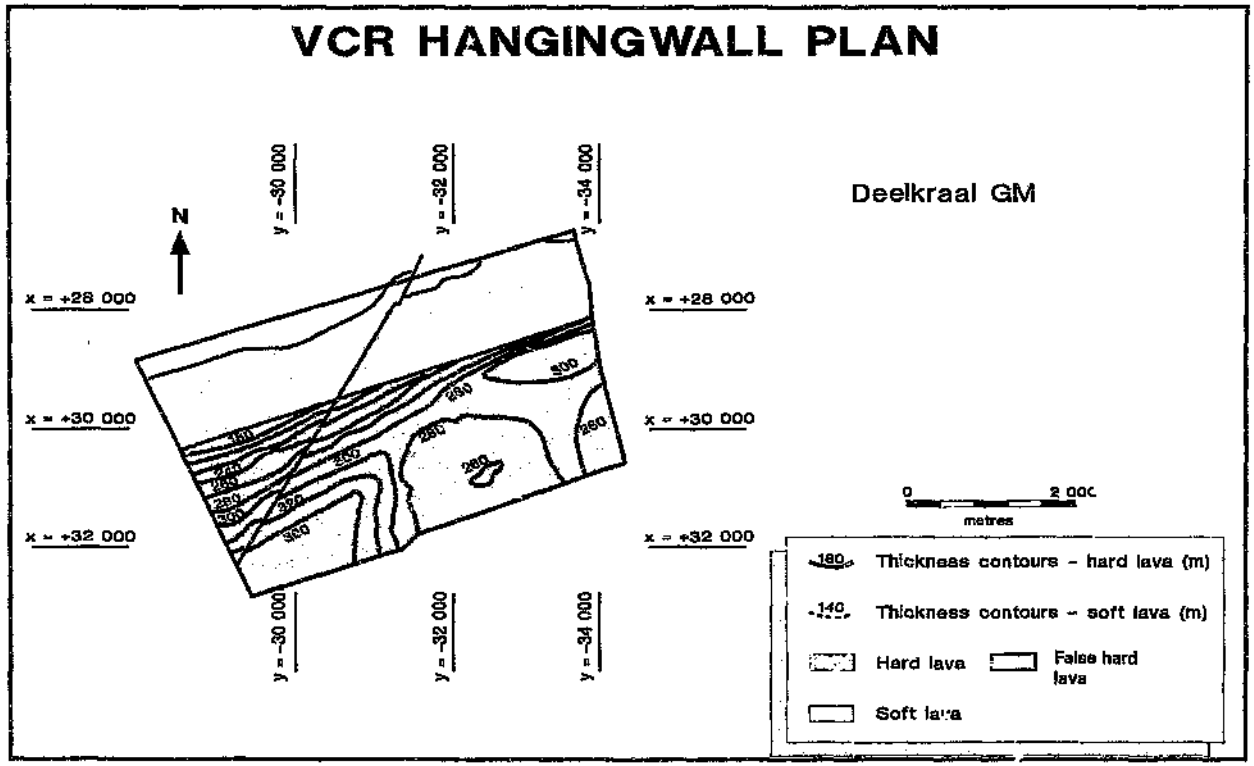

Figure 5.16. VCR hangingwall plan of Deelkraal Gold Mine. Grey colour delineates area of "false" hard lava thickness due to erosion by Black Reef (Schweitzer, pers. comm.,1993).

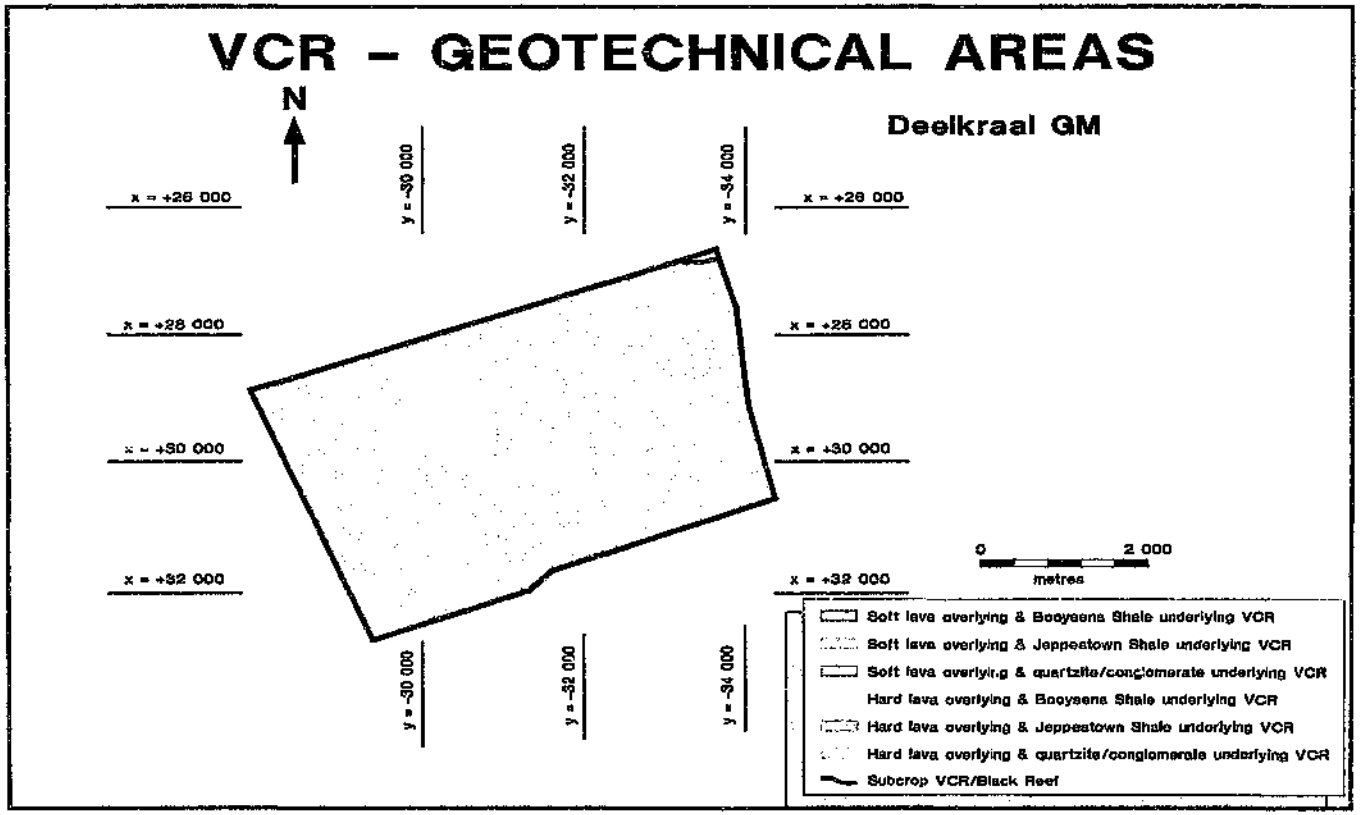

Figure 5.17. Geotechnical plan of Deelkraal Gold Mine (Schweitzer, pers. comm.,1993).

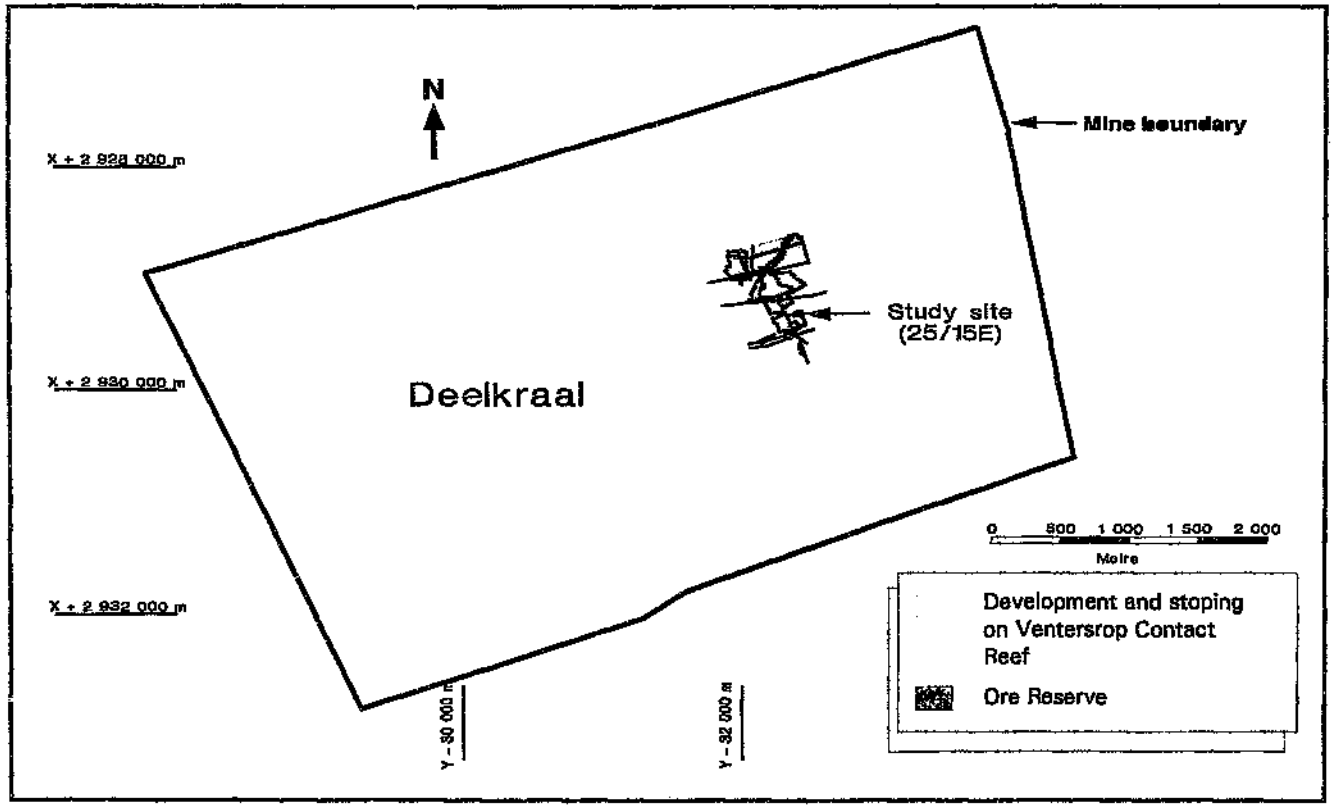

Figure 5.18. Locality of underground monitoring site (Schweitzer, pers. comm.,1993).

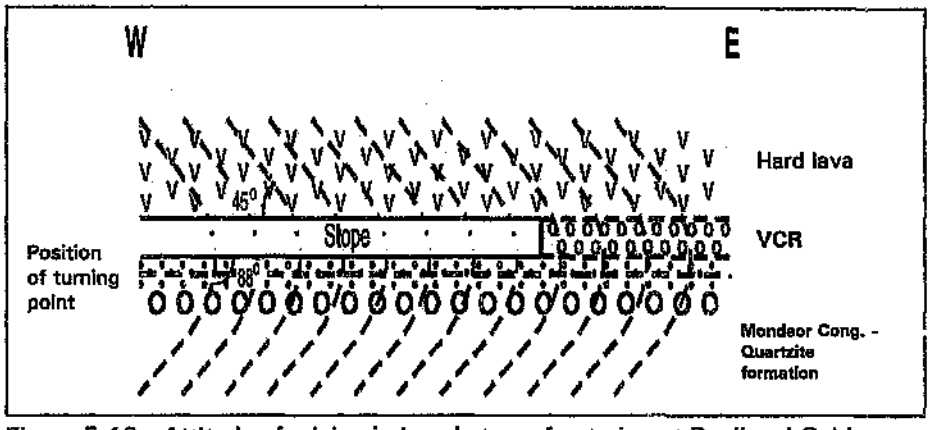

Figure 5.19. Attitude of mining induced stress fracturing at Deelkraal Gold Mine. The point of inflection occurs in the footwall of the excavation.

5.1.2.2 Closure-ride stations

The site is located on 27 Level 15 Line with the depth varying between 2690 m and 2730 m below datum, at a dip of 27 degrees. The positions of the installed stations are shown in Figure 5.20. Measurements were taken since August 1993.

The same methodologies of closure ride station installation and closure rate calculation as explained in Chapter 5.1.1.2 were adopted for this geotechnical area.

At Deelkraal Gold Mine, closure rates are low, on average about 5 mm per day. The closure rates on the uppermost panels, E1 and E5 are slightly higher, with an average of about 6 to 7 mm per day. It is suggested that these differences may be related to different rates of face advance. The information is summarised in Figures 5.21 to 5.25.

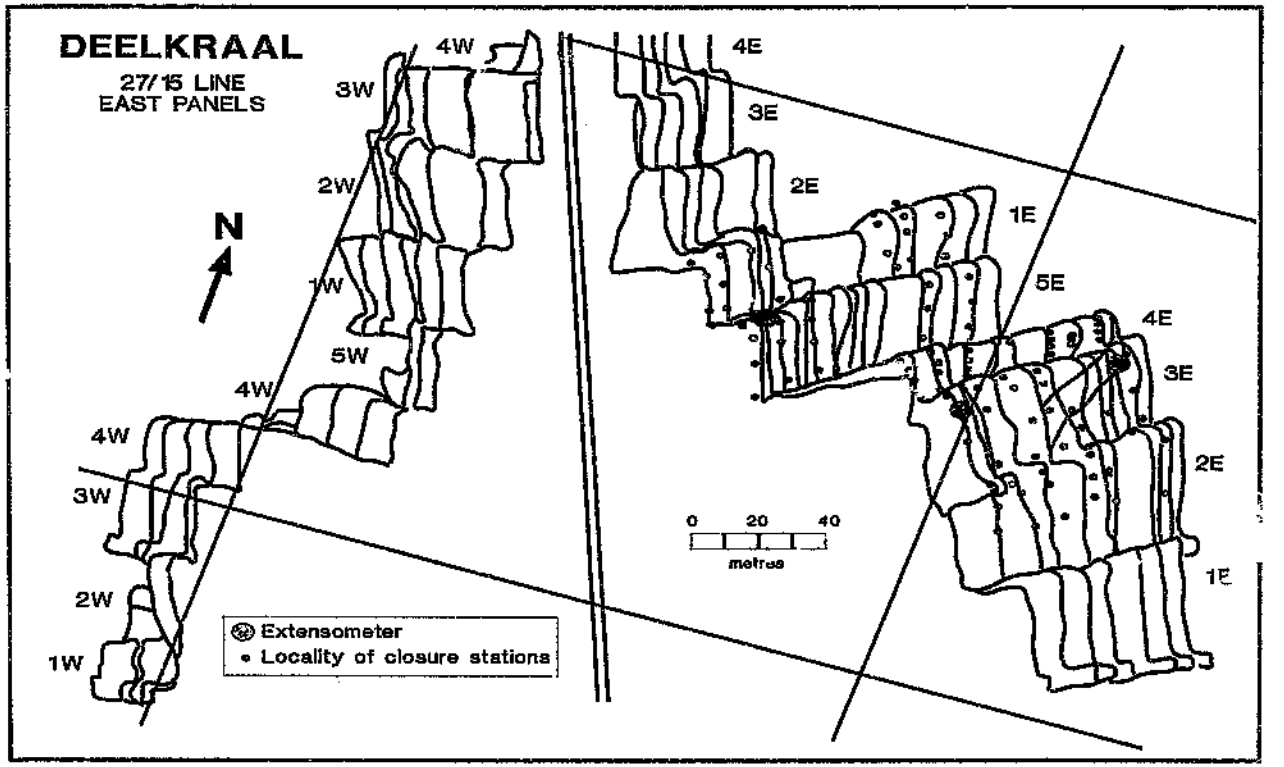

Figure 5.20. The general panel layout, face position, and location of each station at the monitoring site on 27 Level, 15 Line, Deelkraal Gold Mine.

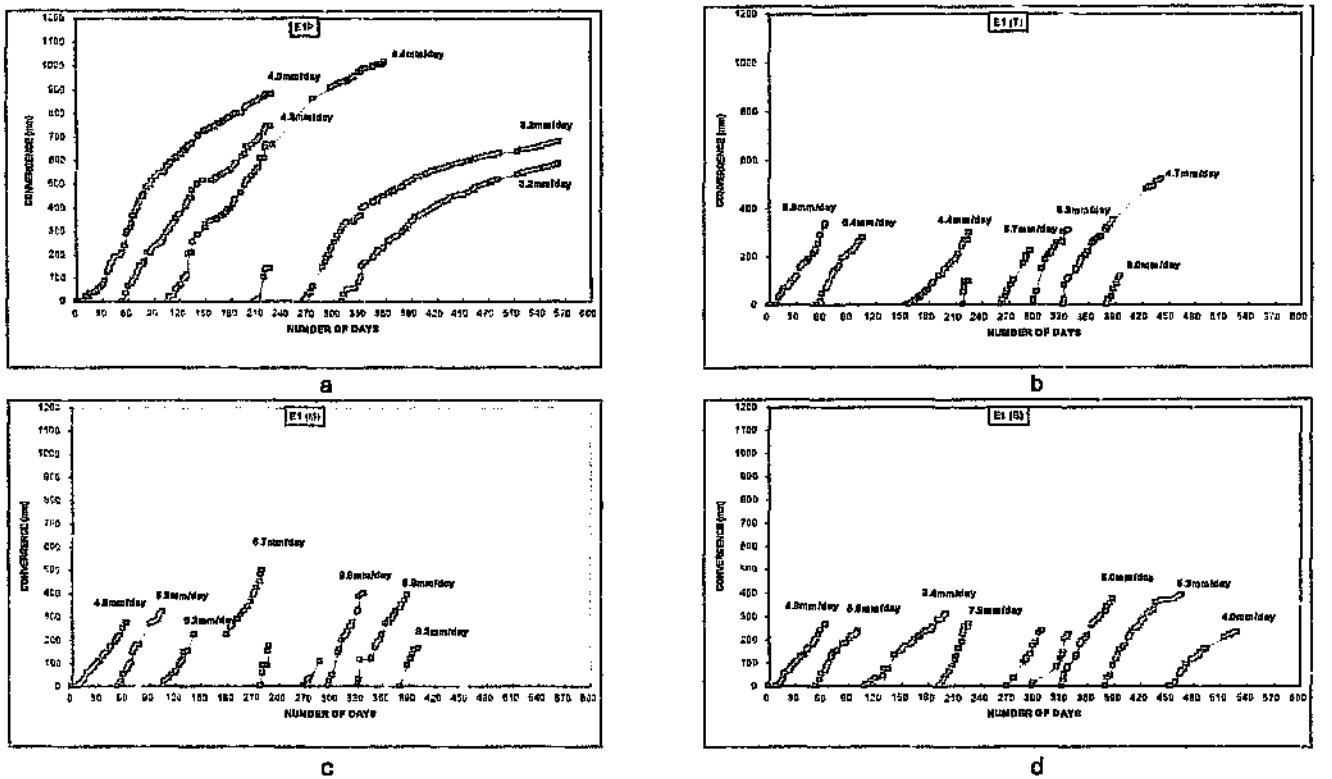

Figures 5.21 a to d. Closure rates at the permanent station (a), and the temporary stations at the top (b), middle (c) and bottom (d) of the face in East 1 panel, 27 Level, 15 Line, Deelkraal Gold Mine.

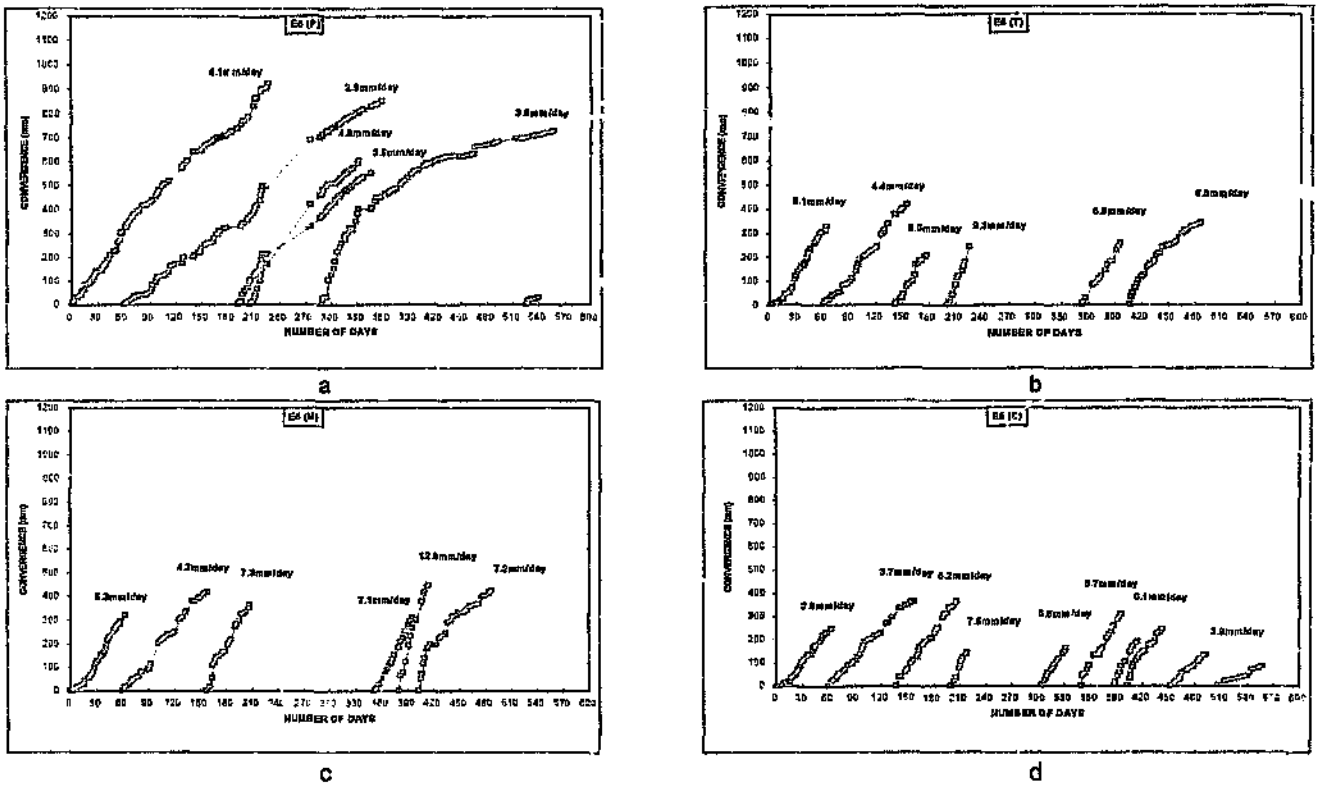

Figures 5.22 a to d. Closure rates at the permanent station (a), and the temporary stations at the top (b), middle (c) and bottom (d) of the face in East 5 panel, 27 Level, 15 Line, Deelkraal Gold Mine.

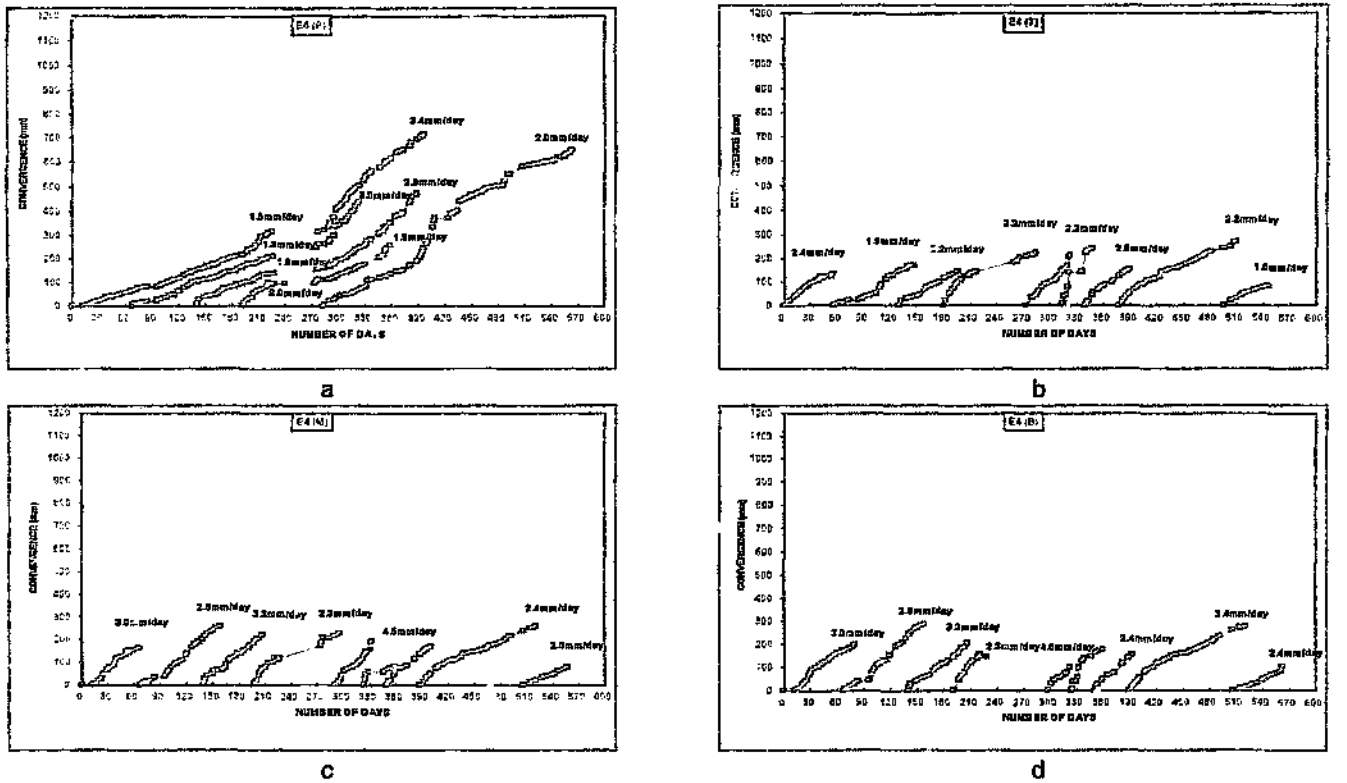

Figures 5.23 a to d. Closure rates at the permanent station (a), and the temporary stations at the top (b), middle (c) and bottom (d) of the face in East 4 panel, 27 Level, 15 Lir·, Deelkraal Gold Mine.

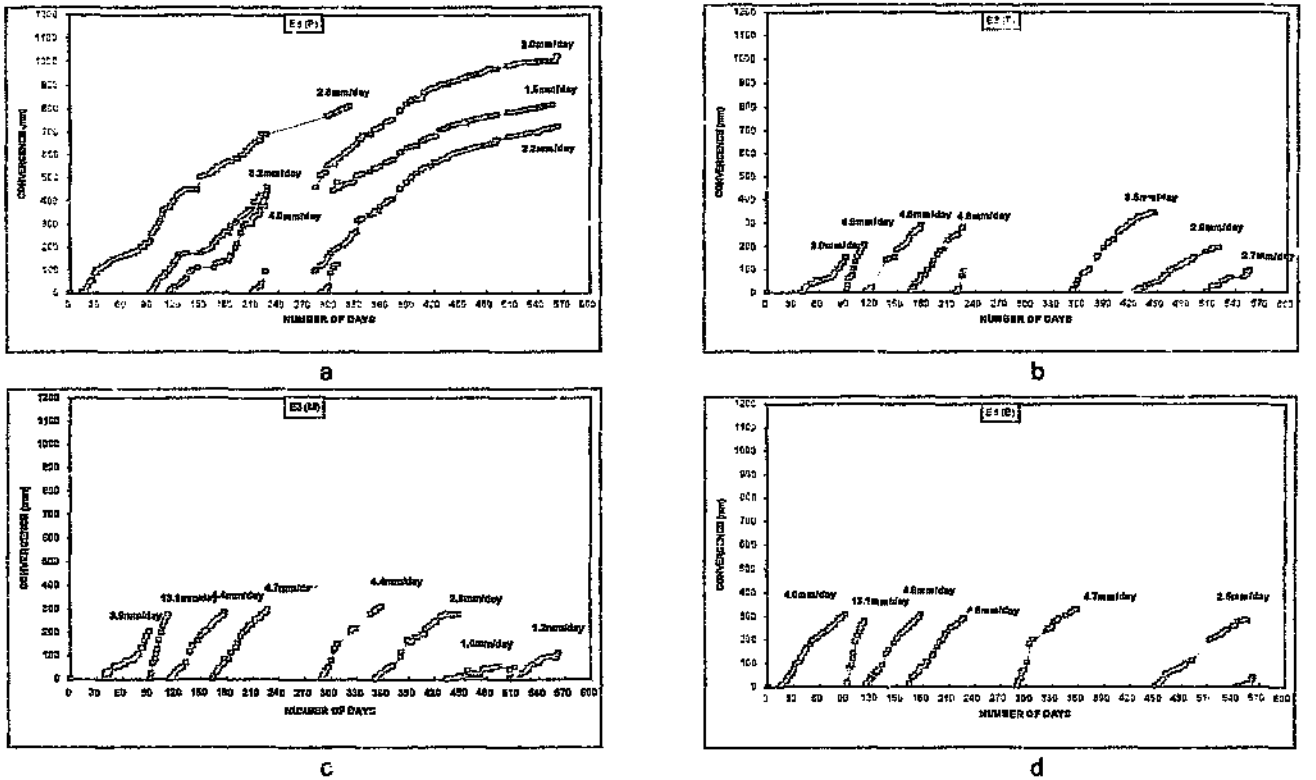

Figures 5.24 to d. Closure rates at the permanent station (a), and the temporary stations at the top (b), middle (c) and bottom (d) of the face in East 3 panel, 27 Level, 15 Line, Deelkraal Gold Mine.

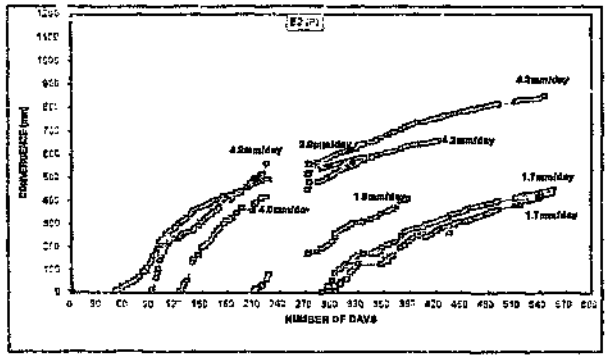

a

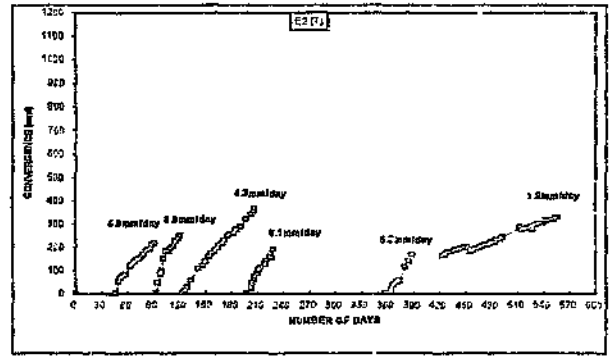

b

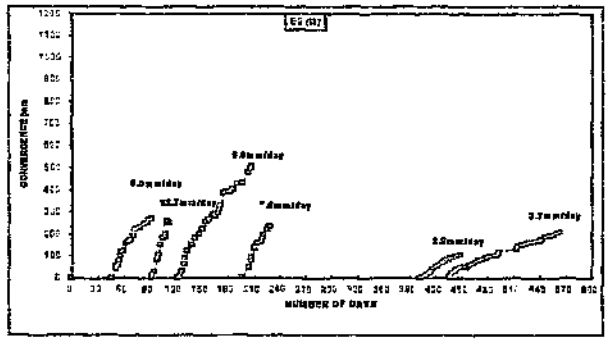

c

Figures 5.25 a to c. Closure rates at the permanent station (a), and the temporary stations at the top (b), and middle (c) of the face in East 1 panel, 27 Level, 15 Line, Deelkraal Gold Mine.

5.1.2.3 Extensometer stations

In order to identify the relative hangingwall and footwall contributions to total closure, a number of boreholes of 10 m depth were drilled in pairs in three different areas along the advanced strike gullies and in the stope. After each hole was drilled, it was mapped for fractures by petroscope or borehole camera. Finally, the holes were equipped with borehole extensometers with anchors set at 2 m intervals. The extensometers were sited in the same panels in which closure-ride stations were installed. In total, three sets of holes, along the East 1, 3, and 4 panels, were drilled and equipped (Fig. 5.26).

Extensometer readings (Figs. 5.27 to 5.29) show that hangingwall and footwall separations occurred. Most of the separation was initiated by a seismic event in both the hangingwall and footwall. While a more complex rock mass behaviour is observed in the hangingwall formation over the following days, the footwall formation did not indicate any further significance over this time period.

Fracture mapping of the boreholes in the hangingwall (Fig. 5.30a/a) was completed on 09/02/1995. Although the real position of the fractures was recorded, it was not possible to measure their dip angles because of technical problems with the petroscope. This borehole was equipped with borehole extensometers (Fig. 5.30a/b) on the same date.

Two seismic events, shown by red crosses in Figure 5.26, with magnitudes of 0.3 and 1.3 were recorded on 7/03/1995. A separation of 63 mm was observed in the first 2 m of the hangingwall (Fig. 5.30a/c), immediately after these seismic events were recorded. During the next two days, the hard lava formation between the second and fourth metres of the hangingwall continued to separate a further 10 mm. During the same period, the hard lava formation between the fourth and sixth metres closed by a total of 12 mm on the existing fractures (Fig. 5.30a/d). In the following three

months, the hard lava formation between the fourth and the sixth metres of the hangingwall closed by further 8 mm, and a further closing of 20 mm was observed in the hard lava formation between the sixth and tenth metres of the hangingwall (Fig. 5.30a/e).

The same type of fracture mapping was also carried out in the footwall borehole, drilled in the same panel. Its position, as well as total number of fractures and borehole extensometers installed, are shown in Figures 5.30b/a and 5.30b/b, respectively. After the two seismic events had occurred, the same amount of separation of strata, as recorded in the hangingwall, was observed in the footwall strata between the first and second metres (Fig. 5.30b/c). No further separation or closing of the formation, in the first 10 m of the footwall, was noted subsequently.

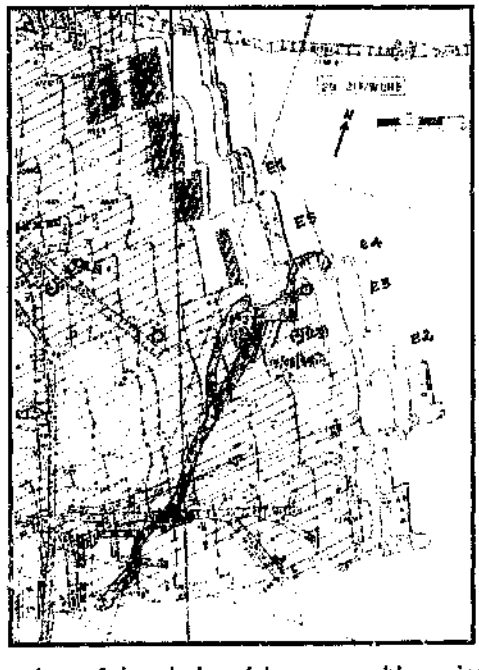

Figure 5.26. Location of boreholes (shown as blue circles) and seismic events (shown as red crosses) on 27 Level, 15 Line, Deelkraal Gold Mine.

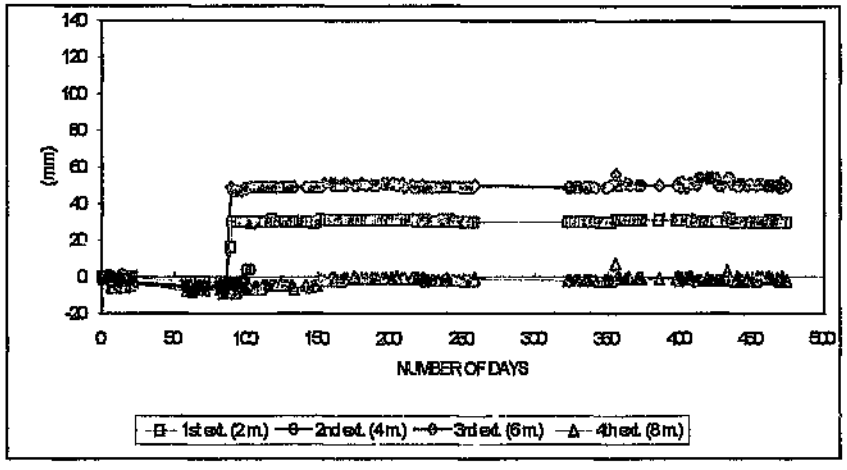

a

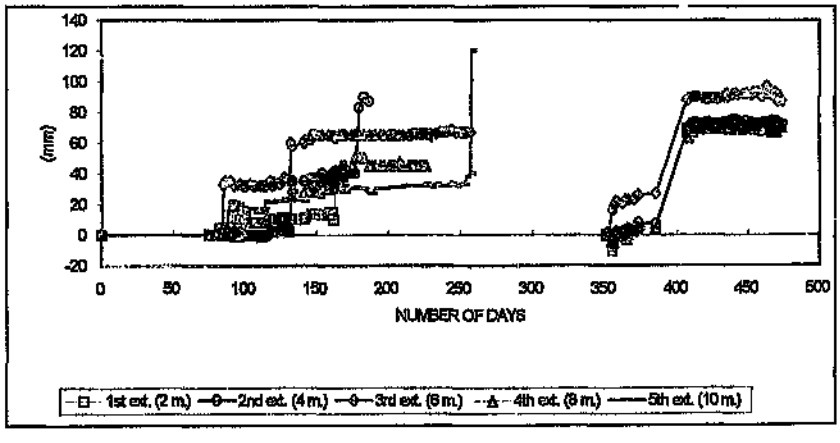

b

Figures 5.27 a and b. Extensometer results from the borehole in the hangingwall (a) and footwall (b), East 1 gully, 27 Level, 15 Line, Deelkraal Gold Mine.

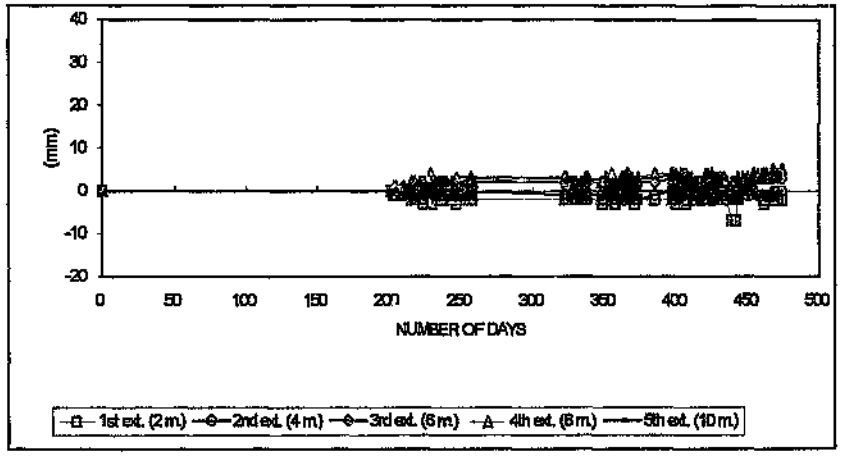

a

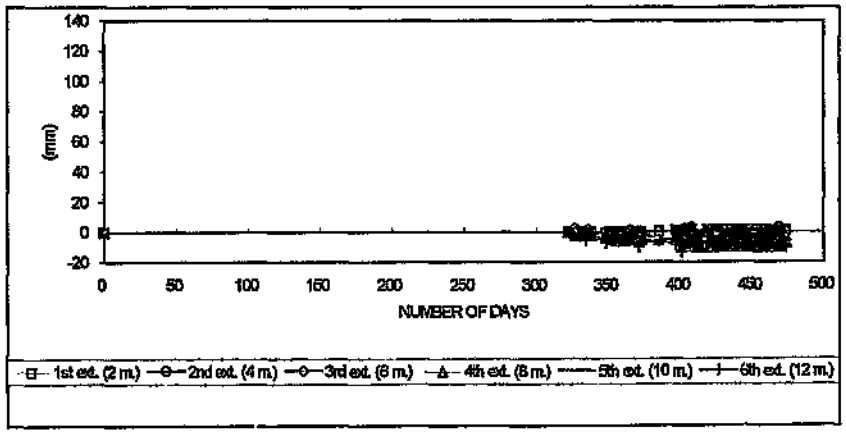

b

Figures 5.28 a and b. Extensometer results from the borehole in the hangingwall (a) and footwall (b), East 4 gully, 27 Level, 15 Line, Deelkraal Gold Mine.

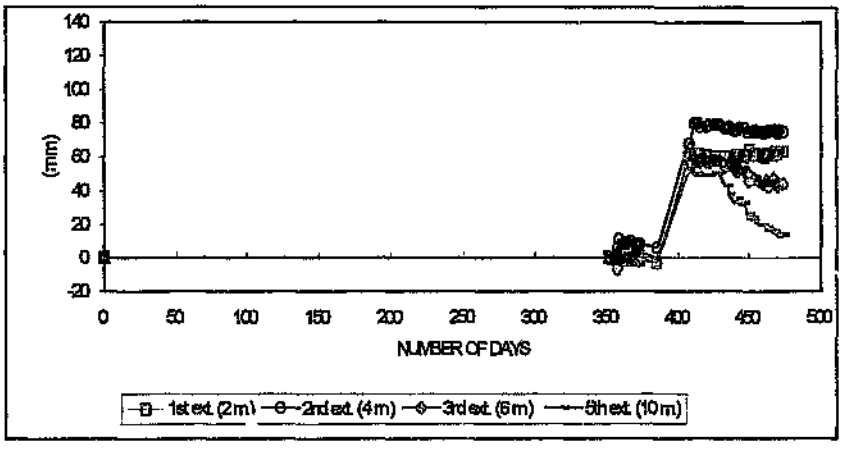

a

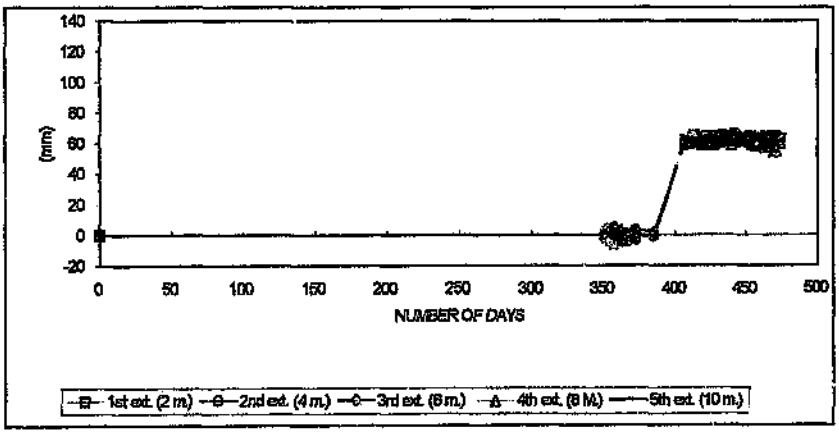

b

Figures 5.29 a and b. Extensometer results from the borehole in the hangingwall (a) and footwall (b), East 3 panel, 27 Level, 15 Line, Deelkraal Gold Mine.

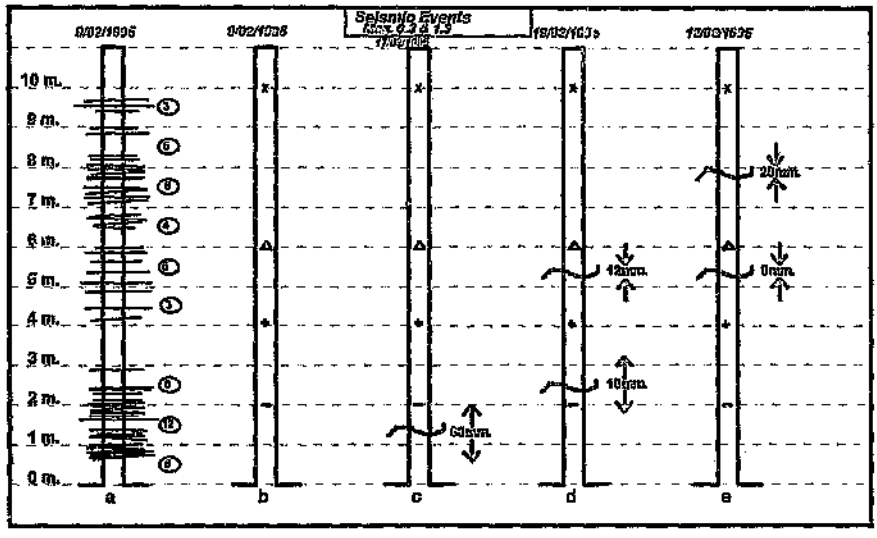

a

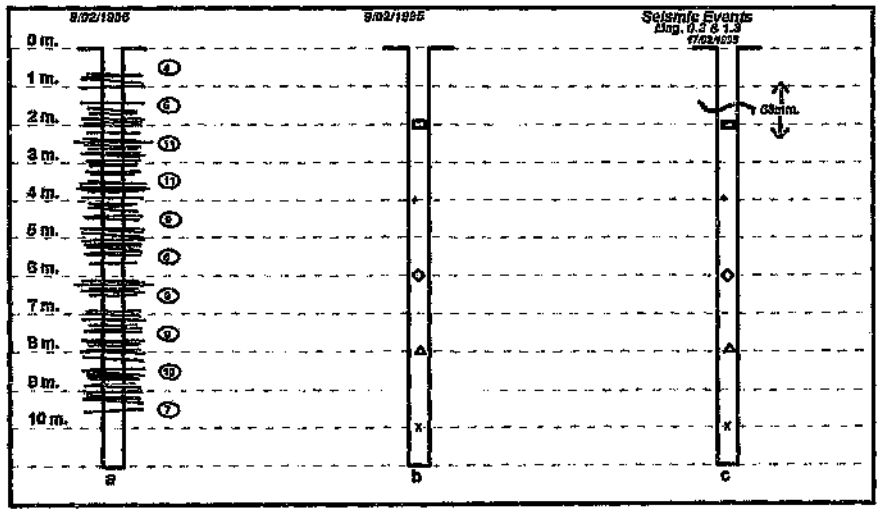

b

Figures 5.30 a and b. Position of fractures and borehole extensometers installed in the boreholes drilled in the hangingwall (a) and footwall (b) and in East 3 panel, 27 Level 15 Line, Deelkraal Gold Mine. Circled numbers refer to the number of fractures that were observed.

5.1.2.4 Analysis of falls of ground sizes

In order to understand differences in the shape and size of blocks that have fallen out of the hangingwall, a study was carried out in the geotechnical area as defined for Deelkraal Gold Mine.

The experimental site was selected at East 3 Panel, 27 Level, 15 Line where the face is about 40 m long and the VCR dips 27° to the NNE-SSW. The study site extended from the face to about 75 m into the back area. The general face layout is shown in Figure 5.31. The production in this panel was stopped some time ago due to pronounced falls of ground in the face area.

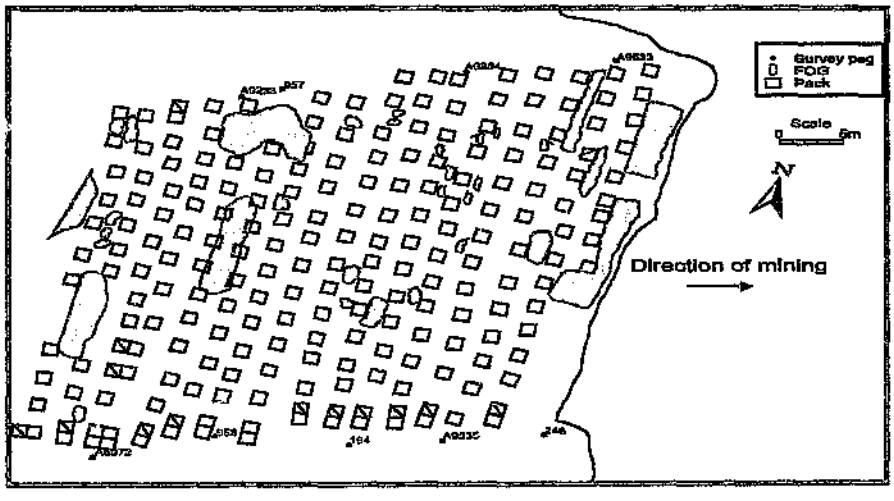

Figure 5.31. Panel layout and the positions of falls of ground (grey area) in E3 panel, 27 Level, 15 Line, Deelkraal Gold Mine.

The face was divided into regions positioned between packs. The sizes of the falls of ground were measured at three points along the strike direction, at the top, middle and bottom of each pack along each line. Along 15 lines, 1748 measurements were taken at different points over an area of 3000 m².

The measurements taken along each section line are shown in Figure 5.31. The data are summarized as follows:

Thickness (cm)	Cumulative %	Thickness (cm)	Cumulative %
10	31.69	110	96.68
20	53.47	120	97.54
30	71.69	130	98.40
40	77.71	140	98.74
50	82.92	150	99.14
60	87.05	160	99.66
70	89.40	170	99.71
80	92.15	180	99.89
90	93.18	190	99.89
100	95.07	200	100.0

Figure 5.32 shows the cumulative percentages of the thickness of falls: 95 % of the fallen blocks are less than 100 cm thick; these blocks are typically 1.0 m / 1.1 m / 0.4 m in size.

In summary; the results obtained at underground monitoring sites are presented; these consider underground measurements with respect to closure-ride and extensometer stations, as well as mining induced stress fracture mapping, and falls of ground.

The results as obtained in two different geotechnical areas show that there are significant differences in the rock mass behaviour in terms of:

- measured closure rates;
- contribution to the total closure in the footwall and hangingwall stratigraphies;
- general orientation of the mining induced stress fractures; and
- the size of falls of ground.

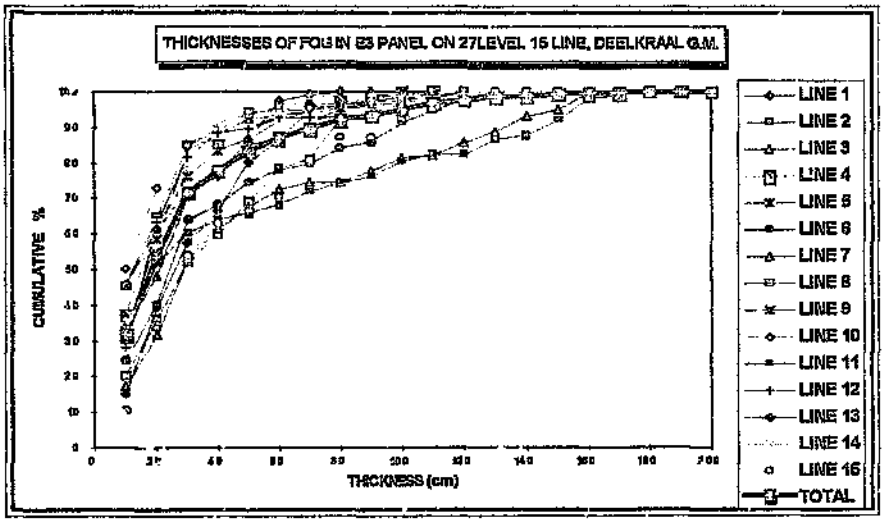

Figure 5.32. Observed thicknesses of falls of ground in E3 panel, 27 Level, 15 Line, Deelkraal Gold Mine. The thick red line delineates the average of all the lines measured in this panel.

CHAPTER 6

6 NUMERICAL MODELLING

The underground measurements and observations indicate significant differences in behaviours of the rock mass surrounding the VCR in various geotechnical areas. These measurements and observations include in particular the closure in the stope and the pattern of fracturing around the stopes. It was suggested that the different rock types could have a significant effect on these differences in various geotechnical areas.

Analysis of the measured underground closure in different geotechnical areas with the elastic convergence would be a good way to compare various geotechnical areas. It is also a very useful means of assessing by how much the laboratory derived Young's Modulus should be reduced to enable the elastic convergences obtained from the model to best fit the observed closure pattern. This technique is applied mainly to simulate in situ closures more accurately when assessing the performance of stope support, in particular backfill. It should be noted that this change to the moduli has some detrimental implications particularly for off-reef results (Johnson, 1994).

The other reason why it was decided to use numerical modelling is to investigate whether numerical modelling could be used to indicate that it is differences in hangingwall and footwall rock properties which cause the fracture patterns in VCR stopes to vary.

Basically two different numerical modelling methods, i.e. Mining Simulation programme (MINSIM-D) and Fast Langrangian Analysis of Continua (FLAC), were applied to research the issues explained above.

6.1 MINSIM-D MODELLING

MINSIM-D is a boundary element program useful for modelling multiple tabular excavations, which may be arbitrarily oriented with respect to one another, producing stresses, displacements and other parameters useful for mine layout planning (Johnson, 1991). It assumes that the rock mass is isotropic and behaves elastically.

In order to obtain realistic closures the laboratory measurements of Young's Modulus in the simple elastic analysis performed are down graded. Down grading of the moduli compensates for the lack of inelastic closure.

6.1.1 East Driefontein Gold Mine

The VCR was digitised in three different planes because of different depth, dip and strike of the VCR at this site. The Jean's Fault separates the VCR into two different planes with an almost 80 m elevation difference in the vicinity of the 37 Line. The third VCR plane is defined along the 34 Line due to a pronounced change in strike of the VCR at this location (Fig. 6.1).

The area modelled extends from the 20 to the 45 longwall faces (Fig. 6.1). Figure 6.2 depicts a fine window showing the mining steps over the same time period as the monitoring site at the 32 Level, 37 Line site.

The original modelling and analysis were carried out using different Young's Moduli of 20 GPa, 40 GPa and 70 GPa (Table 6.1 for input values).

Modelled (MINSIM-D runs) and observed convergence rates are compatible with runs when using a Young's Modulus of 20 GPa (Figs. 6.3 a and b).

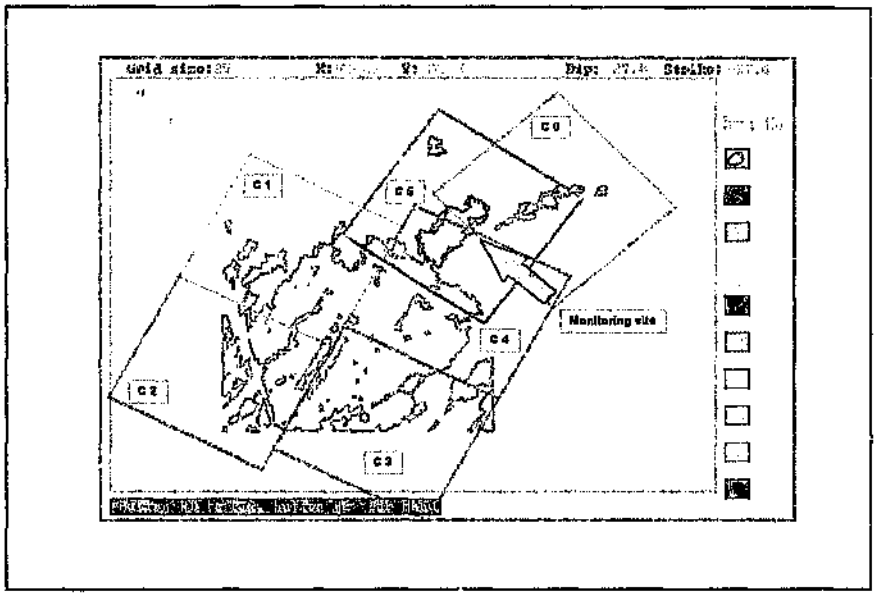

Figure 6.1. Digitised plan showing the extent of mining on the VCR from August 1993 to April 1994, East Driefontein Gold Mine. The six coarse windows (C1-C6) are also shown.

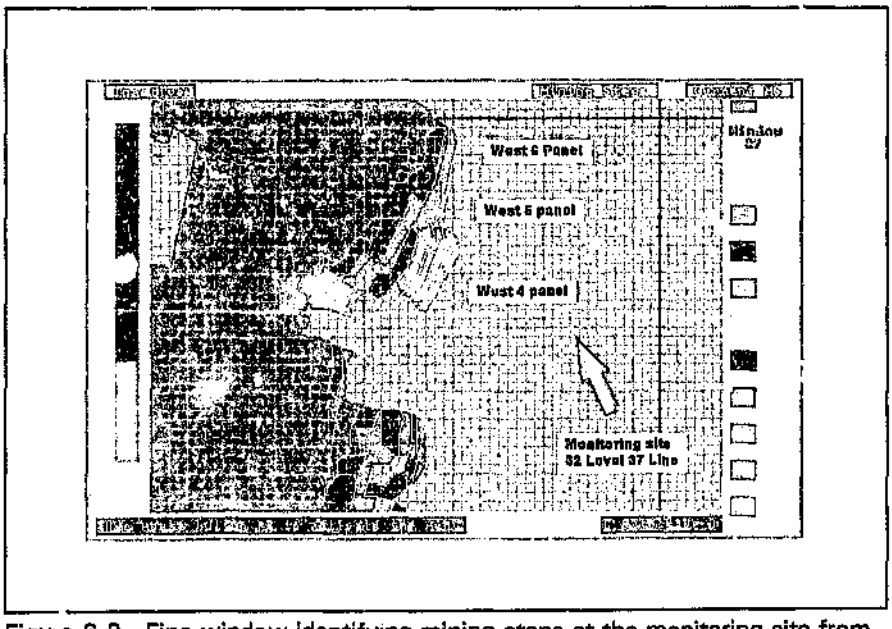

Figure 6.2. Fine window identifying mining steps at the monitoring site from August 1993 to April 1994, 32 Level, 37 Line, East Driefontein Gold Mine.

Table 6.1. Summary of input values as utilised during MINSIM-D modelling for the East Driefontein Gold Mine site.

Number of reef plans digitized	:	3
Number of coarse windows	:	6
Coarse window grid size	:	25 m
Number of fine windows	:	1
Fine window grid size	:	6.25 m
Stoping width	:	1.5 m
Fill width	:	1.4 m
The input value of "a"	:	10
The input value of "b"	:	0.4
Friction angle	:	30°
Poisson's ratio	:	0.2

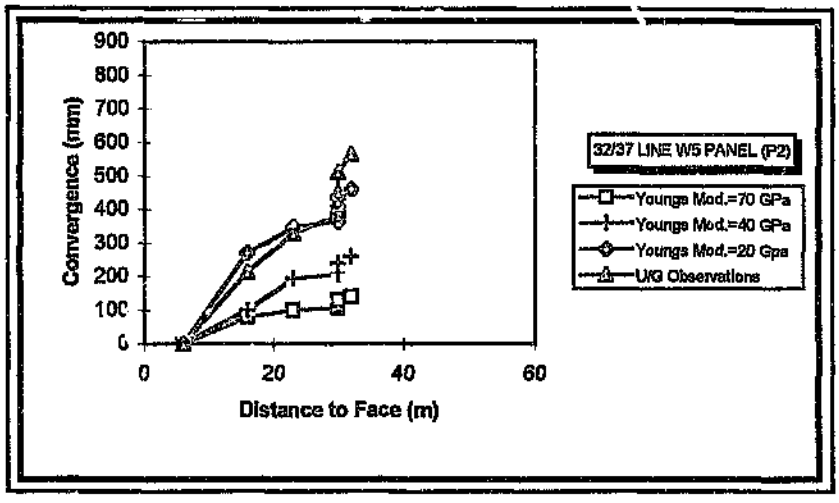

a

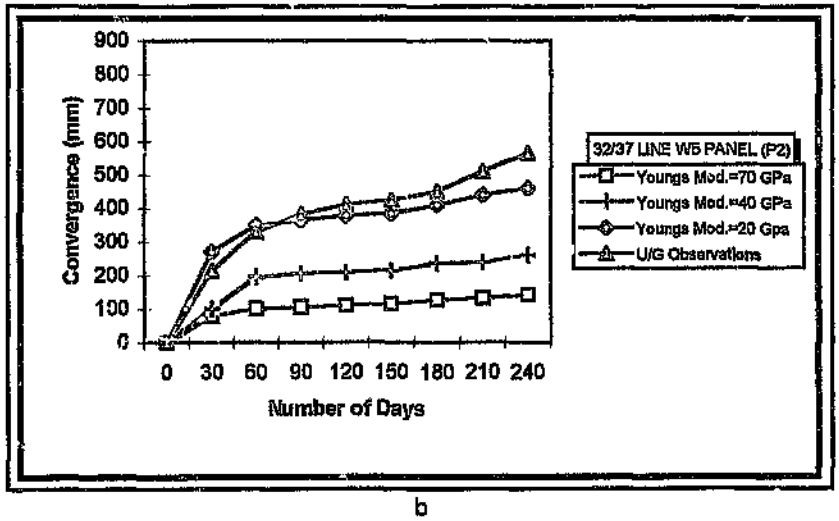

b

Figures 6.3 a and b. Comparison of MINSIM-D runs for different Young's Moduli, with actual underground measurements considering closure versus distance to face (a) and closure versus number of days (b).

6.1.2 Deelkraal Gold Mine

At Deelkraal Gold Mine, the VCR was digitised as one continuous plan. The original modelling and analysis was carried out using different Young's Moduli of 20 GPa, 30 GPa and 70 GPa. All input values are summarised in Table 6.2.

Tabl 6.2. Summary of input values considering during the MINSIM-D modelling for the Deelkraal Gold Mine.

Number of reef plans digitized	:	1
Number of coarse windows	:	4
Coarse window grid size	:	8.0 m
Number fine windows	:	1
Fine window grid size	:	2.0 m
Stoping width	:	1.5 m
Fill width	:	1.4 m
The input value of "a"	:	10
The input value of "b"	:	0.4
Friction angle	:	30°
Poisson's ratio	:	0.2

The area modelled and the mining steps are delineated in Figures 6.4 and 6.5. The results of the modelled and observed convergence rates are shown in Figures 6.6 a to d. MINSIM-D results and underground observations are compatible when using a Young's Modulus value of 30 GPa. A reduction of around 50 % is appropriate for this geotechnical area (Figs. 6.6a to d).

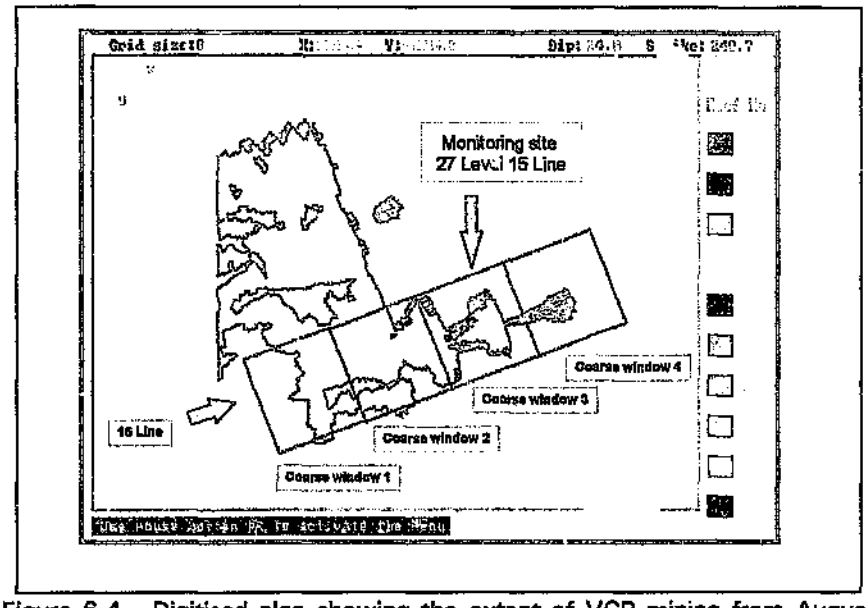

Figure 6.4. Digitised plan showing the extent of VCR mining from August 1993 to May 1994, 15 Line, Deelkraal Gold Mine. The positions of the coarse windows are also indicated.

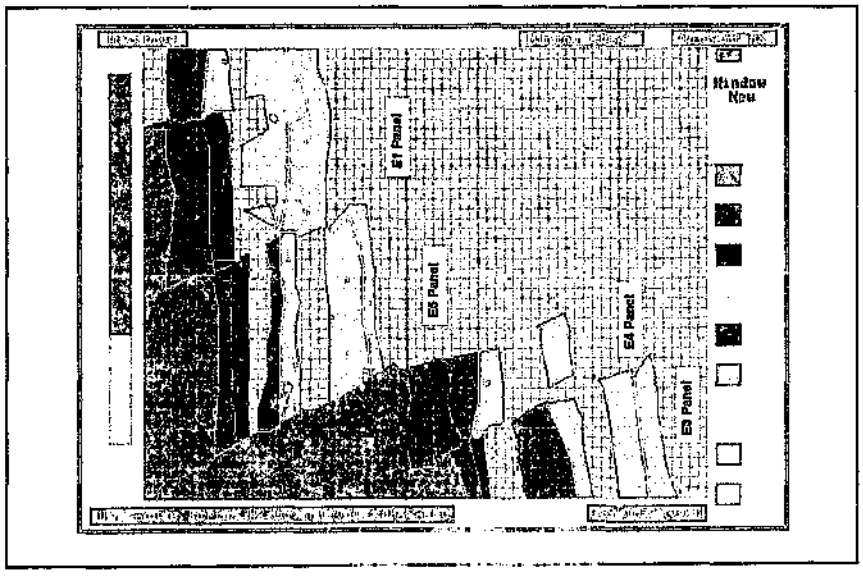

Figure 6.5. Fine window showing mining steps on the monitoring site from August 1993 to May 1994, 27 Level, 15 Line, Deelkraal Gold Mine.

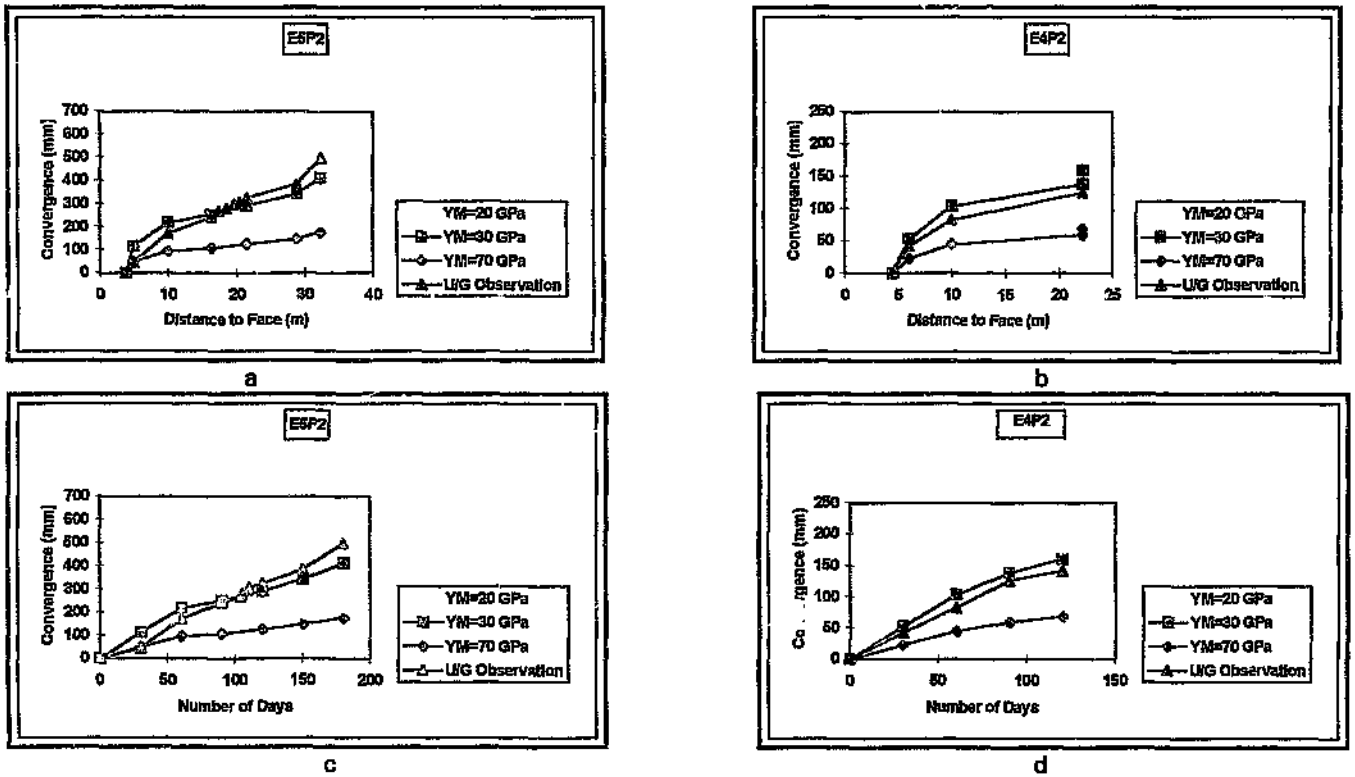

Figures 6.6 a to d. Comparison of MINSIM-D runs for different Young's Moduli with actual measurements taken from underground, in the graphs of closure versus distance to face (a) and closure versus number of days (b).

6.2 FLAC MODELLING

FLAC is two dimensional explicit finite difference code which simulates the behaviour of structures built of soil, rock or other materials which may undergo plastic flow when their yield limit is reached (FLAC Manual, Volume 1, 1993).

FLAC has been used to model the multi material rock mass surrounding a stope. The primary reason why FLAC model has been used is to investigate the mechanism that lead to the observed differences in rock mass behaviour, in particular differences in fracture patterns on Deelkraal and East Driefontein Gold Mines.

The approach used in modelling the rock mass behaviour around the VCR was to set up a simple model; this model was established using FLAC. A simple geometry was used, i.e. a strike section through a stope of uniform width. Different material properties in the hangingwall, reef and footwall were superimposed onto this geometry. Three of the various material constitutive laws available in FLAC were applied in the order of increasing complexity, i.e. elastic, Mohr-Coulomb and Mohr-Coulomb with strain-softening. Initially, before laboratory results became available, the sensitivity of the rock mass behaviour to elastic stiffness and strength properties was analysed using both the elastic and Mohr-Coulomb models. These properties were artificially contrasted in the hanging-and footwalls.

Principal stress directions are taken to be an indication of the direction in which fractures form; extension fractures are known to form parallel to the direction of the major principal stress. A method of displaying this information has been devised with the hypothesised fracture directions plotted as lines in the first grid in the hangingwall and footwall. This information can also be plotted as angle versus stope half span. The constitutive model is not adjusted for the presence of fractures. Initially no

fracture criterion is applied to determine when fractures form just ahead of the face. The fracture directions recorded in this way are compared with those observed underground.

6.2.1 Description of the model

The initial model that developed by Dr. R.A. EVE considers a horizontal stope of uniform width of 1.4 m, at 2500 m depth. In later, to be able to model as same as underground sites where data were collected, some part of this particular model was modified as the reef is parted from both the hangingwall and footwall by defined interfaces above and below the reef. These interfaces are unglued along the contact with the reef. In addition to these two interfaces, another nine interfaces were defined to identify some bedding layers in the sedimentary footwall. All these bedding layers are parallel to the reef and have an individual thickness of 0.5 m. Another two interfaces are included one above and one below the reef. All the interfaces are glued from 100 m ahead of the final face position, to the end of the boundary of the model.

Boundary conditions are defined as follows: the top and bottom of the model are fixed in the y-direction by setting the y-component of the velocity of each grid point to zero; the left-hand side of the model is fixed by applying the x-component of the velocity of each grid point as zero; and to the right hand side a stress condition is applied. The initial maximum principal stress, σ_1, is assumed to act vertically and is applied with a value of 67.5 MPa at the middle level of the model. A "k ratio" of 0.5 is assumed hence the intermediate principal and minimum principal stresses (σ_2 and σ_3) are each assumed to be 33.75 MPa (Fig. 6.7). The results of triaxial and uniaxial tests form the input rock properties as used in the model. The value of tension cut-off was assumed as 10 % of the value of cohesion.

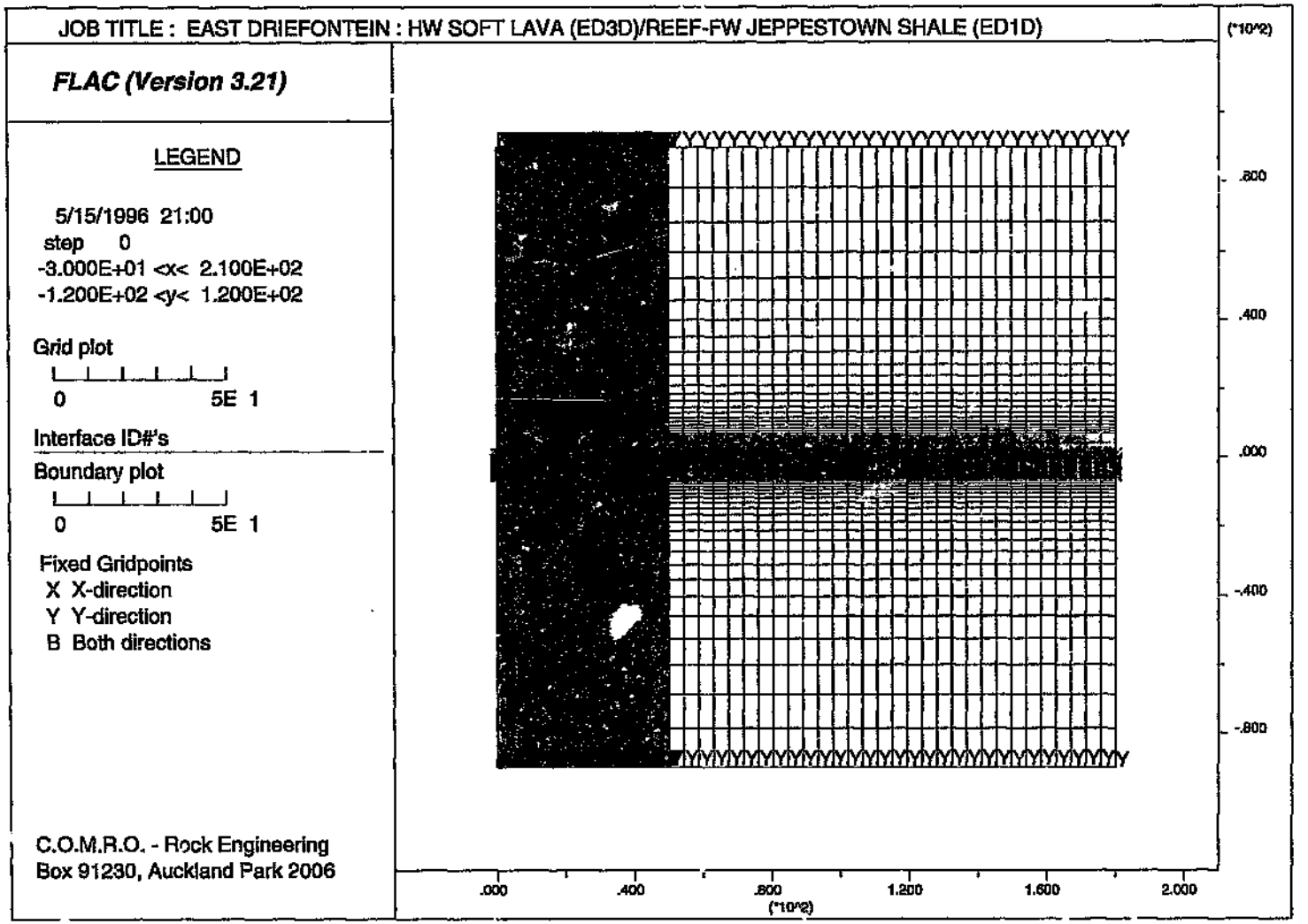

Figure 6.7. The basic model including position of grids, interfaces and boundary conditions.

In the model, the reef is mined from zero to 40 m half span in 0.5 m step face advances. After each mining step, the "zonk" FISH function is used to control unbalanced forces around the excavation. Based on the assumption that fractures form parallel to the major compressive principal stress, σ_1, a FISH function is utilised to record and plot the fracture angle.

As the face advances, the eight zones ahead of the face, in the first layer of the hanging-and footwalls, are examined. All necessary information to calculate fracture angle on the particular zones and the state conditions are stored. At the end of 40 m of excavation, there are eight different output parameters for each zone in the first layer above and below the reef. As the face advances, the zones ahead of the face are initially in an elastic state of failure according to the Mohr-Coulomb criterion and their associated state flag is changed to reflect this plastic failure. By using a FISH function, the information stored is interpreted for two cases, i.e. where each zone is the last elastic, and then when each zone becomes plastic.

6.2.2 Elastic and Mohr-Coulomb models

The elastic model describes the simplest form of the material behaviour. This model is valid for homogeneous, isotropic, continuous materials, which exhibit linear stress-strain behaviour with no hysteresis on unloading. The Mohr-Coulomb plasticity model represents a material, which is yielding in shear, but also includes a tension limit criterion. Table 6.3 summarises the material properties used during the numerical modelling as obtained from laboratory tests of the rocks under consideration (Tables 4.1, 4.2 and 4.3).

The results of the elastic modelling show that there is very little difference in the hangingwall and footwall stress distribution around the stope. Figures 6.8a and b show the modelled principal stresses around the stopes for the two study sites, at East Driefontein and Deelkraal Gold Mines,

respectively. Some further studies on the same model which uses only unrealistical elastic properties for hangingwall and footwall, show noticeable changes in the stress distribution around the stope, but the results of this study are not presented here.

Table 6.3. Material properties used during the numerical modelling.

PROPERTY			DEELKRAAL		EAST DRIEFONTEIN	
			Hangingwall hard lava	Footwall quartzite	Hangingwall soft lava	Footwall Jeppestown shale
Young's Modulus	E	(GPa)	72	64	67	61
Poisson's ratio	ν		0.21	0.14	0.22	0.25
Bulk Modulus	K	(GPa)	41	29	39.6	40.9
Shear Modulus	G	(GPa)	30	28	27.5	24.4
UCS		(MPa)	279	184	106	134
Cohesion	C	(MPa)	73	49	28	40
Internal friction angle		(degree)	35	34	34	28
Tension cut off	T	(MPa)	7.3	4.9	2.8	4.0
Dilation angle	ψ	(degree)	10	10	10	10

The basic parameters in the Mohr-Coulomb plasticity model are defined as density (ρ), bulk modulus (K), shear modulus (S), tension cut-off (T), dilation angle (ψ), internal friction angle (ϕ), and cohesion (C). The results of Mohr-Coulomb modelling indicate that the stress distribution around the stope changes depending on internal friction angle, the dilation angle, the tension cut-off, and the cohesion. Large differences in cohesion appear to have the most pronounced influence.

Initially, the actual results of triaxial and uniaxial tests are employed as the input rock properties in the Mohr-Coulomb model for the first geotechnical area, defined as soft lava hangingwall and Jeppestown shale (Table 6.3).

Figure 6.9 a shows the distribution of principal stress around the stope. Figure 6.9 b shows the directions and angles of the calculated fractures at the first zone of the hangingwall and footwall around the stope.

The modelled hangingwall fractures are much flatter than the observed mining induced stress fractures in this particular geotechnical area at East Driefontein Gold Mine. When the strength of the soft lava hangingwall and footwall is assumed to be 75 % softer than the original values and the strength of the reef is equal to 2/3 of the strength of the footwall, the orientation of the principal stress and the directions and angles of the calculated fractures are dramatically changed (Figs. 6.10 a and b). The modelled fractures in the hangingwall seem to be dipping in the "opposite" direction, whereas the fractures in the footwall are steep and dip away from the face. This compares favourably to the underground observations (Appendix A).

The same model was applied considering the second geotechnical area defined by hard lava hangingwall and quartzite/conglomerate footwall, as found at Deelkraal Gold Mine. Appropriate material properties were utilised. The fractures in the hard lava hangingwall are flat (about 40° to 50°) and dip towards the face, whereas in the footwall they dip steeply away from the face (Figs. 6.11 a and b). This is similar to the underground observations (Appendix B).

6.2.3 Strain-Softening modelling

The implemented strain softening model is a plasticity model based on the Mohr-Coulomb constitutive model. The principal characteristic is that the strain softening model incorporates load shedding upon loading beyond peak strength. The two elastic constants, Young's Modulus (E) and Poisson's

ratio (υ), and three plasticity parameters (cohesion, C; internal friction angle, ϕ; and dilation angle, ψ), define the complete stress-strain characteristic.

The plasticity parameters required in the strain softening model are obtained from a computer program called SS (Ryder,1993). This computer program uses the main output parameters from the rock test analyses and allows the user to re-construct the experimental data by defining tables of cohesion, internal friction angle, and dilation angle values.

In Figure 6.12 a, the left hand diagram shows maximum principal stress, σ_1, versus axial strain and radial strain versus axial strain as obtained in the laboratory. Diagrams on the right show the same relationships as generated for use in the model. Figure 6.12 b presents all the generated input parameters. This figure is for soft lava hangingwall in the geotechnical area defined in East Driefontein Gold Mine. Figures 6.13 a and b show the same parameters for the Jeppestown shale in the same geotechnical area. The same analyses were completed for the second geotechnical area defined as hard lava hangingwall and quartzite-conglomerate footwall in Deelkraal Gold Mine. Figures 6.14 a and b, and 6.15 a and b represent the same parameters for hangingwall and footwall respectively.

The results obtained for the geotechnical area as present at Deelkraal Gold Mine agree with observed, underground fracture angles. For the second geotechnical area (East Driefontein Gold Mine), the analyses show that fractures are formed flatter than those observed. The development of a plastic failure area occurs a few zones ahead of mining, both below and above the stope. This result may be due to the fact that the rocktest analyses are biased towards representing large-scale properties. The results indicate that a change in cohesion with plastic strain offers a mechanism for a large contrast in cohesion to develop between hangingwall and footwall. Large differences in cohesion appear to be more significant than differences in the other plasticity parameters, i.e. internal friction angle ϕ, and dilation ψ.

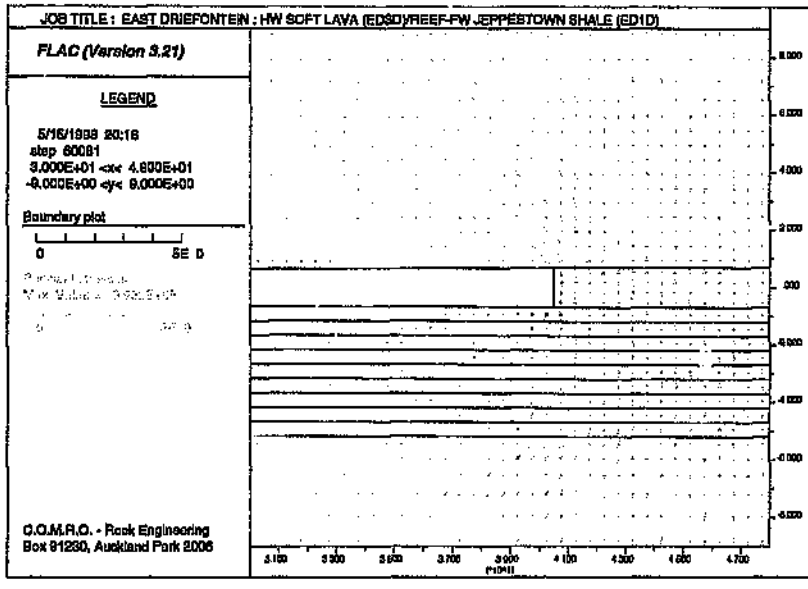

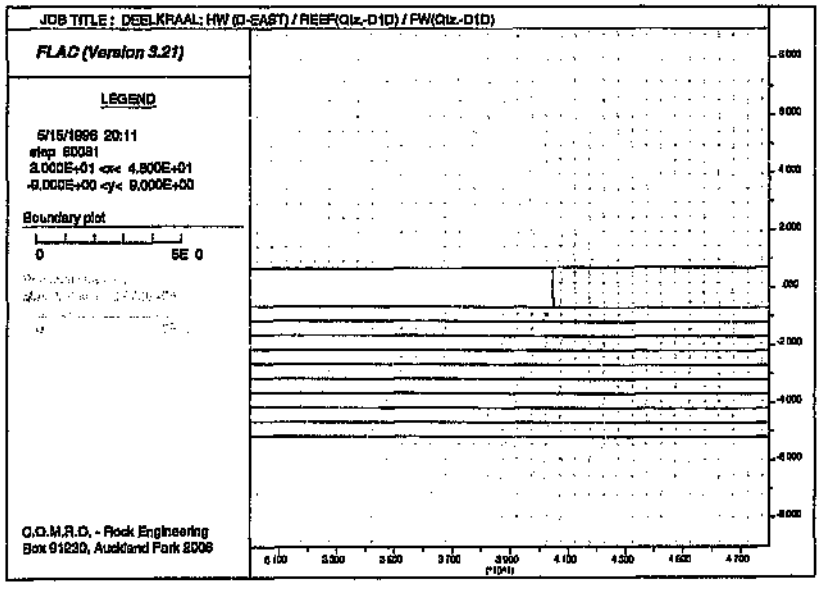

Figures 6.8 a and b. Modelling results considering maximum principal stress around the stopes at East Driefontein (Fig. 6.8 a) and Deelkraal Gold Mines (Fig. 6.8 b).

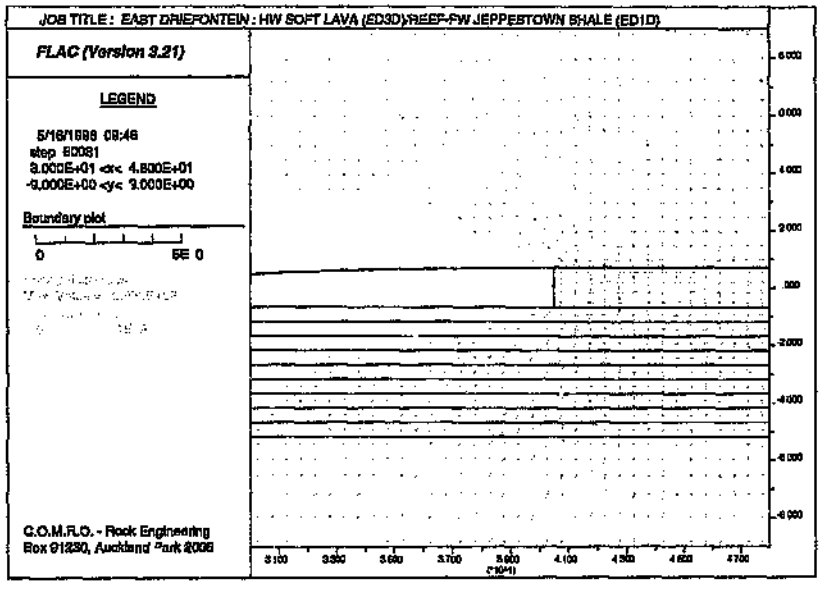

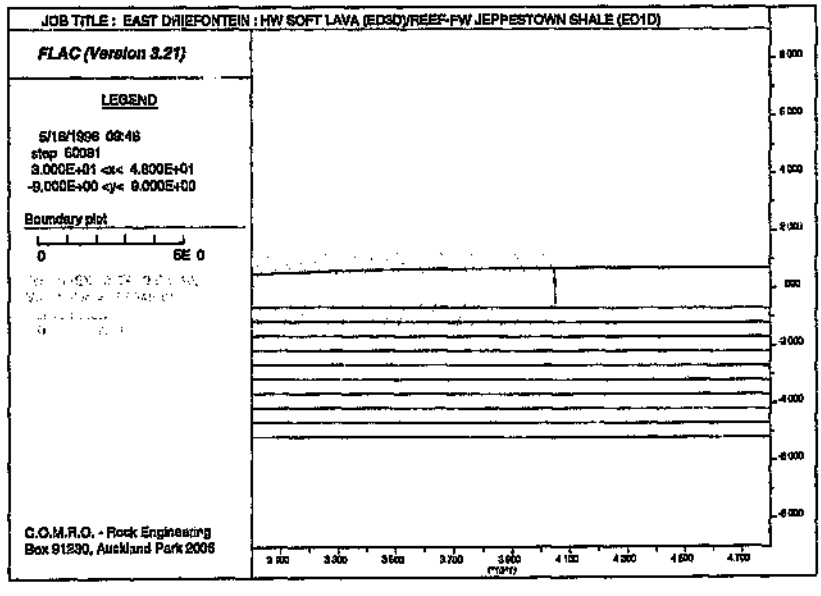

Figures 6.9 a and b. Modelled maximum principal stress, the directions and angles of the calculated fracture around the model stope, East Driefontein Gold Mine, using the Mohr-Coulomb model.

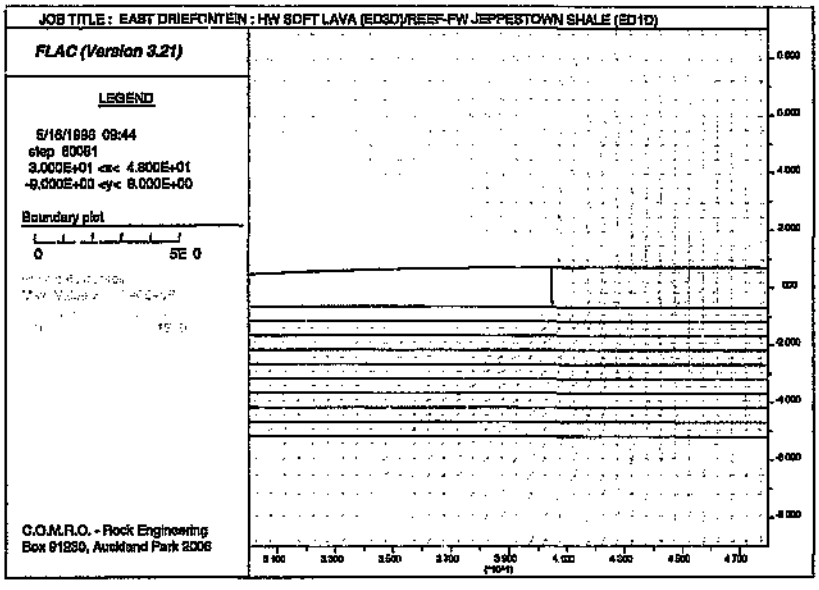

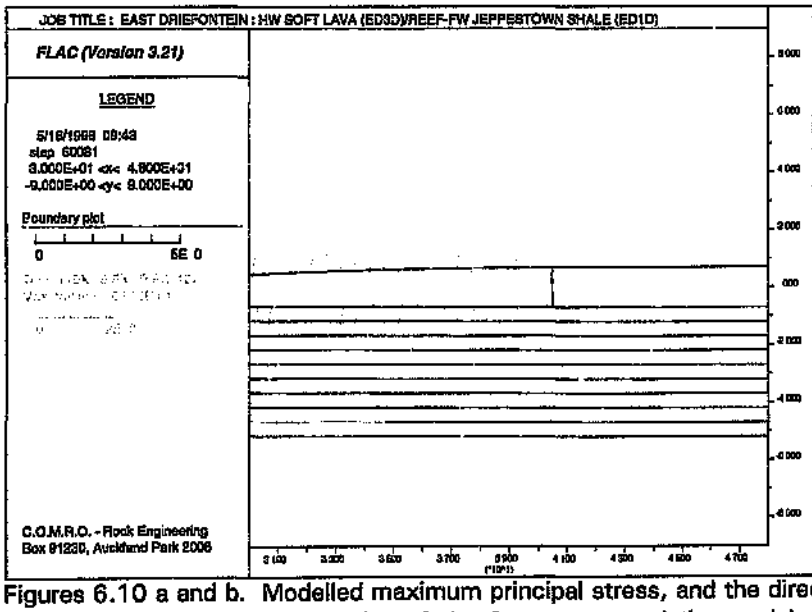

Figures 6.10 a and b. Modelled maximum principal stress, and the directions and angles of the fracture around the model stope, East Driefontein Gold Mine, using the Mohr-Coulomb model. The hangingwall, footwall, and reef strengths were assumed to be 75 % softer than those measured in the laboratory.

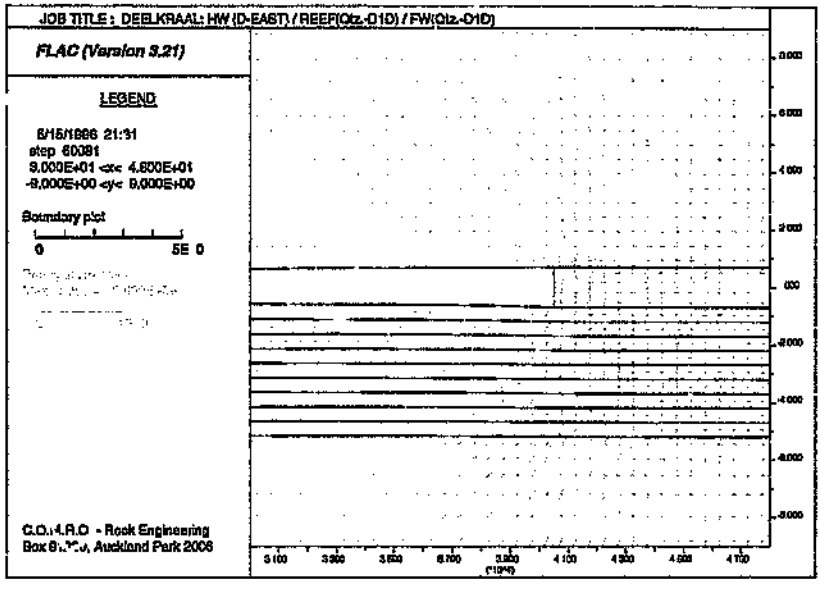

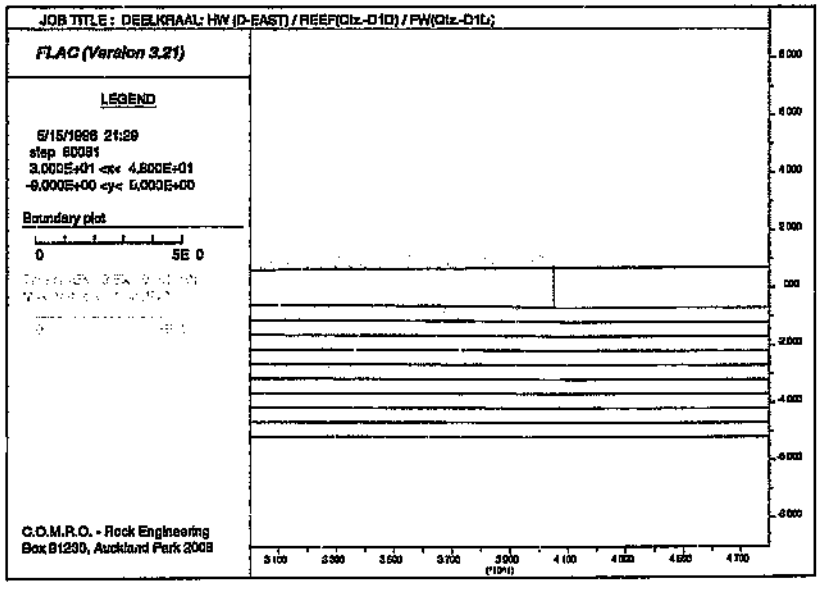

Figures 6.11 a and b. Modelled maximum principal stress, the directions and angles of the calculated fracture around the model stope, Deelkraal Gold Mine, using the Mohr-Coulomb model.

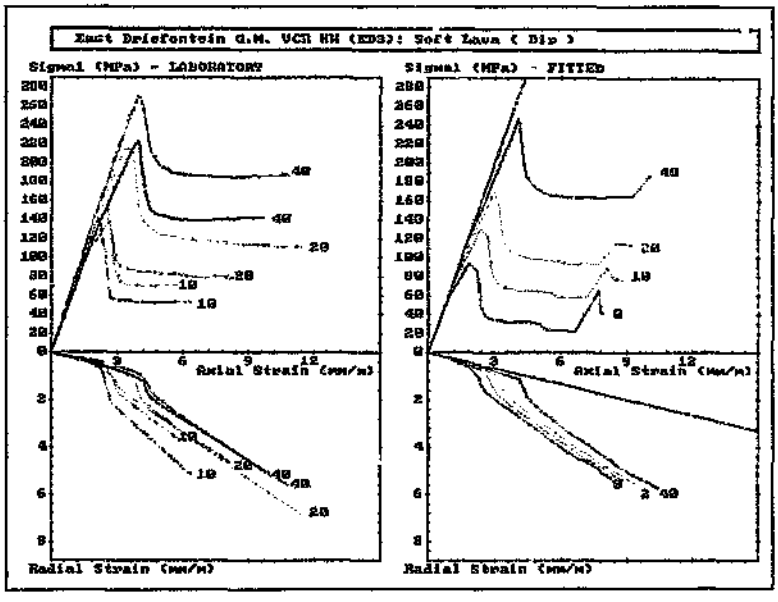

a

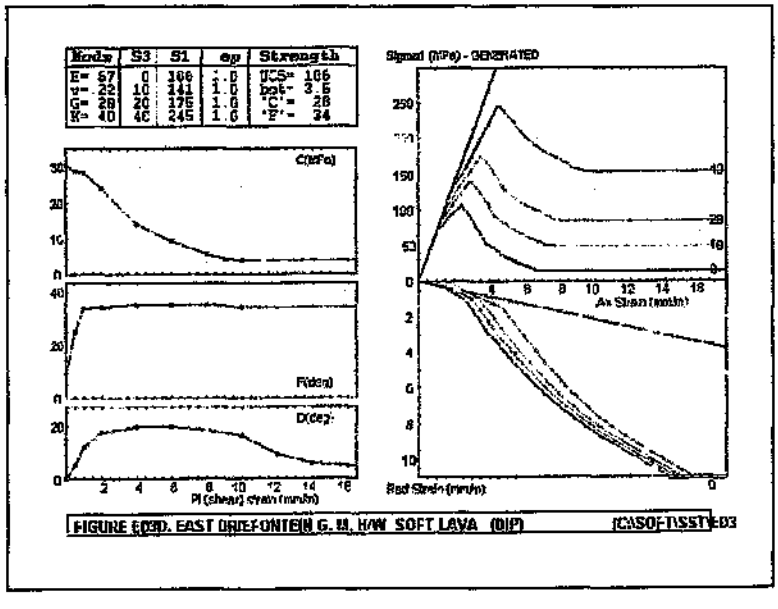

b

Figures 6.12 a and b. Idealised stress-strain characteristics of soft lava hangingwall to use in strain-softening test for East Driefontein site.

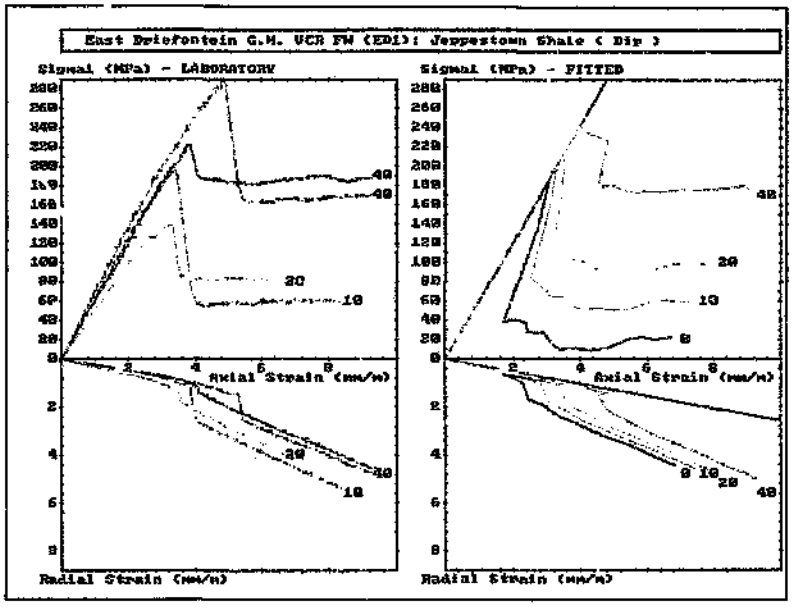

a

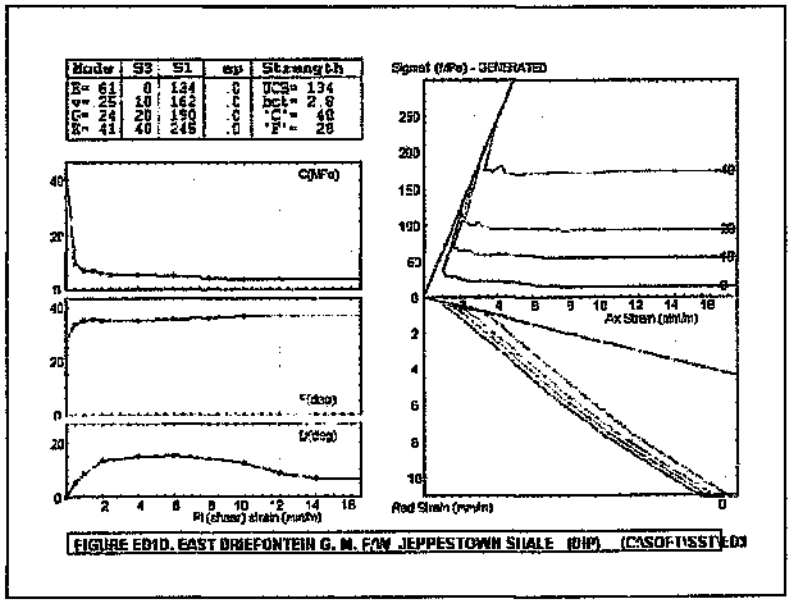

b

Figures 6.13 a and b. Idealised stress-strain characteristics of Jeppestown shale footwall to use in strain-softening tests for East Driefontein site.

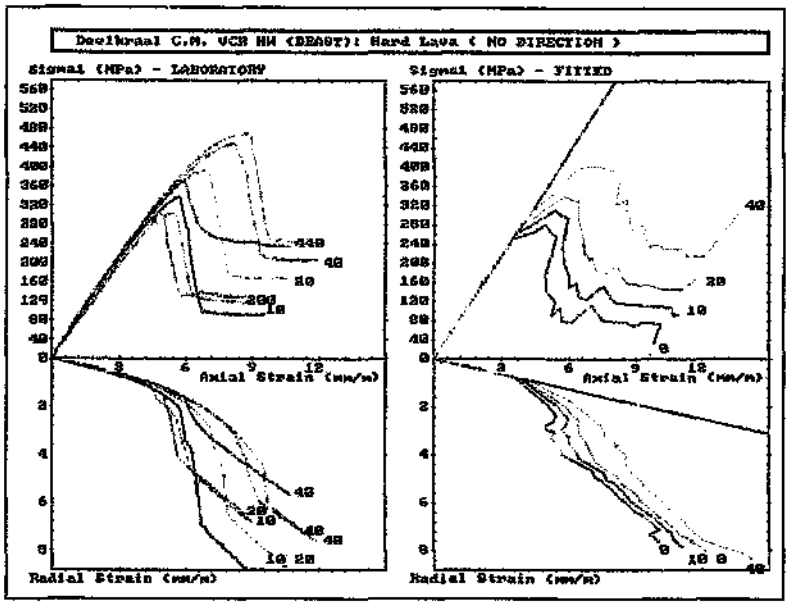

a

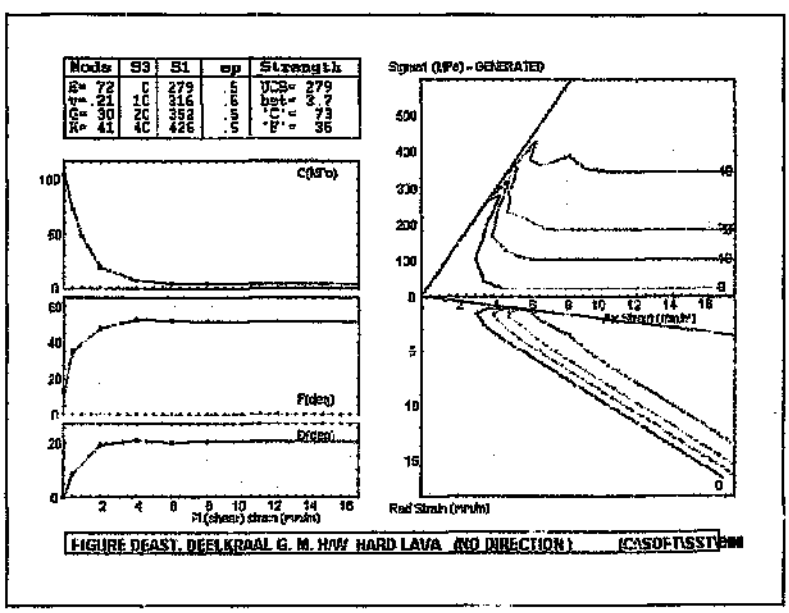

b

Figures 6.14 a and b. Idealised stress-strain characteristics of hard lava hangingwall to use in strain-softening test for Deelkraal site.

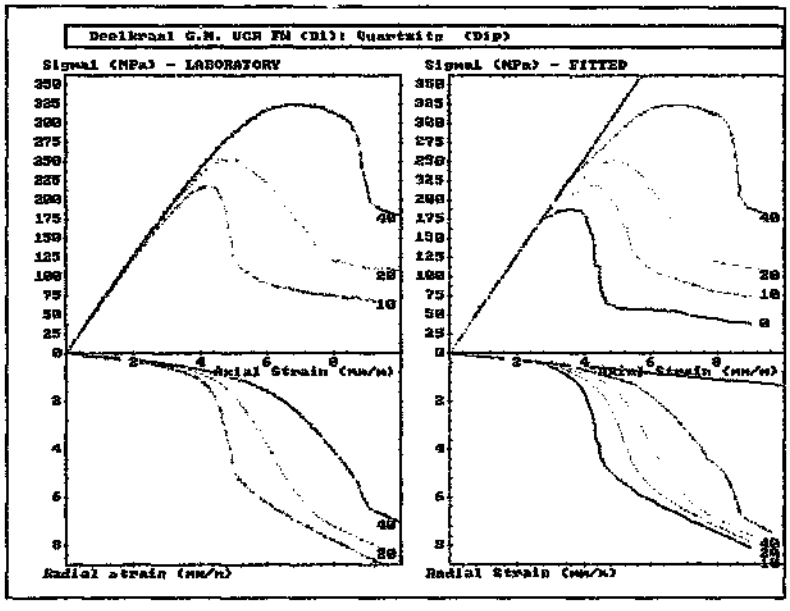

a

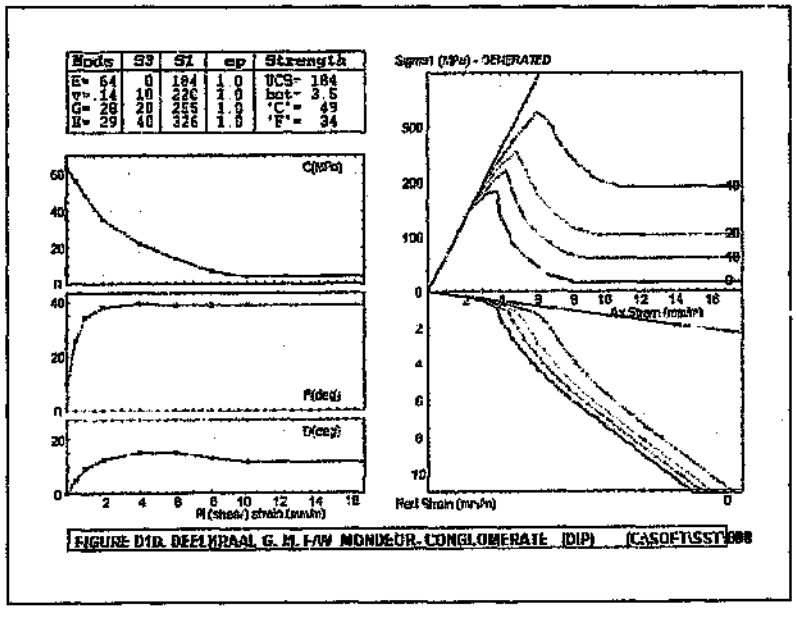

b

Figures 6.15 a and b. Idealised stress-strain characteristics of quartzite-conglomerate footwall to use in strain-softening tests for Deelkraal site.

CHAPTER 7

7 FACTORS TO BE CONSIDERED IN THE DESIGN OF SUPPORT FOR VCR STOPES

The primary motivation behind defining geotechnical areas is the expectation that different combinations of rock types in the hangingwall and footwall of the reef may potentially result in different rock mass behaviour around the VCR stopes, therefore influencing support strategies.

The main areas of work carried out in the different geotechnical areas, in order to determine support requirements for the VCR stopes, were:

- detailed analysis of closure data,
- analysis of accident database information,
- analysis of data on fallout thicknesses.

In order to assist in assessing the VCR support requirements, the information obtained from different geotechnical areas was applied.

This chapter presents :

- a review of Stope Design Analysis (SDA) presented in Section 7.2.
- a determination of a support resistance criterion for rockfalls, and an energy absorption criterion for VCR stopes, having soft lava and hard lava hangingwalls.
- modifications to the SDA, which was developed in the SIMRAC stope and gully support SIMRAC project, GAP 032. Importantly, the effect of face advance on closure taking place was evaluated in detail for the stope face.

7.1 INTRODUCTION

The fundamental function of stope support systems is to control the rock mass in the zone of rock subjected to tensile stresses, and the zone of fractured rock behaving inelastically (Anon, 1988). The design of any support system depends upon knowledge of three fundamental aspects: the nature and extent of the rock to be supported; the deformations to which the support systems will be subjected; and the generated force reaction characteristics of the support systems available for installation (Anon 1988). In the light of this information, geotechnical areas were defined, with the expectation that different combinations of rock types in the hangingwall and footwall of the reef may potentially result in different rock mass behaviour around the VCR stopes, therefore influencing support strategies.

In order to evaluate this hypothesis, sites in various geotechnical areas were monitored and the results obtained were processed, initially using the methodology developed under project GAP 032. During this work it was realised that the closure data could be used more comprehensively by separately analysing results from areas where the rate of face advance was different.

The main areas of work, carried out in the different geotechnical areas in order to determine support requirements, are discussed below:

1- detailed analysis of closure data.

The rate of closure taking place in various geotechnical areas is significantly different. For example, the closure rate has been recorded as 4-5 mm per day and 9-10 mm per day in hard lava (Deelkraal Gold Mine) and soft lava (East Driefontein Gold Mine) hangingwall stopes, respectively. Detail is provided in Chapter 5. The graphs of closure versus number of days show that the rate of closure either decreases or increases depending on the rate of mining taking place in the panel, the effect of the face advance rate on the rate of closure for various geotechnical areas was also analysed.

2- analysis of accident data base information.

The database of fatal accident records was developed in conjunction with SIMRAC project GAP 032. The database was developed using information gathered from the fatal accident inquiries conducted by the Department of Minerals and Energy Affairs (now the Department of Minerals and Energy, DME). The fatal accident inquiries were chosen because reasonably good details were recorded in the documentation. The objective of compiling a database is to provide insights into support performance and other mining issues through back analysis. This work concentrated on the collation of available information into an accessible format so as to enable various factors to be considered when investigating specific information.

3- data on fallout thicknesses.

As part of the accident database work, an analysis of the thicknesses of falls of ground and rockburst ejection has been undertaken for the VCR stopes. The ultimate intention is to develop, for each geotechnical area, a support resistance criterion for the prevention of rockfalls, and an energy absorption criterion for the reduction of damage due to rockbursts.

7.2 REVIEW OF PREVIOUS SUPPORT STRATEGIES DEVELOPED

In South African mines with tabular orebodies, the design of stope support systems has, in most cases, been based on experience, past practices and cost considerations (Roberts, 1995). Generally, a number of factors need to be taken into account in a design: these include the amount and rate of closure taking place; the types, orientation and intensity of hangingwall fracturing; the influence of local geology which determines the volume of the rock to be supported; and the probability of a rockburst. In addition, the size and shape of the excavation and the period for which the support is required needs to be considered (Anon 1988; Roberts, 1995).

In order to assess the hypothesis described in 7.1, the methodology developed as described in the final report of the SIMRAC project, GAP 032, stope and gully support, addresses the project's two main objectives, namely:

- Develop a rationale for the design of stope support systems,
- Determine support resistance criteria for the support of stope gullies for both static and dynamic loading and develop improved support systems for gullies.

The following is a brief summary of the methodology developed under this particular project.

The main factors governing the design of stope support systems are: the mass of rock to be supported, stope closure and the generated force–deformation characteristics of support systems. Approximately 130 support systems are currently used by the industry, utilising various support unit types with variations also in spacing and support dimensions.

Roberts (1995) described all critical parameters in developing a rationale for the design of stope support systems. According to the theory in selecting stope support systems, it is necessary take support density into account and thus it is best to work with support resistance. The support resistance (in kN/m^2) of a support system is given by the product of the force (in kN) offered by the individual support units and the support density (in units/m^2). Support systems may be plotted as a support resistance versus deformation curve. Figures 7.1a and b show a typical support resistance curve of a hydraulic prop and pack spaced such that each prop and pack is supporting 1.5 m^2 and 9 m^2 of the stope hangingwall, respectively. Props show immediate support whereas packs need to be compressed significantly before providing support forces.

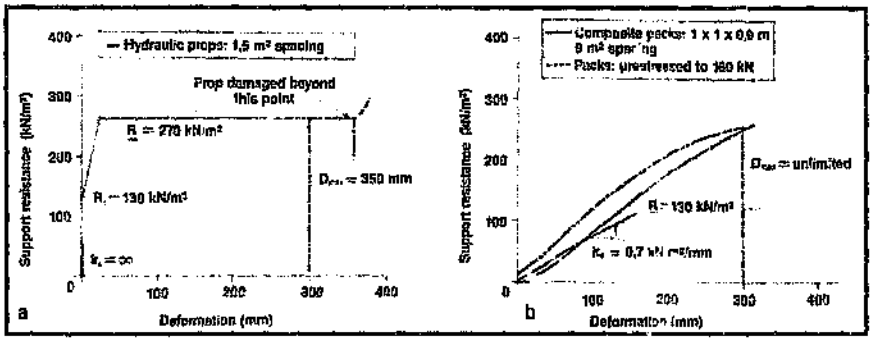

Figures 7.1a and b. Typical support resistance deformation curves (Anon, 1988).

Figure 7.2 (Roberts, pers. comm., 1995) shows a comparison of different support systems by using the concept of support resistance as a function of the distance behind the stope face for a given closure rate; in this case 2 mm per day. The effectiveness of the selected support system can be evaluated for the different closure rates. It is possible to compare various support systems and evaluate then individually as to their suitability at a recorded closure rate (Fig 7.3, Roberts, pers. comm., 1995)

It is well documented (Anon, 1988) that the performance of passive support such as packs is strongly controlled by the closure rates to be expected. Figures 7.4a and b present support deformation curves supplemented with expected closure rate lines. For example, yielding elongates and hydraulic prop/backfill systems may be examined for rockfall and rockburst conditions (Figs. 7.4a and b, Anon, 1988). Typical elongate systems at 3 m^2 spacing and installed 3 m away from the face can provide acceptable support in stopes with low closure rates (2 mm per day), but fail in very high closure environment (50 mm per day) due to inadequate yieldability (Fig. 7.4a). In rockburst conditions, although backfill used alone would fail to supply efficient face area support, hydraulic props accompanied by a backfill system give adequate support resistance (Fig. 7.4b).

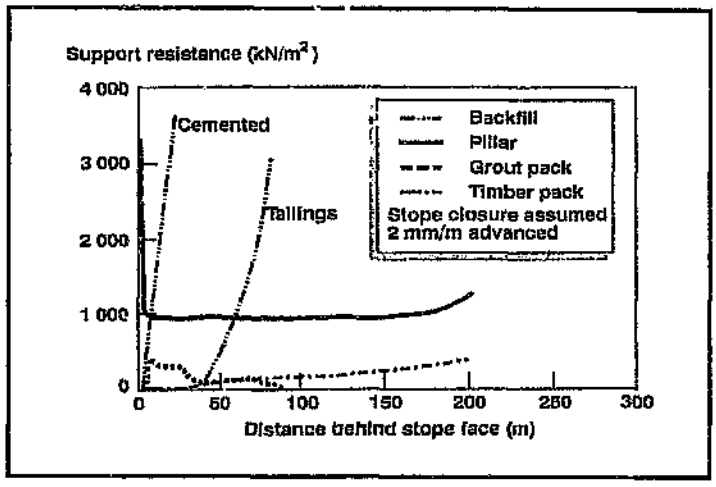

Figure 7.2. Comparison of different support systems (Roberts, pers. comm., 1995).

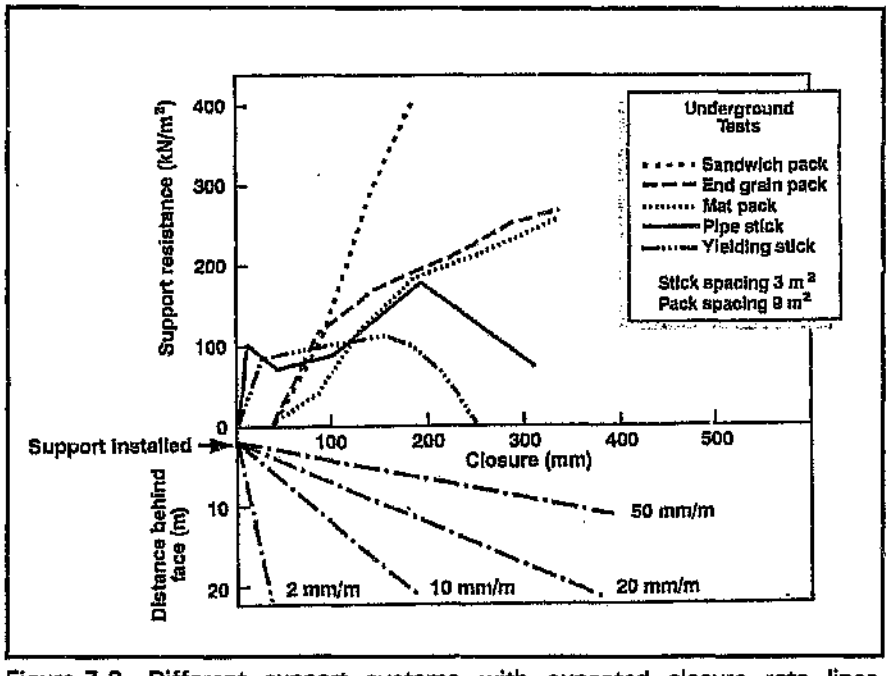

Figure 7.3. Different support systems with expected closure rate lines (Roberts, pers. comm., 1995).

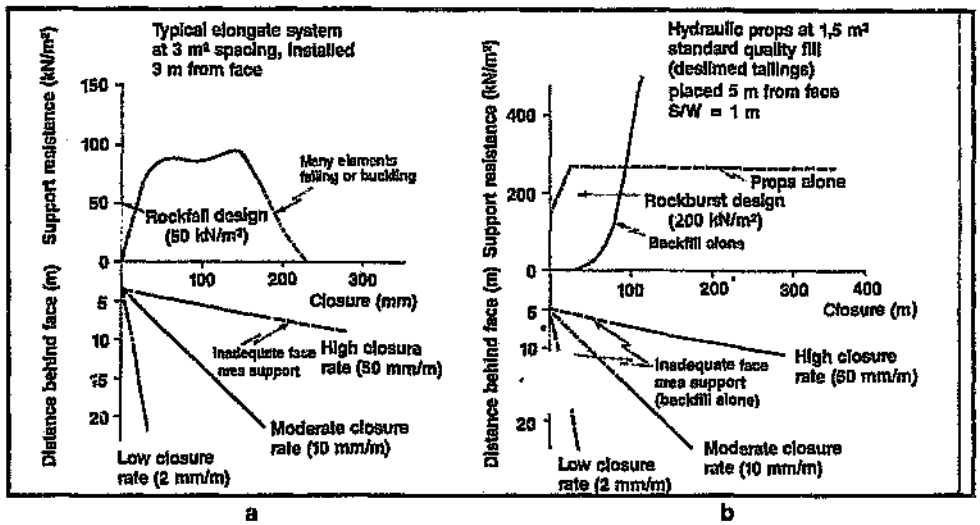

Figures 7. a and b. Selection and design of stope support systems (Anon, 1988).

In the evaluation of this methodology, the variables that should be considered are as follows:

- factors affecting the force-deformation behaviour of the support units constituting the stope support system encompassing, for timber support, the loading rate, and, for all systems, the height of support units.

- the influence of the rock mass on support systems, which encompasses the stope closure rate, dynamic closure velocity during rockbursts, and the spacing of the stope support units.

In addition, a linear relationship between deformation rate and resulting change in pack force (Taggart, 1994) was established as:

$$F_f = F_s\left[1+\frac{\%inc}{100}\right]^{\log\frac{V_f}{V_s}}$$

where F_f is pack force at increased velocity V_f

F_s is pack force at lower velocity V_s and,

% is the empirically derived per cent increase in force per increase in order of magnitude in compression velocity.

Using this relationship the force-deformation behaviour and consequently the energy absorption ability of timber packs may be determined for high deformation rates typical of some rockbursts.

The common assumption when considering the relationship between the height of the pack and its stability is that packs with height-to-width ratios exceeding two are considered unstable, particularly during dynamic closure (Roberts, 1996). Furthermore, underground studies and testing carried out on different support systems showed that the stability of yielding timber elongates decreases with increasing height and with increasing amount of stope closure and, therefore, the height-to-width ratio of these units should not exceed 10 (Roberts, 1996). Underground observations showed that hydraulic props and extensions, which exceed 2.5 m in length, are unstable during dynamic loading (Roberts, 1996). Tests undertaken on a variety of mechanical props indicated that lengths between 2.3 m and 2.7 m should be regarded as the upper limit for medium duty mechanical props (Roberts, 1996). The ability to absorb energy of those props is extremely limited and they have no energy absorption function in rockburst prone stopes.

The influence of the characteristics of a particular rock mass can cause significant differences in the size and geometry of blocks to be supported in the hangingwall and the stope closure rate. It is therefore necessary that the distribution of geological structures, bedding thickness and mining induced stress fractures in the rock mass be known as they influence the size of rock

blocks and thus the spacing of support units in a support system, while the closure rate influences the choice of support units particularly if they are required to absorb energy should a rockburst occur. The expected stope closure rate and mining cycle are also important in determining the absolute amount of stope closure that will act on the support system, and thus whether the remaining yieldability will allow sufficient energy to be absorbed should a rockburst occur. For the purposes of assessing support system behaviour, the dynamic closure velocity is assumed to be 3 m per second.

Other outputs from the GAP 032 SIMRAC project, which are relevant to this project, were derived from the UDEC modelling. This work showed that if support spacing is increased, the required capacity of the units increases by more than the amount simply derived by maintaining average resistance. The main benefit derived from reducing spacing is likely to be improved hangingwall conditions and thus a reduced rockfall hazard. The influence of load spreaders and sensitivity of bedding plane spacing were also analysed. The test results for a support resistance of 66 kN/m^2 and spacing held constant at 2 m and 3 m showed that the detrimental effects of the punching mechanism at 2 m spacing are present and not as pronounced as they are for a 3 m spacing. The stability of the hangingwall improves significantly with increased bedding plane spacing, while the influence of changes in support parameters seems to be less marked. The model to determine the effect of the back area support indicated that a significant improvement in hangingwall conditions was obtained. The limitation with this model is the modelling method used to represent the backfill, as a back area support would tend to exaggerate the influence of the backfill on the face area as the lack of confinement along the face of the backfill was not taken into account. In order to determine support spacing, there is insufficient data to establish a complete design procedure.

7.2.1 Evaluation of the support resistance and energy absorption ability of various support systems

The support resistance of a support system is defined as the force applied by the support system per square metre of hengingwall and is typically represented as kN/m^2. The basic parameters affecting the support resistance are force-deformation behaviour of individual support units, their spacing and the amount of closure that has acted on the support system. The determination of the ability of a stope support system to absorb energy in order to reduce the damage due to rockbursts is not simple. It depends on the ability of the support system to yield during rapid deformation, normal stope closure, spacing of the support units and velocity of the dynamic stope closure.

An example given by Roberts (1996), namely the force-deformation curve of a profile prop, for a closure rate of 3 m per second, to generate dynamic conditions, is shown in Figure 7.5 a. When the support force is divided by the number of square metres per unit, the values for the support resistance versus deformation are as shown in Figure 7.5 b. In this figure, the area under the curve is the total energy absorption ability of the support system (kJ/m^2). Figure 7.5 c shows the curve of energy absorption-deformation for this support system. This represents the decreasing amount of energy with respect to increasing deformation (E_{finite}) that can be absorbed by the support system per square metre of hangingwall. The equation below indicates the process that was used to assess a profile prop support system as in Figure 7.5 c and in Figure 7.6.

$$E_{available} = E_{finite} - E_{stope\ closure} \qquad \text{(Roberts, 1996).}$$

where: E_{finite} is the amount of energy available to be absorbed by the support system prior to any stope closure.

$E_{available}$ is the available energy that can be absorbed by the support system, during a rockburst for example, taking into account previous stope closure.

$E_{stope\ closure}$ is the energy absorbed by normal stope closure prior to a rockburst.

The other support systems, such as mine poles, hydraulic props, RSS grout packs and timber packs, were also examined.

It was also concluded that most of support units and support systems have a finite amount of energy that can be absorbed during deformation. It is assumed that the energy absorption ability of pack support systems is limited to 50 % deformation as some pack types, notably composite packs, RSS grout packs and some of the "end grained" packs, clearly do lose structural integrity after large deformations (Roberts, 1996).

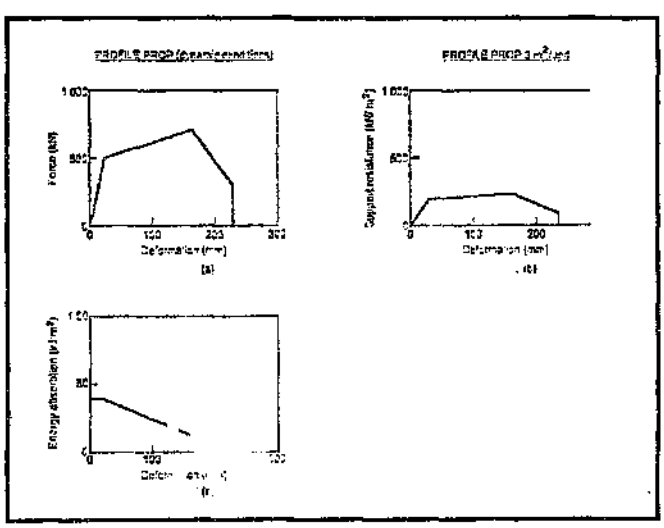

Figures 7.5a to c. The force-deformation (a), support resistance-deformation (b) and energy absorption-deformation behaviour of profile props (Roberts, 1996).

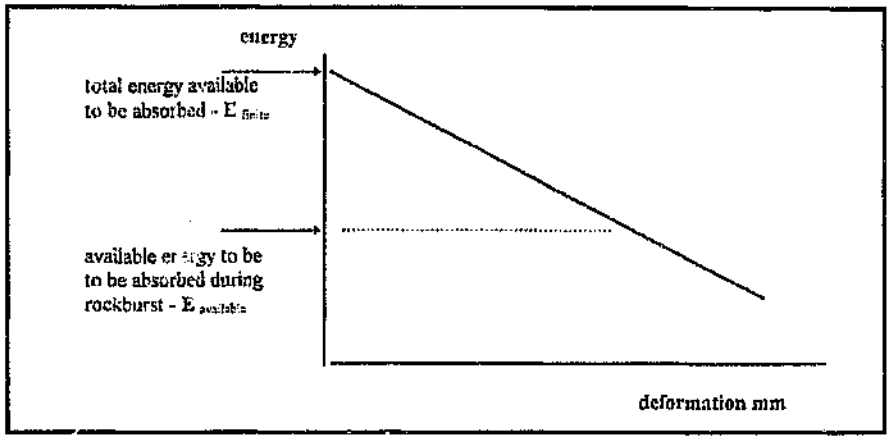

Figure 7.6. Energy-deformation curve showing the decrease in energy absorption ability with increasing deformation (Roberts, 1996).

7.2.2 Analysis of the graphical representation of SDA

The support design methodology for testing support resistance-deformation curves of support systems against support resistance criteria for different reefs was analysed (Roberts, 1996).

In order to determine the support resistance for any distance behind the stope face and for any closure rate, a graphical representation of the stope design methodology was produced, as shown in Figure 7.7.

Consider point A some distance behind the stope face, a horizontal line is traced until it intersects with the line representing the appropriate stope closure rate, point B. From point B a vertical line is traced to point C on the support resistance - deformation curve of the support system. From C a horizontal line is traced back to the x-axis to point D, where the support resistance of that particular support system for the specific closure rate can be determined.

The graphical representation of the support design methodology was extended by separating the face and permanent support areas into two different areas and plotting the support resistance-deformation curves of the support systems used in both the face and permanent support areas (Fig. 7.8). For example, a mine pole and mechanical prop support systems are compared in the face area, whereas a timber pack support system is compared with a yielding timber prop support system (Fig. 7.8).

The energy absorption ability of support systems with respect to the energy absorption criterion can be evaluated by using the support system design methodology as discussed above. The graphical representation for determining the energy that can be absorbed ($E_{available}$) for any distance behind the stope face and for any closure rate is produced in Figure 7.9.

Consider point A some distance behind the stope face, a horizontal line is traced until it intersects with the line representing the appropriate stope closure rate, point B. From point B a vertical line is traced to point C on the energy-deformation curve of the support system. From C a horizontal line is traced back to the x-axis to point D, where the energy that remains to be absorbed by the system ($E_{available}$) can be determined for that particular support system and for that specific closure rate.

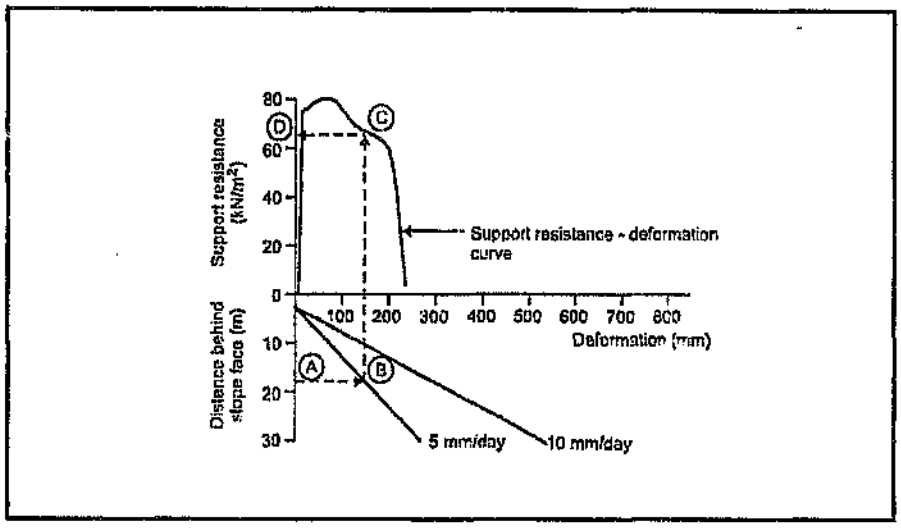

Figure 7.7. The support resistance-deformation curve, as a function of stope closure and distance behind the stope face props (Roberts, 1996).

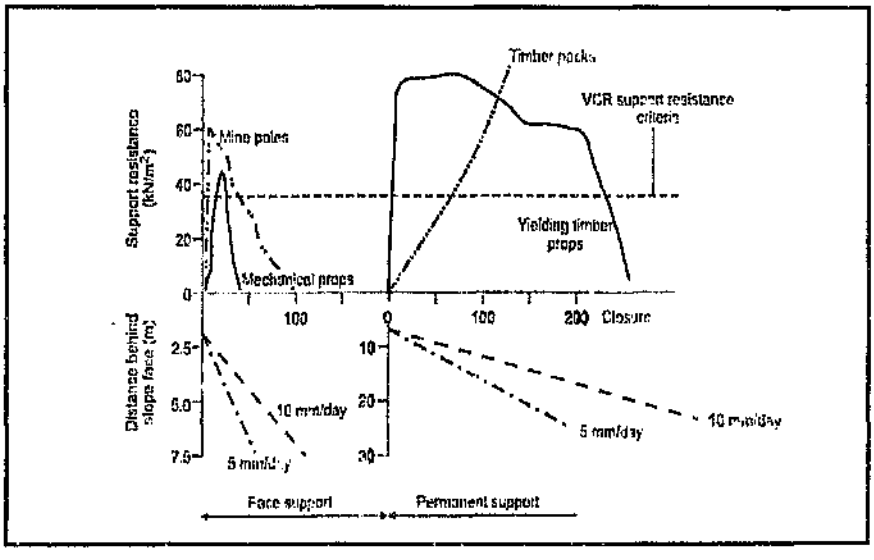

Figure 7.8. The support resistance-deformation curves of various support systems, as a function of stope closure and distance behind the stope face, for the face and permanent support areas (Roberts, 1996).

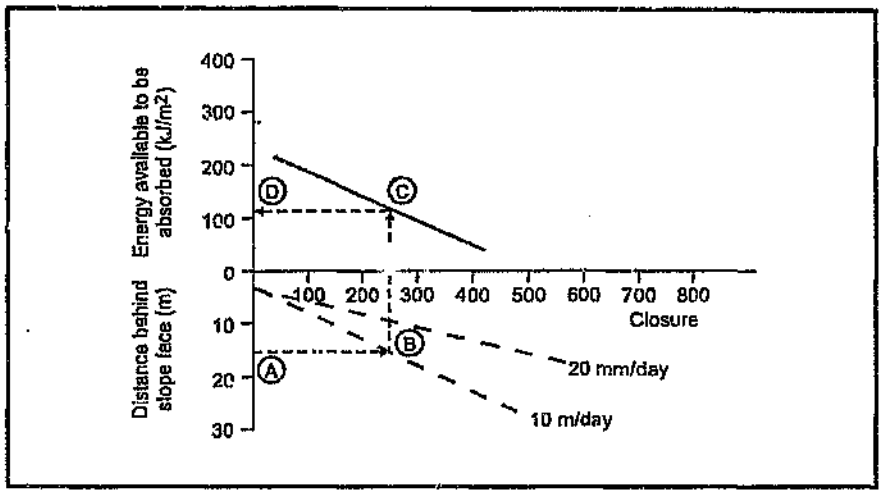

Figure 7.9. Energy absorption-deformation curve as a function of stope closure and distance behind the stope face props (Roberts, 1996).

The graphical representation may be further extended by plotting the velocity curve at the left hand side of the graph. In order to determine the critical velocity that would destroy the support during dynamic conditions, the velocity curve of a particular support system (Fig. 7.10), is drawn using the following formula (Roberts, 1996):

$$\text{The critical velocity, } V_o = \sqrt{\frac{E_{available} - mgh}{\frac{1}{2}m}}$$

where:

$E_{available}$ = the energy-absorbing ability of the support unit at any given time, which will be specific to each support unit and will depend on its position behind the stope face and on the stope closure rate (kJ/m^2)

M = the mass of the ejected hangingwall (kg)

G = gravity (m/s^2)

h = distance of yieldability left in the support unit after stope closure has acted upon it (m)

Consider point A some distance behind the stope face, a horizontal line is traced until it intersects with the line representing the stopes closure rate, point B. From point B a vertical line is traced to point C on the energy-deformation curve of the support system. From C a horizontal line is traced back to the x-axis to point D, where the energy that can be absorbed ($E_{available}$) can be determined for that particular support system and for that specific closure rate. From point D, a horizontal line is followed until it intersects with the curve of velocity at the left hand side of the graph, point E. From point E a vertical line is traced to point F on the minus part of the x axis, thus giving the critical velocity (V_c) which could be handled by using energy ($E_{available}$) available to be absorbed.

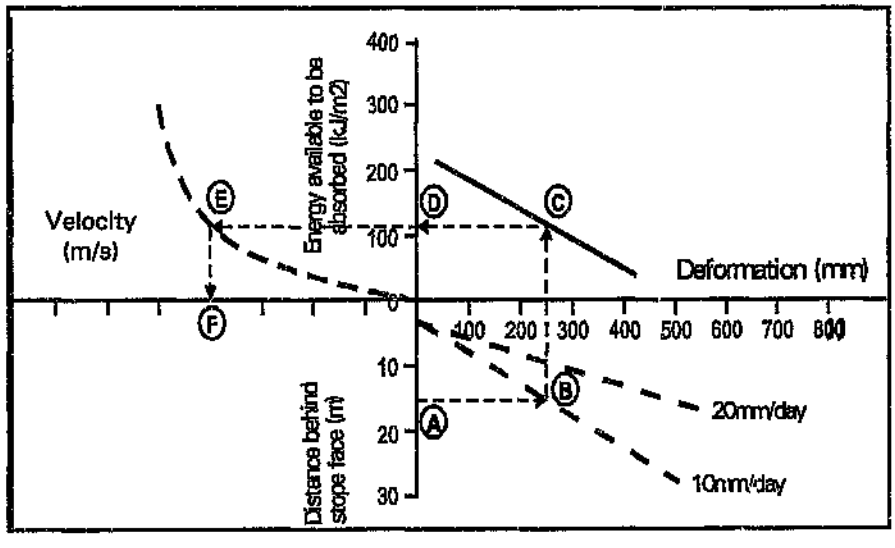

Figure 7.10. Determination of critical velocity (V_c) using an energy-deformation curve as a function of stope closure and distance behind the stope face (Roberts, 1996).

The comparison of the critical velocity variations for various support systems having a constant energy absorption capability but different yield capabilities showed that the difference in the critical velocities, V_c, for all the various support systems is, as could be expected, negligible. Figure 7.11 shows a horizontal line intersecting with the Y-axis where the energy absorption criterion is the same for all four different support systems. The vertical lines from the intersection of this horizontal line with all four velocity curves to the x-axis give the critical velocities for each of the support systems.

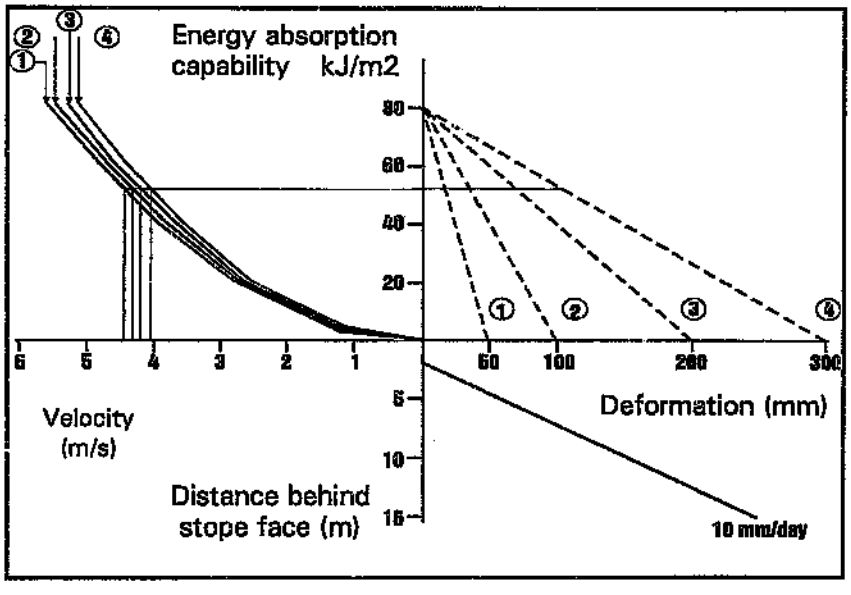

Figure 7.11. Critical velocity variation for a constant energy absorption capability (Roberts, 1996).

Figure 7.12 shows a comparison between various support systems with different yield ranges, i.e. much closer to the options that could be considered for practical applications underground. For example, three support systems, shown as A,B and C, with different yield ranges will have

different energy absorption capabilities for the same amount of deformation at some distance behind the stope face. At this point, the critical velocities to be handled by each support system are significantly different, the higher velocities being associated with the systems with the larger yieldability. However, with a low force high/yieldability system, consideration needs to be given as to whether the "h" yield limitations are violated or not.

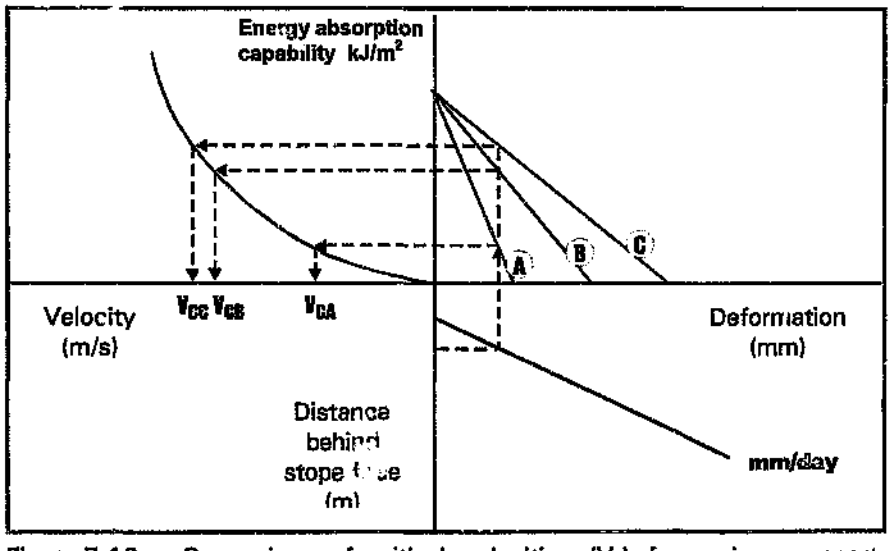

Figure 7.12. Comparison of critical velocities (V_c) for various support systems with different energy absorption ability as a function of stope closure and distance behind the stope face (Roberts, 1996).

7.3 VCR SPECIFIC SUPPORT DESIGN METHODOLOGY

The support design rationale developed in GAP 032 (Roberts, 1996) was applied as a basis for assessing support requirements for VCR mines. The consequences of the measured characteristics of the rock mass behaviour around VCR stopes was thoroughly investigated, in particular the varying closure rates observed. The rate of closure is the key issue in the support

design methodology. The rate of face advance also plays an important role as it not only determines the period over which support is deformed at the given closure rate, but also influences the closure rate.

The South African mining industry has historically used a stope support resistance of 50 kN/m² in the design of stope support systems in stopes where the major hazard is rockfalls (Anon, 1988). Also, in stopes, which are subjected to seismicity and rockbursts, a general energy absorption criterion has been applied which stipulates that the support systems should be capable of absorbing 60 kJ energy per square metre of hangingwall, thus requiring them to have a yielding capability.

7.3.1 An estimation of the support resistance requirements for the soft lava and hard lava in the VCR stopes.

It should be noted that most VCR stopes are subjected to seismicity and rockburst, rather than rockfall, problems. In the design of VCR stope support, the rockburst energy absorption criterion should usually be applied. Nevertheless, it is necessary to ensure that the design is capable of controlling rockfall problems, which account for 30 % of the fatalities (Roberts and Jager, 1991).

The accident database covers all rock related fatalities on South African tabular gold mines that occurred during the last six years, from 1990 to 1995 (Table 7.1). The analysis this database indicates that 32.3% of total fatalities occurred between 1990 and 1996 are rockfall fatalities. Figures 7.13 and 7.14 show the cumulative percentages of rockfall thicknesses in VCR stopes where the hangingwall is defined as soft and hard lavas, respectively. In the calculation of the required support resistance for stope support systems, it is assumed that the designed support system should prevent 95 % of all fallouts (Table 7.2).

Table 7.1. Summary of rock related (rockburst and rockfall) fatalities on South African tabular gold mines that occurred during last six years from 1990 to 1995 (Source: RSA, DME, 1996).

Year	Rockburst	Rockfall	Total
1990	32	17	49
1991	21	25	46
1992	63	14	77
1993	42	24	66
1994	45	13	58
1995	23	15	38
TOTAL	226 (67.7 %)	108 (32.3 %)	334

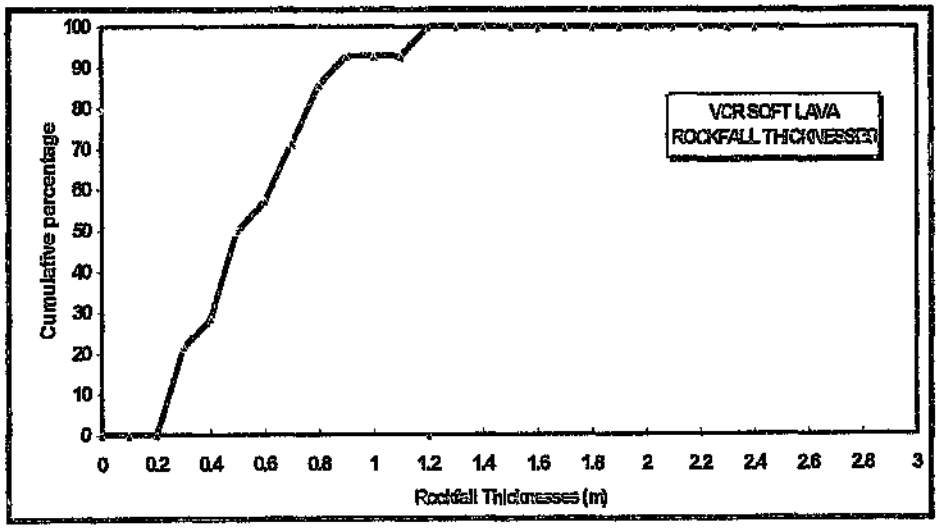

Figure 7.13. Analysis of fallout thicknesses in VCR stopes with soft lava hangingwall from 1990 to 1995 (Source: RSA, DME, 1996).

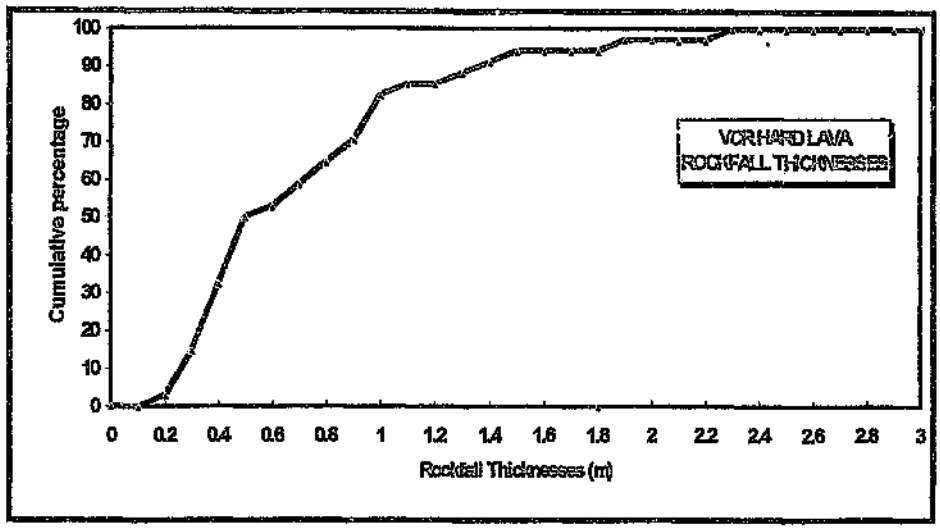

Figure 7.14. Analysis of fallout thicknesses in VCR stopes with hard lava hangingwall from 1990 to 1995 (Source: RSA, DME, 1996).

Table 7.2. The fallout thickness for the 95 % frequency level and the associated support resistance criteria for VCR soft and lavas.

REEF	95 % fallout frequency	Support resistance criteria
	m.	kN/m²
VCR Soft Lava	1.2	33.0
VCR Hard Lava	1.8	49.5

7.3.2 Estimation of the energy absorption criteria for VCR stopes having soft lava and hard lava in the hangingwall.

In order to reduce rockburst damage, the currently used energy absorption criterion is 60 kJ/m². The basis of this criterion is that a 3 m thickness of hangingwall formation accelerated to 3 m per second has to be brought to rest in less than 300 mm. The kinetic energy and change in potential energy

for this case is 60 kJ/m² and thus this energy imparted to the rock has to be absorbed by the support.

To quantify ejection thicknesses for the soft and hard lavas, all data from fatal accidents that occurred in the six years from 1990 to 1995 have been analysed. Figures 7.15 and 7.16 show cumulative percentage curves of the ejected block thickness from rockbursts measured at the sites of fatal accidents for soft and hard lava.

Using these block ejection thicknesses, it is possible to calculate a minimum energy absorption requirement per square metre of stope hangingwall that a support system should be able to provide to stabilise the hangingwall in 95 % of the cases.

Energy absorption criterion or $E = (0.5)\, m\, v^2 + m\, g\, h$

where:
- E = energy absorption criterion (kJ)
- m = mass of the ejected hangingwall (kg)
- v = velocity of ejection (m/s)
- g = gravity (m/s²)
- h = distance of yieldability left in the support unit after stope closure has acted upon it (m)

In this calculation, it is assumed that the density of the formation, the velocity of ejection, and gravity have the following values: 2750 kg/m³, 3 m/s and 9.8 m/s², respectively. Tables 7.3 and 7.4 list the minimum energy absorption requirements per square metre of stope hangingwall for yield limitations, "h", for support systems.

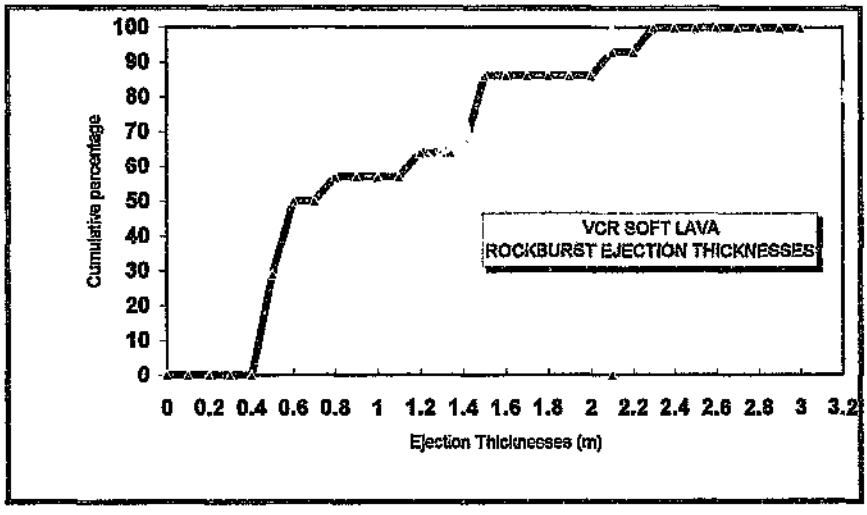

Figure 7.15. Analysis of rockburst ejection thicknesses in VCR stopes with soft lava hangingwall using data from 1990 to 1995 (Source: RSA. DME, 1996).

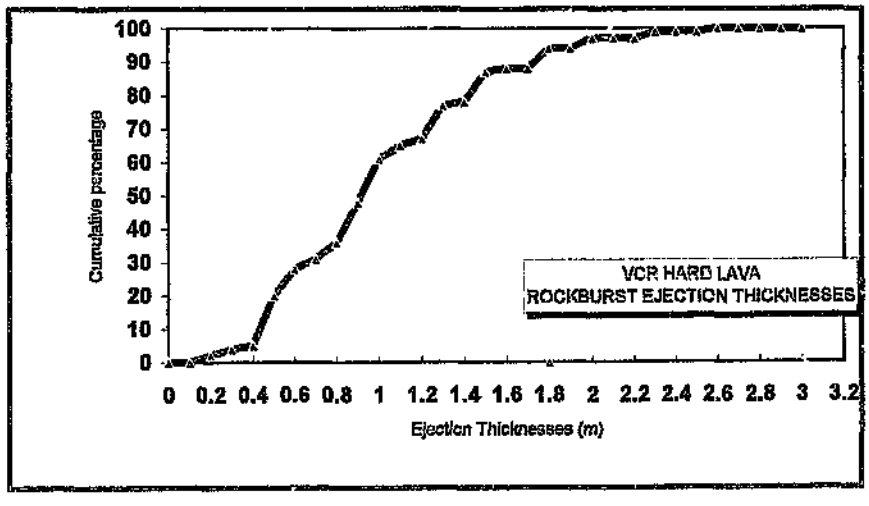

Figure 7.16. Analysis of rockburst ejection thicknesses in VCR stopes with hard lava hangingwall using data from 1990 to 1995 (Source: RSA, DME, 1996).

Table 7.3 The minimum energy absorption requirements per m^2 of soft lava hangingwall.

SOFT	LAVA						
Ejection thickness (95%)	Velocity of ejection	Density	Mass	Yield limitation	Kinetic Energy (J)	Potential Energy (J)	Energy Absorption Requirement
m	m/sec	kg/m3	t	m	(0.5*M*V2)	(M*G*H)	kJ/m2
2.1	3	2750	5775	0.05	25987.5	2830	28.8
2.1	3	2750	5775	0.1	25987.5	5660	31.6
2.1	3	2750	5775	0.15	25987.5	8489	34.5
2.1	3	2750	5775	0.2	25987.5	11319	37.3
2.1	3	2750	5775	0.25	25987.5	14149	40.1
2.1	3	2750	5775	0.3	25987.5	16979	43
2.1	3	2750	5775	0.35	25987.5	19808	45.8

Table 7.4. Minimum energy absorption requirements per m^2 of hard lava hangingwall.

HARD	LAVA						
Ejection thickness (95%)	Velocity of ejection	Density	Mass	Yield limitation	Kinetic Energy (J)	Potential Energy (J)	Energy Absorption Requirement
m	m/sec	kg/m3	t	m	(0.5*M*V2)	(M*G*H)	kJ/m2
1.8	3	2750	4950	0.05	22275	2426	24.7
1.8	3	2750	4950	0.1	22275	4851	27.1
1.8	3	2750	4950	0.15	22275	7277	30
1.8	3	2750	4950	0.2	22275	9702	32
1.8	3	2750	4950	0.25	22275	12128	34.4
1.8	3	2750	4950	0.3	22275	14553	36.8
1.8	3	2750	4950	0.35	22275	16979	39.3

Assuming that the support system must absorb the energy during yielding of 0.2 m, typical of the yieldability of hydraulic props and yielding timber props, then the minimum energy absorption requirements per square metre for hard lava and soft lava hangingwalls are given in Table 7.5.

Table 7.5. The fallout thickness for the 95 % frequency level and the associated energy absorption criterion for VCR soft and lavas.

REEF	95 % fallout frequency	Energy absorption criterion
	m.	kJ/m^2
VCR Soft Lava	2.1	37.3
VCR Hard Lava	1.8	32.0

7.3.3 The effect of average face advance rate on rate of stope closure.

One of the most important parameters used in the support design methodology is the rate of stope closure. The closure is used to determine whether the remaining yieldability will allow sufficient energy to be absorbed should a rockburst occur.

As previously presented, closure ride stations were installed in different panels to monitor the deformation taking place in the formation around the stope, in different geotechnical areas. The analysis of the measurements shows that the closure rates in different areas vary quite significantly. Another finding is that the general trend of the closure rate with time or distance to face is not linear. The rate of closure in the first 10 m from the face, however, can be considered to be approximately linear. Analysis also shows that the closure rate is very dependent on the rate of face advance. For instance, at the East Driefontein study site, the West 6 and West 5 panels were stopped for five months because of a pronounced roll of the reef. It is of interest that, during this period, stope closure was reduced to a rate of 3 mm per day. Once mining recommenced, a large increase in closure rate to 8 mm and 10 mm per day was recorded. Similar observations were made in different geotechnical areas.

In order to analyse the effect of face advance in both geotechnical areas, all readings taken within 10 m of the face at all stations installed were taken into account.

The equation for the linear line in the graph of deformation versus distance behind the stope face (the fourth quadrant, Fig. 17) in the defined SDA, which allows comparison of the stope support systems for different closure rates, is:

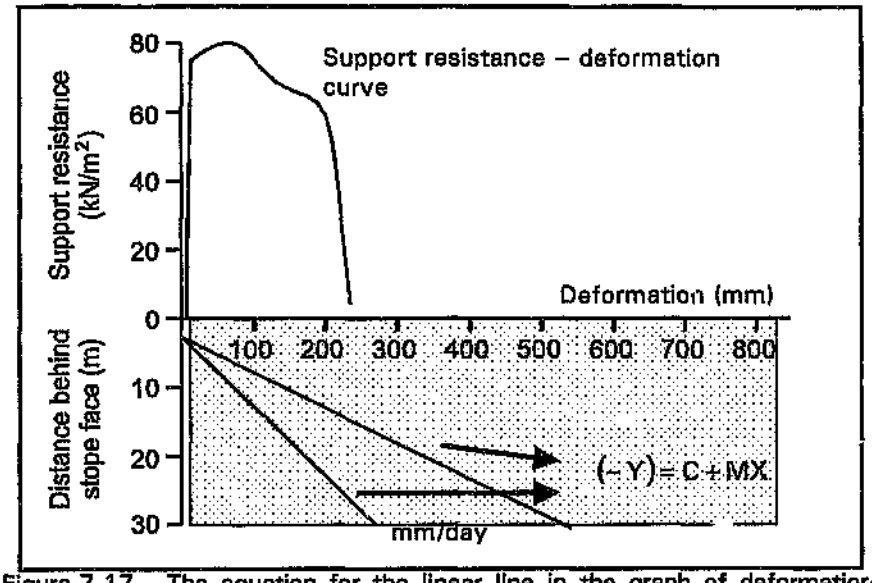

Figure 7.17. The equation for the linear line in the graph of deformation versus distance behind the stope face (the fourth quadrant) in the defined SDA.

$$(-Y) = C + MX$$

where:

Y = distance behind the stope face, (m)

C = distance to face from the first row of the support unit, (m)

M = slope of the linear line, as related to face advance rate

X = deformation, (mm)

This equation can be written as follows;

$$-Y(m) = C(m) + \left(\frac{Z(m)}{AC\left(\frac{mm}{day}\right) * D(days)} \right) * X(mm)$$

where:

Z = total face advance, (m)

AC = average closure rate, (mm/day)

D = total monitoring time, (days)

and the slope of the linear line will be as follows;

$$M = \left(\frac{Z(m)}{AC\left(\frac{mm}{day}\right) * D(days)} \right)$$

The motivation behind this is to calculate the slope of the line in the graph of average face advance per month versus "slope" for each geotechnical area. The rate of the face advance during the monitoring period was assumed to be the same. From the best fit line for this graph, it would be possible to have a value of "slope" depending on the average face advance designed in a particular panel.

7.3.3.1 Soft lava hangingwall

The measurements from only five closure-ride stations installed in the face area in West 5 and West 6 panels were available for analysis. All measurements analysed show very good correlation. For instance, Figure 7.18 shows a typical graph of closure versus number of days for this geotechnical area.

The value of "slope" for this particular closure-ride station was calculated as below:

Initial distance to face (m)	= 3.1 m.
Final distance to face (m)	= 10.2 m.
Z, total face advance (m)	= 7.1 m.
X, total closure (mm)	= 186 mm.
D, total days	= 16 days
AC, average closure rate (mm/day)	= 11.6 mm/day
and the calculated value of "slope"	= 0.038

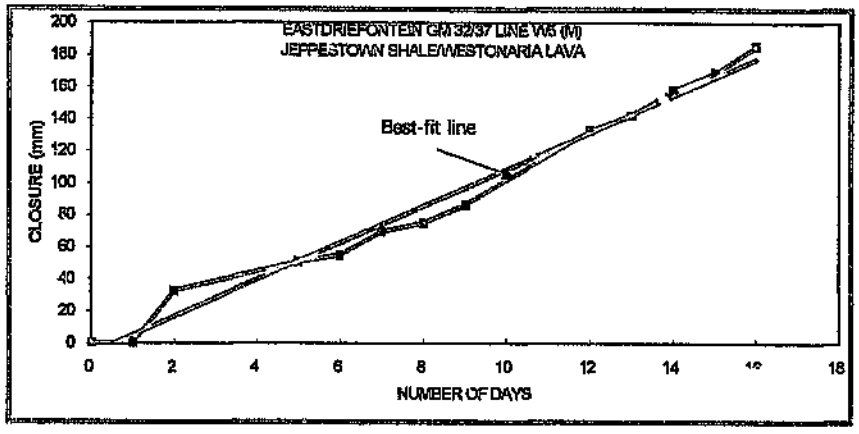

Figure 7.18. Closure measured in the closure-ride station installed in the face area at the middle of the West 5 panel, East Driefontein Gold Mine, 32 Level, 37 Line. $R^2=0.985$.

The same calculation was done for all other stations available and Table 7.6 summarises all the information and correlation factors (R^2). It is concluded that VCR face advance rates are very well correlated with total closure recorded in the geotechnical area as considered at East Driefontein.

Table 7.6. All stations installed in the face area where the hangingwall is soft lava, with all parameters to be used in the process.

Station	From (m)	To (m)	Z (m)	D (days)	X (mm)	Average face advance (m/month)	AC (mm/day)	VALUE OF SLOPE	R^2
W5MID1	5.0	10.6	5.6	28	274	6.0	9.8	0.020	0.9824
W5MID2	3.1	10.2	7.1	16	186	13.3	11.6	0.038	0.9850
W5TOP1	3.4	10.8	7.4	15	169	14.8	11.3	0.044	0.9869
W6TOP2	4.2	10.6	6.4	26	317	7.4	12.2	0.020	0.9603
W6TOP1	3.3	10.0	6.7	20	174	10.1	8.7	0.039	0.9370

The next step is to draw a graph between the value of the "slope" and average face advance per month for each station. Figure 7.19 shows the best fit line for those five stations with a correlation factor of 0.86.

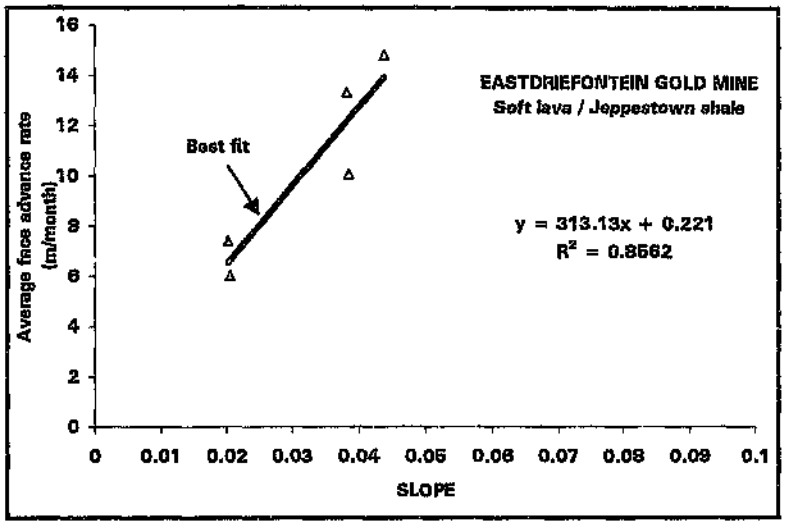

Figure 7.19. Graph showing the relationship between average face advance per month versus the value of the "slope" for five closure-ride stations analysed with the best fit line having a correlation factor of 0.86.

The equation of the best fit line in the graph above is $Y = 313.13\,X + 0.221$, which gives the relationship between the average face advance and the closure taking place at this point. For instance, if the design requires 5 m, 7.5 m or 10 m average face advance per month as Y, the value of "**X**" in the equation above will be 0.0153, 0.0232 and 0.0312, respectively.

In the design methodology, the fourth quadrant of the graph requires information about closure rate in millimetres per day. If the average face advance per month is assumed for this area, the linear line between distance to face and closure on this part of the graph could be drawn easily by assuming the value of closure varies from 0 to 300 or any required level in the face area.

Figure 7.20 shows the relationship between the closure taking place and average face advance per month.

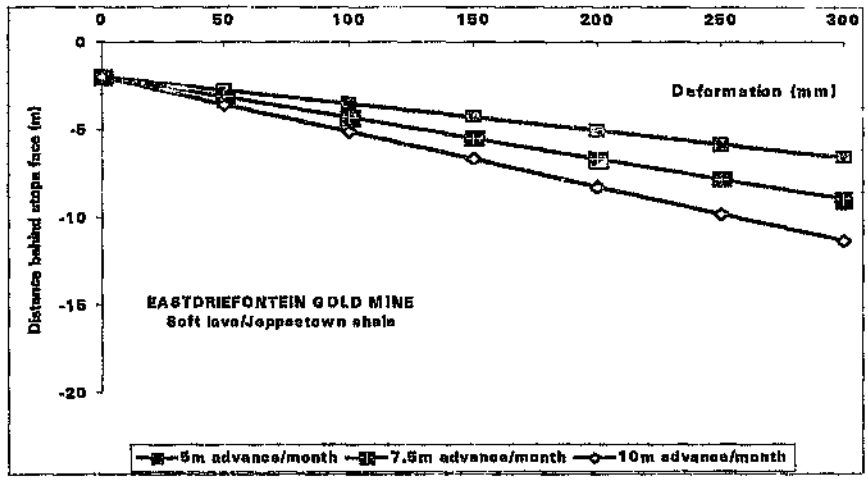

Figure 7.20. Calculated relationship between closure and average face advance in a stope with soft lava hangingwall in East Driefontein Gold Mine, 32 Level 37 Line.

7.3.3.2 Hard lava hangingwall

The same procedure as applied to the area of soft lava hangingwall was followed in analysing the measurements taken from the closure-ride stations installed in five panels in a geotechnical area defined as hard lava hangingwall and quartzite-conglomerate footwall in Deelkraal Gold Mine. Table 7.7 summarises all measurements taken into account during the analysis with the calculated value of the "slope" for each closure-ride station.

Figure 7.21 shows the relationship between average face advance per month and the value of the "slope" for all closure-ride station analysed with the best line having a correlation factor of 0.82. Figure 7.22 represents the observed relationship between closure and face advance in a stope with hard lava hangingwall in Deelkraal Gold Mine, 27 Level 15 Line.

Table 7.7. List of stations installed in the face area where the hangingwall is hard lava, with all parameters to be used in the process.

Station	From (m)	To (m)	Z (m)	D (days)	X (mm)	Average face advance (m/month)	AC (mm/day)	VALUE OF SLOPE	R^2
E1TOP1	6.5	10.9	4.4	26	173	5.08	6.65	0.025	0.993
E1TOP2	4.2	10.5	6.3	28	138	6.75	4.93	0.046	0.887
E1MID1	5.3	12.6	7.3	38	271	5.76	7.13	0.027	0.967
E1BOT1	5.0	11.6	6.6	31	184	6.39	5.94	0.036	0.969
E1BOT2	2.4	10.9	8.5	33	133	7.73	4.03	0.064	0.877
E1BOT3	4.6	9.5	4.9	34	270	4.32	7.94	0.018	0.971
E1BOT5	2.6	10.6	8.0	37	260	6.49	7.03	0.031	0.973
E5TOP4	5.1	10.2	5.1	34	215	4.50	6.32	0.024	0.971
E5MID3	5.1	10.2	5.1	28	212	5.46	7.57	0.024	0.893
E5BOT3	2.7	11.2	8.5	42	206	6.07	4.90	0.041	0.985
E5BOT5	2.2	10.0	7.8	34	222	6.88	6.53	0.035	0.928
E4TOP1	5.1	9.9	4.8	17	99	8.47	5.82	0.048	0.983
E4TOP3	4.6	10.3	5.7	19	109	9.00	5.74	0.052	0.968
E4TOP5	4.3	9.5	5.2	15	69	10.40	4.6	0.075	0.967
E4MID1	5.1	10.5	5.4	17	66	9.53	3.88	0.082	0.963
E4MID2	4.5	10.6	6.1	62	192	2.95	3.10	0.032	0.972
E4MID4	3.4	11.4	8.0	31	113	7.74	3.65	0.071	0.948
E4MID5	4.4	10.2	5.8	18	74	9.67	4.11	0.078	0.993
E4BOT1	5.5	9.9	4.4	62	225	2.13	3.63	0.02	0.983
E4BOT5	3.2	9.0	5.8	15	65	11.60	4.33	0.089	0.964
E4BOT6	4.4	10.0	5.6	17	77	9.88	4.53	0.073	0.002
E3TOP1	3.0	10.2	7.2	47	209	4.60	4.45	0.034	0.982
E3TOP2	3.8	9.5	5.7	27	137	6.33	5.07	0.042	0.979
E3TOP3	4.7	10.0	5.3	37	193	4.30	5.22	0.027	0.981
E3MID1	4.2	10.2	6.0	29	153	6.21	5.28	0.039	0.981
E3MID2	4.6	10.3	5.7	37	216	4.62	5.84	0.026	0.949
E3BOT1	4.9	10.0	5.1	62	258	2.47	4.16	0.02	0.975
E3BOT3	5.2	10.4	5.2	36	200	4.33	5.56	0.026	0.985
E3BOT4	4.3	10.1	5.8	29	135	6.00	4.66	0.043	0.970

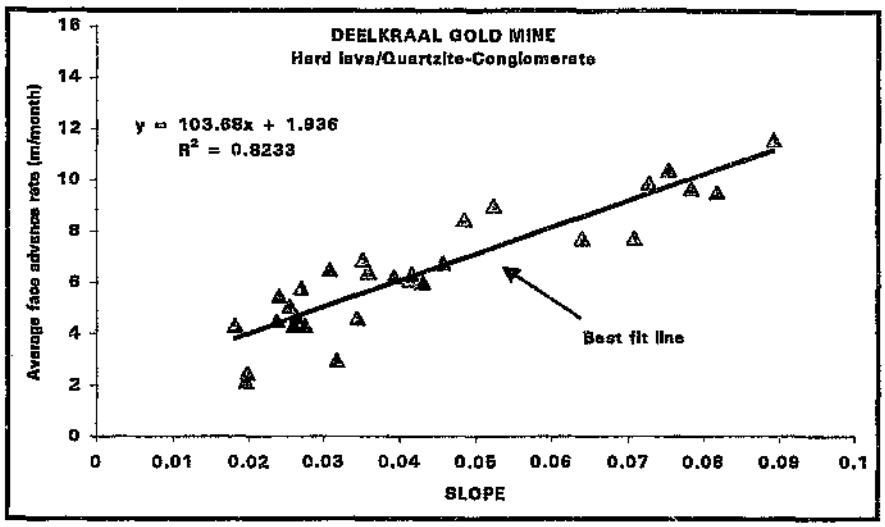

Figure 7.21. Graph showing the relationship between average face advance per month and the value of the "slope"; the best fit line has a correlation factor of 0.82.

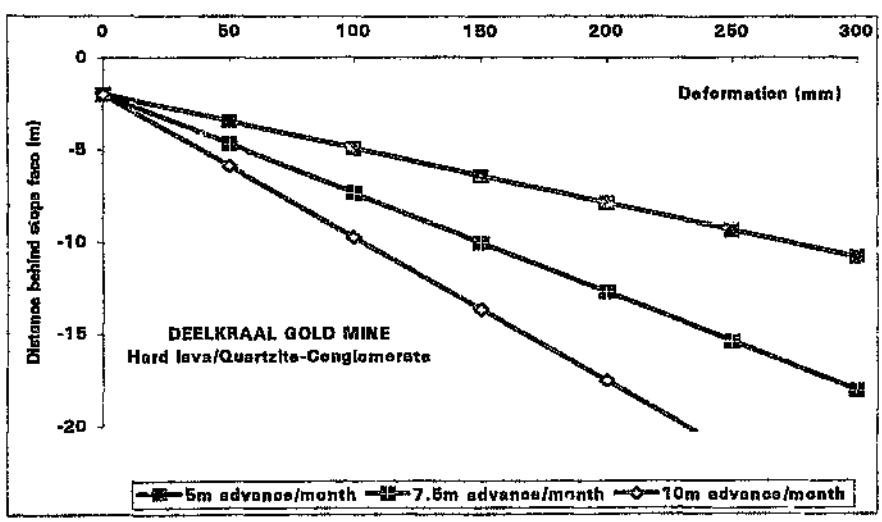

Figure 7.22. Calculated relationship between closure and average face advance in a stope with hard lava hangingwall in Deelkraal Gold Mine, 27 Level 15 Line.

A summary of these calculations is shown graphically in Figure 7.23. The solid and dashed lines representing an energy absorption criterion level as well as designed face advance rates, for example 5 m and 10 m per month, are for soft lava and hard lava hangingwalls respectively.

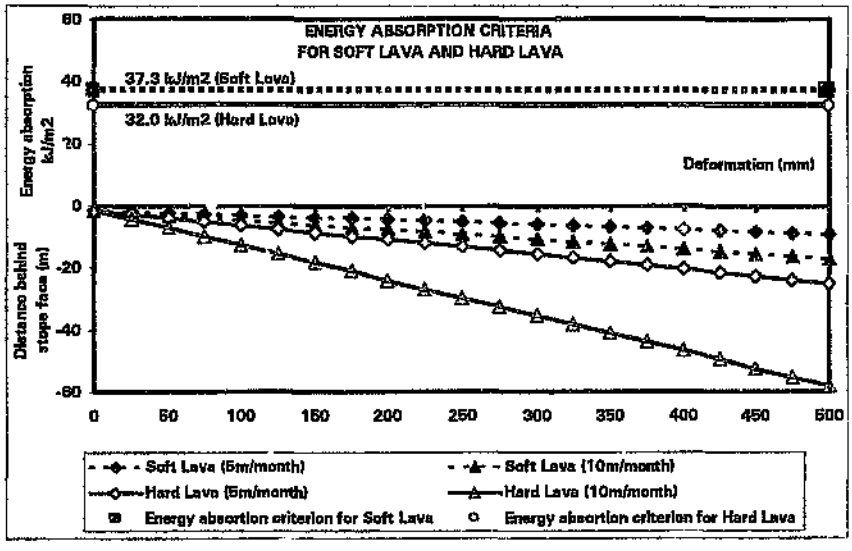

Figure 7.23. Summary of energy absorption criteria for soft lava and hard lava hangingwalls for different face advance rates.

The rate of face advance plays an important role as it not only determines the period over which support is deformed at the given closure rate, but also it influences the closure rate. The effect of face advance rate on closure rate deals directly with the amount of compression seen by a support unit a certain distance behind the stope face, whatever the rate of face advance may be. The effect of different face advance rates on the amount of closure experienced at a particular distance behind the face, and hence amount of available energy to be absorbed by the support system, is shown in Figure 7.24. This is a very important finding as a support system suitable

for one rate of face advance could be unsuitable when the rate of face advance slows. The total amount of energy available on a support unit in a stope with a high face advance rate will be higher than when with a low face advance rate (Fig. 7.24).

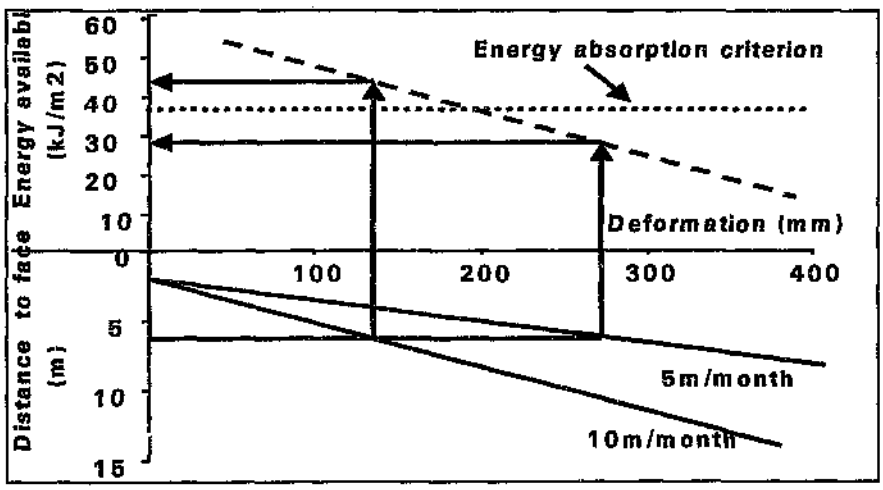

Figure 7.24. The effect of different face advance rates on the amount of closure experienced at a particular distance behind the face and hence amount of available energy to be absorbed by the support system.

CHAPTER 8

8 CONCLUSION AND PROPOSED FUTURE STUDIES

8.1 SUMMARY AND CONCLUSIONS

The basic expectation behind defining "geotechnical areas" is to observe and quantify different rock mass behaviour in the different combinations of rock types in the hangingwall and footwall of the reef. All mines where the VCR is currently being mined are defined in terms of different geotechnical areas based only on rock types in the hangingwall and footwall.

In order to determine the variation in rock mass behaviour in different VCR geotechnical areas, underground monitoring has been carried out at two different Gold Fields mines over a period of two years. The first site was selected at East Driefontein Gold Mine where the soft lava overlies Jeppestown shale. The other site was at Deelkraal Gold Mine. There the geotechnical area is defined as hard lava overlying quartzite-conglomerate.

At the East Driefontein site, mining of West 6 and West 5 panels was stopped for five months because of pronounced rolling of the reef. It is of interest that during this period stope closure was reduced but continued at a rate of 3 mm per day. Once mining recommenced, a large increase in closure rates to 8 mm and 10 mm per day were recorded. At the Deelkraal site, average closure rates of about 5 mm per day were recorded. It is of significance that closure rates are consistently lower than those measured at East Driefontein Gold Mine.

MINSIM-D modelling is used to compare actual closures measured with the expected convergences and it is found that the measured closures can be fitted with reduction in moduli of 70 % and 60 % for the soft and hard

lavas, respectively. This suggests that more inelastic behaviour is taking place in geotechnical areas with soft lava overlying Jeppestown shale than in areas with hard lava overlying quartzite-conglomerate.

A number of extensometers were installed at both sites in order to identify the relative contributions of hangingwall and footwall to the total closure in the stope. Measurements have shown that separation of the hangingwall formation is localised in nature and occurs primarily as a result of seismic events in the area where soft lava overlies the VCR. No significant contribution to closure was observed in the footwall shales. The extensometer measurements showed that the hangingwall and footwall contribute equally to the closure rates in the area where hard lava overlies the VCR.

Stress around the face of the stope, where the fractures are assumed to form, is influenced by the variation in stiffness and extent of damage between the footwall and hangingwall. Fractures are assumed to form in a direction associated with the direction of maximum compressive principal stress. This direction changes with distance ahead of the face.

Visits to underground monitoring sites were made to identify and map mining induced stress fracturing and the orientation of joints, faults, and dykes within the footwall and hangingwall of the VCR. The general orientation of mining induced stress fractures in the footwall at the underground monitoring site in the soft lava/Jeppestown shale geotechnical area is steep (about 70° to 80°) and away from the face. The orientation of fractures observed in the soft lava hangingwall is anomalous, dipping in the "wrong" direction when compared to reefs that have sedimentary footwall and hangingwall rocks or to areas where the VCR is overlain by hard lava. Visits to the opposite side of the longwall showed the same configuration of the mining induced stress fracturing relative to the face.

In the hard lava/quartzite-conglomerate geotechnical area, the general direction of mining induced stress fracturing in the quartzite-conglomerate footwall is steeply (about 70° to 80°) dipping away from the face similar to the first geotechnical area. However, the fractures in the hard lava hangingwall are significantly flatter (about 45° to 55°) and dip towards the face. The point of inflection of fractures in this combination of hangingwall and footwall rock types appears to be in the footwall.

There are thus clear distinctions between the patterns of mining induced stress fracturing from the two geotechnically defined regions. The consequences of differences in natural and mining induced structural features between the two geotechnical areas is that, at Deelkraal, the blocks of rock which can fall out are as large as 1.0 m / 1.1 m / 0.4 m, whereas at East Driefontein, they are smaller, about 0.3 m / 0.35 m / 0.4 m. This has a significant influence on the design of support for the two conditions.

A large number of rock samples were collected from both the hangingwall and footwall on different mines. Uniaxial compressive strength tests were carried out in each of three directions relative to the reef plane. The testing indicates a general homogeneity in rock properties with respect to dip, strike, and stratification. Two types of hangingwall lava do, however, exhibit large differences in rock properties, and mineralogical differences identified in the soft lava led to a further subdivision of this formation from a physical rock property point of view. More than 1000 point load tests were performed on nine underground borehole cores. The UCS values for the Talcose high-Mg basalt are generally less than 150 MPa. Olivine cumulate and mottled high-Mg basalt have UCS values generally exceeding 150 MPa. The soft lava therefore may be subdivided, from a rock engineering point of view, into two categories.

In elastic modelling, only unrealistically large differences in elastic properties between the hangingwall and footwall resulted in significant changes in the

stress distribution and orientation around the stope. To investigate the influence of rock failure and inelastic behaviour on stress distribution around a stope face, FLAC modelling was set up for the simplest stoping geometry and various material constitutive laws were used. Mohr-Coulomb and Strain-softening modelling indicated that plastic parameters such as internal friction angle (ϕ), tension cut-off (T), dilation angle (ψ) and cohesion (C), affect the stresses around the stope. Large differences in cohesion appear to be the most significant.

In order to determine support resistance criteria for the control of rockfalls and energy absorption criteria for the control of rockbursts for both soft and hard lava hangingwalls in VCR stopes, the main input parameters were taken from the database of fatalities which is an output of the SIMRAC stope and gully support project GAP 032 (Roberts, 1996). In these calculations, all fatalities that occurred during six years, 1990-1995, were used and it was assumed that the designed support system should prevent 95 % cumulative percentages of all fallouts and block ejection due to rockburst conditions. The support resistance for VCR soft lava and hard lava hangingwalls is calculated as 33.0 kN/m^2 and 49.5 kN/m^2 respectively. In the calculation of energy absorption criteria, two major assumptions were made: the support system has the ability to yield 0.2 m, typical of the yieldability of hydraulic props and yielding timber props; and the velocity of ejection during rockburst conditions is 3 m/s. The calculations show that the energy absorption criteria for the control of rockbursts for soft and hard lava hangingwalls in VCR stopes are 37.3 kJ/m^2 and 32.0 kJ/m^2, respectively.

8.2 RECOMMENDATIONS

In further studies, the definition of the geotechnical area should be further refined by including the distribution and frequency of geological features, such as faults, joints and rolls, in addition to the combination of hangingwall and footwall rock types.

Inclined holes should be drilled from the stope into the hangingwall and footwall in order to obtain better information on the fracture mechanism. If extensometers were installed into some of these holes after establishing the position of fractures by means of petroscope observations, it would be possible to obtain further information on how the rock mass behaves ahead of the face, where the rock is failing.

Ground penetrating radar (GPR) which is the electromagnetic analogue of seismics, could also give useful information on fracturing in the hanging-and footwalls.

Further studies will have to consider the early identification of rolls, possibly by considering the characteristics of jointing and mining induced stress fracturing before intersection of the rolls.

In numerical modelling, models should consider the reef parallel weakness planes in the immediate hangingwall, footwall bedding at different distances from the stope, major faults, and the contact between soft and hard lava. A method to effectively modify values from laboratory testing for use as input values in numerical models needs to be determined. The input values obtained from the rock test analysis should be rescaled down in a systematic formulation.

The basic parameter used in the support design methodology, developed under the SIMRAC stope and gully support project GAP 032 (Roberts, 1996)

is the rate of stope closure. The closure is used to determine if the remaining yieldability will allow sufficient energy to be absorbed should a rockburst occur. Underground monitoring results from closure ride stations in different geotechnical areas shows that the closure rates vary quite significantly and the general trend of the closure rate with time is not linear. The rate of closure in the first 10 m from the face can be considered to be approximately linear. It has also been observed that the closure rate is very dependent on the rate of face advance. In order to analyse the effect of face advance rate on closure rate, results from all stations installed within 10 m of the face were taken into account. The results for the face area show a very good correlation and make it possible to develop a support system design that is dependent on rate of face advance. The closure rate/face advance rate correlation, as defined in this study for the VCR, needs to be established for the other gold-bearing horizons of the Witwatersrand Basin. The analysis for the back area shows that the number of the stations and quality of readings are not sufficient for a good correlation between the rate of face advance and closure taking place.

In the determination of rockburst and rockfall control criteria for the support system design methodology, a limited database of six years was used. The expansion of this database will be required.

In the stope support design methodology, the basic assumptions are that the support system should be able to stabilise the hangingwall in 95 % of the cases, and the velocity of ejection during rockburst conditions is 3 m/s with a yieldability of 0.2 m. A further study, on higher or lower percentages of cases requiring stabilising of the hangingwall, needs to be undertaken. The rockburst closure velocity is likely to be different within different geotechnical areas, and additional investigation in this area is also necessary. The maximum height of 0.2 m, typical of the yieldability of hydraulic props and yielding timber props, should be discussed in terms of the variability between different support systems.

REFERENCES

ANON (1988). An industrial guide to methods of ameliorating the hazards of rockfalls and rockbursts. Chamber of Mines of South Africa, 114 pp.

ARMSTRONG, R.A., COMPSTON, W., RETIEF, E.A. and WELKE, H.J. (1986). Ages and isotopic evolution of the Ventersdorp volcanics. Ext. Abstr., Geocongress'86, Geol. Soc. S. Afr., Johannesburg, p. 89-92.

BARTON, E.S., BARTON, J.M. Jr, CALLOW, M.J. , ALLSOPP, H.L. , EVANS, I.B. , WELKE, H.J. (1986). Emplacement ages and implications for the source region of granitoid rocks associated with the Witwatersrand Basin. Ext. Abstr., Geocongress'86, Johannesburg, p. 93-97.

CHAPMAN, K.M., TUCKER, R.F., KIDGER, R.J. (1986). The Klerksdorp Goldfield. In: Witwatersrand Gold - 100 years. Geol. Soc. S. Afr., p. 173-197.

CHUNNETT, I.E. (1994). The VCR - A Historical perspective. S. Afr. J. Geol., 97/3, p.239-246.

COETZER, K.J.B., LAMBERT, P.E., (1993). Stratigraphy, geochemistry and distribution of the Westonaria Formation on East Driefontein Gold Mine. Ext. Abstr., VCR Mini Symposium, The VCR Revisited, Geol. Soc. S. Afr.

CSIR Mining Technology. Rock Engineering. Stope Catalogue (1993).

DE KOCK, W.P. (1940). The VCR : Its nature , Mode of occurrence and economic significance, with special reference to the Far West Rand. Trans. Geol. Soc. S. Afr., Vol. 43, p. 85-108.

DEELKRAAL GOLD MINE CO. LTD. (1992). Annual Report. pp. 21.

DRIEFONTEIN GOLD MINE CO. LTD. (1992). Annual Report. pp. 26

ELANDSRAND GOLD MINE CO. LTD. (1992). 19th Annual Report. pp.21

EVE, R.D. (1994). Personnel communication. CSIR, a Division of Mining Technology.

FLAC (Fast Lagrangian Analysis of Continua) (1993). FLAC Manuals, Version 3.2, ITASCA Consulting Group, USA.

GÜLER, G. (1996). Measurement and prediction of the rock mass of the Ventersdorp Contact Reef stopes. Prediction and performance in rock mechanics and rock engineering. ISRM Symposium, EUROCK'96, Italy, 1996. pp.1071-1078.

GÜRTUNCA, R.G., ADAMS, A.D. (1991). Determination of the in situ modulus of the rock mass by the use of backfill measurements. J. S. Afr. Inst. Min. Metall., Vol. 91, no. 3., March. 1991. p. 81-88.

GÜRTUNCA, R.G., LEACH, A.R., YORK, G., TRELOAR, M.L. (1993). In situ performance of cemented backfill in a deep-level South African gold mine. Minefill 93, Johannesburg, SAIMM, p. 121-128.

HAMMAN, J.P.E. (1993). Personnel communication. Rock Engineering Department, Elandsrand Gold Mine, Carletonville.

JOHNSON, R.A. (1991). MINSIM-D Package. Overview and program operation. Chamber of Mines of South Africa.

JOHNSON, R.A. (1994). Regional Support Modelling - Assessment of an alternative approach. The application of numerical modelling in geotechnical engineering. Int. Soc. for Rock Mech., SANGORM, Pretoria, 1994. p. 25-30.

KLOOF GOLD MINE CO. LTD. (1992). Annual Report. pp.24

KNOWLES, A.G. (1966). A paleocurrent study of the VCR at Western Deep Levels Limited on the Far West Rand. M.Sc. Thesis, University of Witwatersrand, Johannesburg, 125 pp.

McKINNON, S.D. (1989). Protection of Deep Vertical Shaft Systems. Ph.D. Thesis, University of Witwatersrand, Johannesburg.

NICOLAYSEN, L.O., BURGER, A.J., LIEBENBERG, W.R. (1962). Evidence for the extreme age of certain minerals for the Dominion Reef conglomerate and the underlying granite in the Western Transvaal. Geochim. Cosmochim. Acta, 26: 15-23.

PELLETIER, R.A. (1937). Contributions to the geology of the Far West Rand. Trans. Geol. Soc. S. Afr.,40, p. 127-162.

PIPER, P., GÜRTUNCA, R.G. (1987). SANGORM News, February, Johannesburg, Editor R. BRUMMER, 20 pp.

REPUBLIC OF SOUTH AFRICA, DEPARTMENT OF MINERALS AND ENERGY, (1996). South African mines reportable accident statistics system (SAMRASS) and guidelines for the classification of accidents, Revised December 1996.

ROBERTS, M.K.C. (1994). Personnel communication. CSIR, a Division of Mining Technology.

ROBERTS, M.K.C. (1995). Stope and gully support, Final Report, Project GAP032, Safety in Mines Researcl 'dvisory Committee (SIMRAC).

ROBERTS, M.K.C., JAGER, A.. '). An analysis of falls of ground and rockburst fatalities. Mine Sa.. .y and Health Congress 91, Chamber of Mines of South Africa, Johannesburg , p. 181-200.

RYDER ,J. (1993). *Personnel communication*. CSIR, a Division of Mining Technology.

SCHWEITZER, J.K. (1987). ". .R., COMRO Internal Technical Note 60/87.

SCHWEITZER, J.K. (1993). Personnel communication. CSIR, a Division of Mining Technology.

SCHWEITZER, J.K. (1994). Personnel communication. CSIR, a Division of Mining Technology.

SCHWEITZER, J.K., VAN NIEKERK A.W., ASHWORTH, S.G.E., A.W., HENCKEL, J. (1994). Interrelationship between geomorphology, stratigraphy, and gold grade in the Ventersdorp Contact Reef, eastern portion of Elandsrand Gold Mine., S. Afr. J. Geol.,1994, 97/3, p 339-347.

SCHWEITZER, J.K., VAN NIEKERK, A.W., HENCKEL, J. (1994). Paleoenvironmental reconstruction of parts of the fluvia' ~ stem that deposited the VCR at Elandsrand Gold Mine, COMRO Refe.ence Report 21/91.

SMITH, G.L., VLIESTRA, D. (1992). Absolute stress measurements using the "Doorstopper Technique" at Kloof Gold Mine., COMRO Internal Note, R08/92.

SOUTH AFRICAN COMMITTEE FOR STRATIGRAPHY (SACS),1980. Lithostratigraphy of the Republic of South Africa , South West Africa / Namibia and Republic of Bophuthatswana, Transkei and Venda. Handbook Geol. Surv. S. Afr., 8, 633 pp.

SWART, H. (1995). Personnel communication. Johannesburg Consolidated Investment Company, Limited (JCI), Group Geological Services-Research, Randfontein.

TAGGART, P.N. (1994). Dynamic laboratory testing of pack based support elements. Part 1. The laboratory evaluation of timber and composite packs, single rise pack elements and grout based prestressing. Interim project report, GAP 032.

TAGGART, P.N. (1994). Dynamic laboratory testing of pack based support elements. Part 2. The laboratory evaluation of two types of grout based prestressing systems. Interim project report, GAP 032.

TANKARD, A.J. JACKSON, M.P.A., ERIKSSON, K.A., NOBDAY, D.K., HUNTER, D.R., MINTER, W.E.L. (1982). Crustal evolution of Southern Africa. Springer, New York, 523pp.

TURNER, P.A. (1979). The planar auriferous Witwatersrand conglomerates : Pediment mantles of the Proterozoic. Ext. Abstr. Geocongress'79 (Part 1), Geol. Soc. S. Afr., p. 359-375.

VAAL REEFS EXPLORATION and MINING CO.LTD. (1992). 49th Annual Report. pp.25

VENTERSPOST GOLD MINE CO. LTD. (1992). Annual Report. pp.17.

WESTERN DEEP LEVELS CO.LTD. (1992). 35th Annual Report. pp.22.

YORK, G., SQUELCH, A.P. (1992). The behaviour of cemented backfill and the surrounding rock mass at Western Deep Levels South Mine. Johannesburg, COMRO, Reference Report no. 18/92, pp. 27.

VLIETSTRA, D. (1995). In-situ stress measurements at Kloof Gold Mine using the "Doorstopper Technique". Johannesburg. CSIR Mining Technology, Internal Note no. RE 1/95.

APPENDIX A

Mining induced stress fracturing : East Driefontein Gold Mine.





Photographs A1 and A2: Fractures observed in hangingwall along West 6 Gully in 32 Level 37 Line at # 4 shaft, East Driefontein Gold Mine. The arrow shows the direction of mining operations. A2 is a close-up of A1.

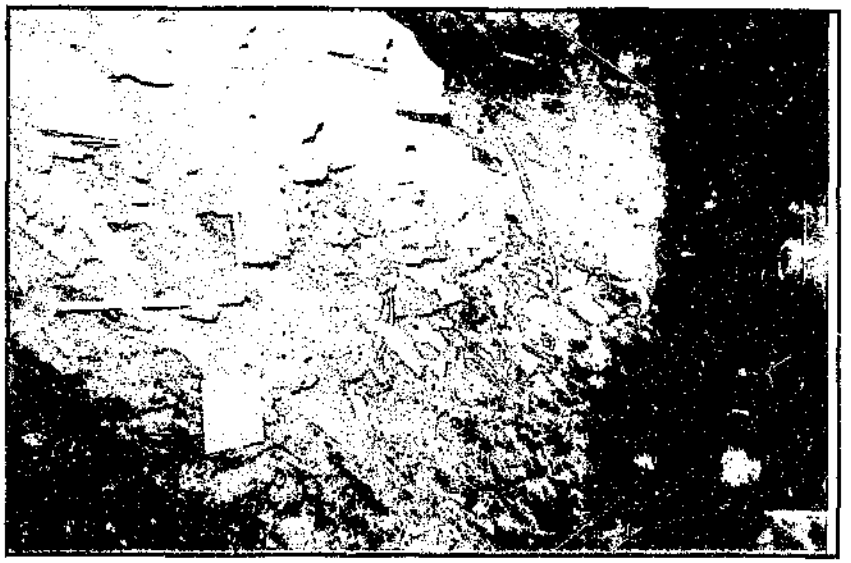

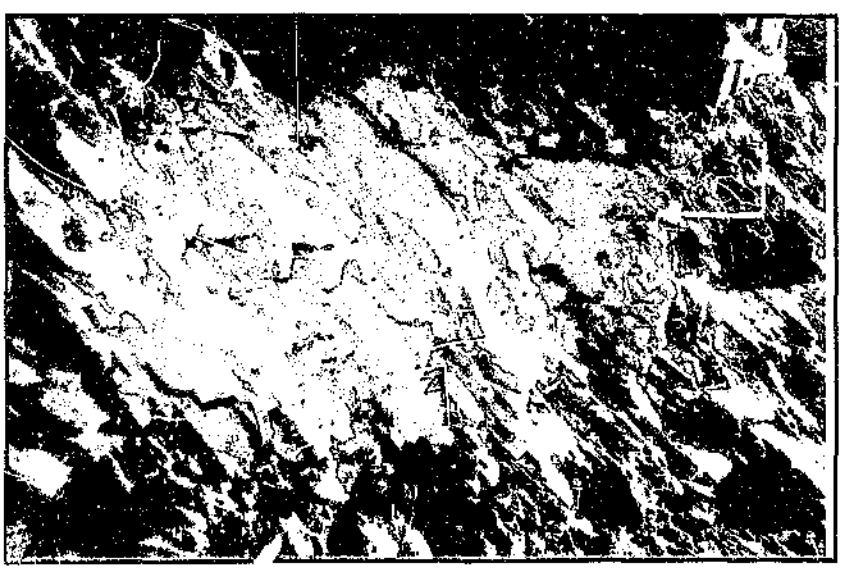

Photographs A3 and A4: Fractures observed in footwall along West 6 Gully in 32 Level 37 Line at # 4 shaft, East Driefontein Gold Mine. The arrow shows the direction of mining operations. A4 represents the close-up of A3.





Photographs A5 and A6: Fractures observed in hangingwall in West 5 Stope in 32 Level 37 Line at # 4 shaft, East Driefontein Gold Mine. The arrow shows the direction of mining operations.





Photographs A7 and A8: Fractures observed in hangingwall in West 7 Stope (above) and in West 6 Stope (below) 32 Level 37 Line at # 4 shaft, East Driefontein Gold Mine. The arrow shows the direction of mining operations.

APPENDIX B

Mining induced stress fracturing : Deelkraal Gold Mine





Photographs B1 and B2: Fractures observed in hangingwall in East 1 panel on 27 Level 15 Line Deelkraal Gold Mine. The arrow shows the direction of mining operations.

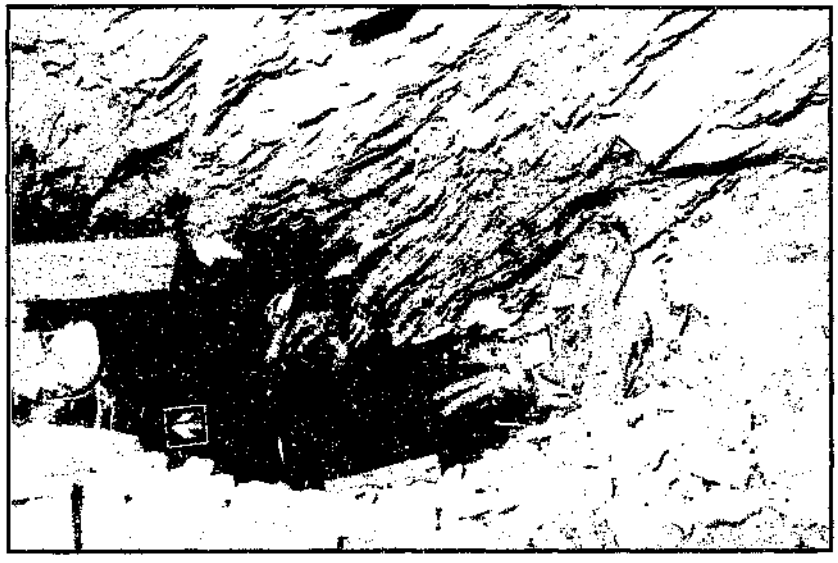



Photographs B3 and B4: Fractures observed in hangingwall in East 5 panel on 27 Level 15 Line Deelkraal Gold Mine. The arrow shows the direction of mining operations.

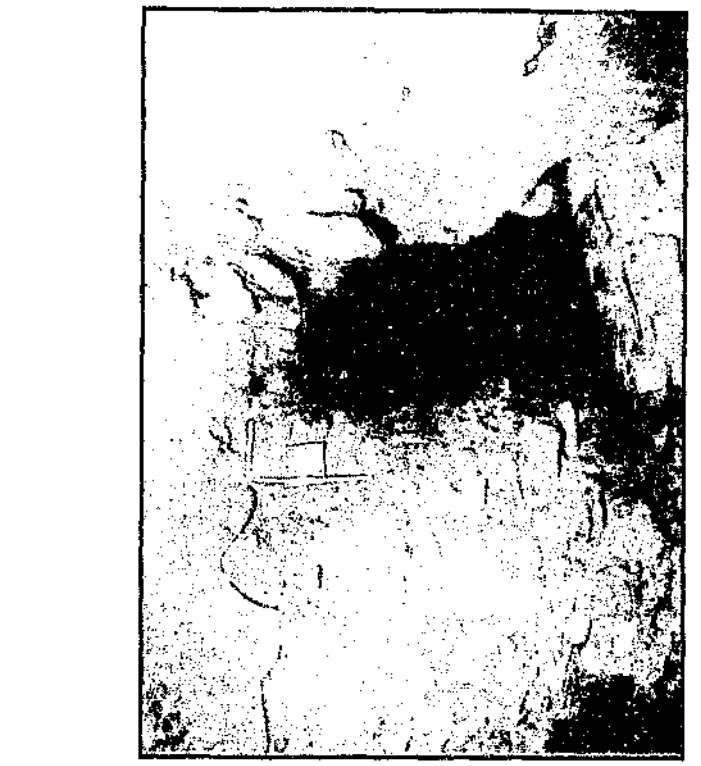



Photographs B5 and B6: Fractures observed in hangingwall and footwall along East 4 panel and fractures in hangingwall in East 4 panel on 27 Level 15 Line Deelkraal Gold Mine. The arrow shows the direction of mining operations.





PhotographsB7 and B8: Fractures observed in hangingwall in East 3 panel and East 2 panels on 27 Level 15 Line Deelkraal Gold Mine. The arrow shows the direction of mining operations.

Author: Guler, Gokhan.
Name of thesis: Analysis of the rock mass behaviour as associated with Ventersdorp Contact Reef Stopes, South Africa - Gokhan Guler.

PUBLISHER:
University of the Witwatersrand, Johannesburg
©2015

LEGALNOTICES:

Copyright Notice: All materials on the University of the Witwatersrand, Johannesburg Library website are protected by South African copyright law and may not be distributed, transmitted, displayed or otherwise published in any format, without the prior written permission of the copyright owner.

Disclaimer and Terms of Use: Provided that you maintain all copyright and other notices contained therein, you may download material (one machine readable copy and one print copy per page)for your personal and/or educational non-commercial use only.

The University of the Witwatersrand, Johannesburg, is not responsible for any errors or omissions and excludes any and all liability for any errors in or omissions from the information on the Library website.